AD-A184 356 EFFECT OF TIME AND TEMPERATURE ON TRANSFORMATION TOUGHENED ZIRCONIAS(U) ARMY LAB COMMAND WATERTOWN MA MATERIAL TECHNOLOGY LAB L J SCHIOLER JUN 87 1/2

UNCLASSIFIED MTL-TR-87-29 DE-AI05-840R-21411 F/G 11/2 NL

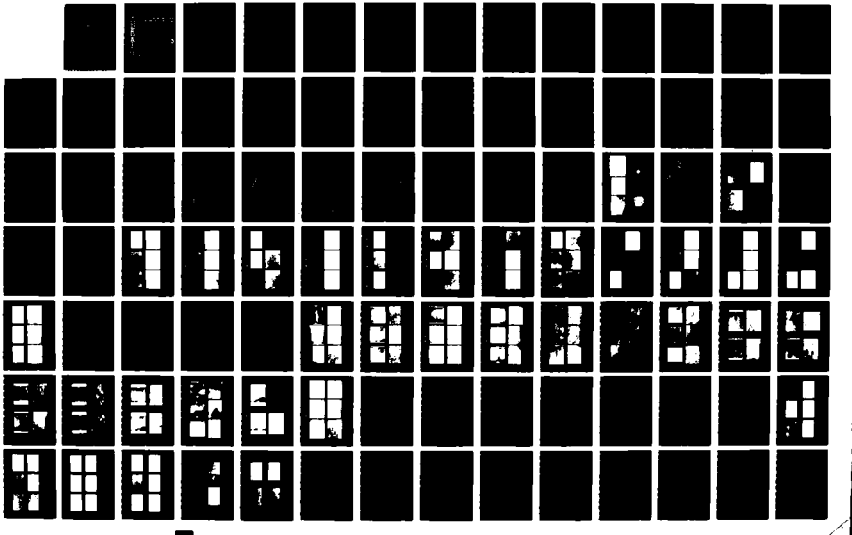

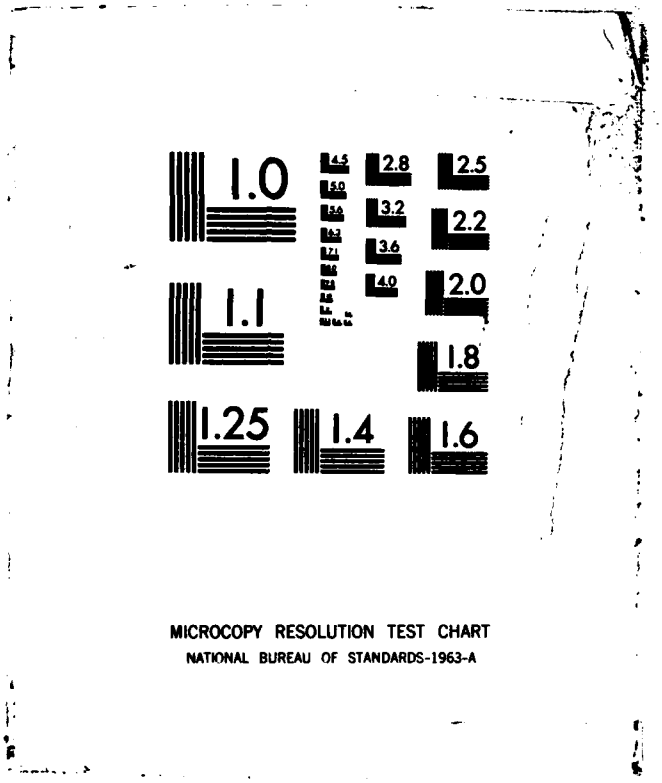

MICROCOPY RESOLUTION TEST CHART
NATIONAL BUREAU OF STANDARDS-1963-A

ENERGY

(2)

AD

MTL TR 87-29

EFFECT OF TIME AND TEMPERATURE ON TRANSFORMATION TOUGHENED ZIRCONIAS

LISELOTTE J. SCHIOLER

June 1987

Prepared under
Interagency Agreement DE-AI05-840R-21411

by
U.S. ARMY MATERIALS TECHNOLOGY LABORATORY
WATERTOWN, MASSACHUSETTS 02172-0001

U.S. DEPARTMENT OF ENERGY

Office of Vehicle and Engine Research and Development
Ceramics Technology for Advanced Heat Engines Programs

The findings in this report are not to be construed as an official Department of the Army position, unless so designated by other authorized documents.

Mention of any trade names or manufacturers in this report shall not be construed as advertising nor as an official indorsement or approval of such products or companies by the United States Government.

DISPOSITION INSTRUCTIONS

Destroy this report when it is no longer needed.
Do not return it to the originator.

UNCLASSIFIED

SECURITY CLASSIFICATION OF THIS PAGE (When Data Entered)

REPORT DOCUMENTATION PAGE		READ INSTRUCTIONS BEFORE COMPLETING FORM
1. REPORT NUMBER MTL TR 87-29	2. GOVT ACCESSION NO.	3. RECIPIENT'S CATALOG NUMBER
4. TITLE (and Subtitle) EFFECT OF TIME AND TEMPERATURE ON TRANSFORMATION TOUGHENED ZIRCONIAS		5. TYPE OF REPORT & PERIOD COVERED Final Report 6. PERFORMING ORG. REPORT NUMBER
7. AUTHOR(s) Liselotte J. Schioler		8. CONTRACT OR GRANT NUMBER(s)
9. PERFORMING ORGANIZATION NAME AND ADDRESS U.S. Army Materials Technology Laboratory Watertown, Massachusetts 02172-0001 SLCMT-MCC		10. PROGRAM ELEMENT, PROJECT, TASK AREA & WORK UNIT NUMBERS Interagency Agreement DE-AI05-840R-21411
11. CONTROLLING OFFICE NAME AND ADDRESS U.S. Department of Energy Office of Vehicle and Engine Research and Development Washington, D.C. 20545		12. REPORT DATE June 1987 13. NUMBER OF PAGES 91
14. MONITORING AGENCY NAME & ADDRESS(if different from Controlling Office)		15. SECURITY CLASS. (of this report) Unclassified 15a. DECLASSIFICATION/DOWNGRADING SCHEDULE

16. DISTRIBUTION STATEMENT (of this Report)

Approved for public release; distribution unlimited.

17. DISTRIBUTION STATEMENT (of the abstract entered in Block 20, if different from Report)

18. SUPPLEMENTARY NOTES

19. KEY WORDS (Continue on reverse side if necessary and identify by block number)

Zirconia	Ceramic materials
Toughened ceramics	Mechanical properties
Ceramics	Microstructure
Fracture toughness	

20. ABSTRACT (Continue on reverse side if necessary and identify by block number)

(SEE REVERSE SIDE)

DD FORM 1 JAN 73 1473 EDITION OF 1 NOV 65 IS OBSOLETE

UNCLASSIFIED

SECURITY CLASSIFICATION OF THIS PAGE (When Data Entered)

Block No. 20

ABSTRACT

The effects of exposure to elevated temperatures (900 to 1300°C) for times ranging from 50 to 500 hours on toughened oxide ceramics intended for use in heat engines were examined. The materials were magnesia stabilized transformation toughened zirconia, yttria stabilized tetragonal zirconia polycrystal, and zirconia toughened alumina, as well as untoughened zirconias for comparison. The materials were heat treated, and physical and mechanical properties were then measured at room temperature. High temperature mechanical tests performed were stress rupture and stepped temperature stress rupture.

The results of the tests indicate that the mechanical properties of magnesia stabilized transformation toughened zirconia degrade substantially after relatively short times at the moderate temperatures expected in low heat rejection diesel engines. The yttria stabilized tetragonal zirconia polycrystal and the untoughened partially stabilized zirconia materials appear to be more stable against the effects of time at temperature.

CONTENTS

	Page
INTRODUCTION.	1
SCREENING OF MATERIALS.	2
ROOM TEMPERATURE TESTING OF BEND SPECIMENS.	6
HIGH TEMPERATURE TESTING OF BEND SPECIMENS.	14
ZIRCONIA TOUGHENED ALUMINA.	17
CONCLUSIONS	22
Appendix A. Polishing Procedure for Zirconia Toughened Materials	55
Appendix B. Phase Analysis of Zirconia System Using X-Ray Diffraction. . .	56

INTRODUCTION

Many of the ceramic materials being investigated for use in heat engines, especially the so-called "adiabatic" diesel engine, are toughened with zirconia. These materials include transformation toughened zirconia (TTZ) and tetragonal zirconia polycrystal (TZP), as well as zirconia toughened alumina (ZTA), among others. Zirconia based materials are of interest due to their low thermal conductivity (necessary for good thermal insulation) and high thermal expansion (desired for attachment of the ceramic to the metal in the engine), as well as their outstanding failure strength and fracture toughness.

The room temperature mechanical properties of these zirconia materials have been studied, but little was known about the effects of exposure to moderate temperatures (1000°C) on these properties. The effects of time-at-temperature become important as the "adiabatic" (or low-heat-rejection) diesel is expected to operate at temperatures of about 1000°C and for lifetimes of >5000 hours. This operating temperature (1000°C) is in the range where a stable phase transformation of zirconia occurs, and is also high enough for grain growth in the material. Both phase transformation and grain growth can cause degradation of mechanical properties such as strength and fracture toughness.

Both TTZ and TZP are partially stabilized zirconias, but the stabilizers used are different in each: MgO and CaO are commonly used in TTZ, and Y_2O_3 is used in TZP, although other rare earth oxides are being investigated for use in the TZP material. The main toughening mechanism of TTZ occurs as small (~0.2 μm) metastable tetragonal precipitates in the large (10-40 μm) matrix grains which transform to the stable monoclinic phase as a crack propagates through the material, absorbing some of the fracture energy (thus the designation "transformation toughening"). The precipitate microstructure is formed during an "ageing" anneal of the zirconia material at temperatures typically greater than 1400°C. The tetragonal precipitates will spontaneously transform to the monoclinic phase due to the lattice mismatch stress if they become larger than about 0.2 μm, with an accompanying loss of strength and toughness in the bulk material. This decrease in mechanical properties with increasing ageing time is commonly referred to a "overageing."

The TZP material has a totally different microstructure from that of the TTZ; it consists of fine (~2 μm) tetragonal grains, with some monoclinic phase only as an impurity at the grain boundaries. In this material, the tetragonal phase is metastable and exists at room temperature only because the grain size is so small. The exact mechanism for the toughening in this material is not well understood. If grain growth occurs at elevated temperatures, it would be expected that the tetragonal grains in TZP would transform to the monoclinic phase with the resulting degradation of properties.

This research project, to determine the effect of time-at-temperature on the properties of toughened ceramics, was carried out in two parts. The first part was a screening of several materials to determine if the expected phase and related density change did indeed occur and at what temperatures and times the effect became severe. In the second part, billets of several different brands of zirconia-based materials were obtained. Bend specimens were machined from the billets and were then heat treated. After the heat treatments, a variety of tests were performed on the specimens, including fast fracture and fracture toughness testing. High temperature testing consisting of stress rupture and stepped temperature stress rupture was also performed.

SCREENING OF MATERIALS

In the screening, small coupons (5 × 5 × 3 mm in size) of five materials [three TTZs, one TZP, and a fully stabilized zirconia (FSZ) for comparison] were examined. The coupons were cut from a few bend specimens supplied by the Cummins Engine Company. Table 1 gives the available information on these five materials. The as-received density and sonic modulus of elasticity (MOE) of each coupon was measured. The phase content was determined via x-ray diffraction techniques on polished surfaces, and photomicrographs were taken of the samples. One coupon of each material was heat treated in a laboratory furnace in air at each of five temperatures for a given time. The coupons were polished; density, MOE, and phase content were again determined; and photomicrographs were taken. The coupons were then placed back in the furnace for another heat treatment. This procedure of heat treatment and property determination was repeated several times for each coupon. The temperatures and total times examined were 900, 1000, 1100, 1200 and 1300°C, and 50, 100, 250, and 500 hours respectively. The heat treatments consisted of a fast heat to temperature (~4 hours), a hold at temperature, and natural cooling. Since the furnaces cooled rapidly from temperature to less than 800°C (a temperature at which no changes were expected in the materials), the heat up and cooling times of the heat treatments were ignored.

Table 1. MATERIALS USED IN THE SCREENING OF ZIRCONIA MATERIALS

Material	Code	Stabilizer	Supplier	Supplier's designation
C	TTZ	MgO	Nilsen, USA	Unknown
G	TTZ	MgO	Coors Porcelain Co.	ZDM (1981)
J	FSZ	Y_2O_3	Coors Porcelain Co.	ZDY (1981)
K	TTZ	MgO	American Feldmuehle Corp.	Unknown
M	TZP	Y_2O_3	NGK Sparkplug	Unknown

Table 2 gives the measured densities of the coupons after heat treatment. No standard deviations are given, as only one sample for each time and temperature was available. This is also the reason why the densities do not change smoothly. The general trend, though, is for the density to decrease from the as-received value (zero hours) as the time of the heat treatment increases, with the amount of the decrease in density increasing with increasing temperature. The magnesia stabilized materials (C, G, and K) showed the largest change in density with heat treatment, while the yttria stabilized materials showed the least change. The decrease in density was due mainly to an increase in volume with little or no decrease in mass. Figures 1a through 1e show the percent change in density as a function of time and temperature for the five coupon materials.

The coupons were carefully polished after the heat treatments to remove the surface layer caused by machining and heat treatments, and to expose a "bulk" surface. Appendix A gives the polishing procedure. X-ray diffraction patterns of the "bulk" surfaces were obtained in order to determine the phase content (Appendix B). The magnesia stabilized materials showed increases in the monoclinic phase content after short times at relatively low temperatures (Table 3), while material M, which is yttria stabilized, did not show any large change in phase content until longer times at higher temperatures. Material J, which is fully stabilized by yttria, did not show any change in phase content, as shown in Table 3. Figure 2

Table 2. DENSITY OF THE COUPONS AFTER HEAT TREATMENTS*

	ρ (g/cm^3) 0 hr	ρ (g/cm^3) 50 hr	ρ (g/cm^3) 100 hr	ρ (g/cm^3) 250 hr	ρ (g/cm^3) 500 hr
Material C					
900°C	5.692	5.596	5.652	5.650	5.623
1000°C	5.668	5.704	5.591	5.642	5.615
1100°C	5.709	5.644	5.581	5.563	5.508
1200°C	5.713	5.584	5.562	5.535	5.482
1300°C	5.689	5.559	5.394	5.365	5.170
Material G**					
900°C	5.125	5.095	5.067	5.030	5.023
1000°C	5.166	5.136	5.073	5.134	5.093
1100°C	5.078	5.051	5.824	4.936	4.890
1200°C	5.051	4.908	4.808	4.790	-
1300°C	5.059	-	-	-	-
Material J					
900°C	5.504	5.488	5.502	5.460	5.406
1000°C	5.522	5.526	5.484	5.495	5.473
1100°C	5.552	5.540	5.478	5.478	5.443
1200°C	5.503	5.479	5.435	5.400	5.380
1300°C	5.494	5.475	5.419	5.377	5.236
Material K					
900°C	5.705	5.727	5.709	5.701	5.664
1000°C	5.737	5.718	5.649	5.628	5.565
1100°C	5.723	5.598	5.556	5.550	5.509
1200°C	5.717	5.591	5.550	5.487	5.485
1300°C	5.720	5.610	5.392	5.376	5.310
Material M					
900°C	5.731	5.723	5.690	5.679	5.650
1000°C	5.690	5.688	5.634	5.654	5.637
1100°C	5.722	5.708	5.714	5.708	5.658
1200°C	5.701	5.659	5.691	5.607	5.651
1300°C	5.729	5.675	5.636	5.682	5.548

* Estimated error in the measured densities is $\pm$ 0.5%

** Densities were not determined on some of the G coupons as they were chipped after heat-treatment

shows the volume percent monoclinic phase as a function of time and temperature for four of the five coupon materials. (Material J is not shown, as it did not show any changes in phase content throughout the heat treatments.) Although high resolution microscopy was not performed on the magnesia stabilized materials for verification, the assumption is that the change in monoclinic phase content is due to spontaneous transformation of the metastable tetragonal precipitates as they grew larger than the critical size.

The phase content of the zirconia coupons was calculated as volume percents of monoclinic and [tetragonal + cubic] phases. The amounts of cubic and tetragonal phases were not determined separately. Some of the coupons were 100% monoclinic after heat treatments, i.e., no peaks were apparent on the powder x-ray diffractogram in the position where the tetragonal and cubic peaks would be expected. This implies that not only the tetragonal phase, but the cubic phase as well transformed to monoclinic. This phenomenon is not easily explained; it could be due to several causes. If the stabilizer, MgO, has volatilized from the coupon, the remaining material would be more susceptible to stable phase transformation. There is, however, no evidence from chemical analysis that this occurred. Another cause for the apparent loss of all the tetragonal and cubic phases would be the formation of an

Table 3. MONOCLINIC PHASE CONTENT OF THE ZIRCONIA COUPONS AS A FUNCTION OF TIME-AT-TEMPERATURE*

	Volume Percent Monoclinic			
	50 hr	100 hr	250 hr	500 hr
Material C (as-received = 25.7 volume % monoclinic)				
900°C	34.2	20.7	34.1	32.1
1000°C	38.7	56.7	61.4	71.5
1100°C	59.5	72.5	93.1	100.0
1200°C	82.8	100.0	96.5	100.0
1300°C	97.8	100.0	99.2	99.5
Material G (as-received = 79.5 volume % monoclinic)				
900°C	77.3	83.6	92.2	99.7
1000°C	100.0	96.0	100.0	100.0
1100°C	100.0	100.0	100.0	100.0
1200°C	100.0	100.0	97.0	100.0
1300°C	100.0	100.0	100.0	100.0
Material K (as-received = 14.1 volume % monoclinic)				
900°C	15.2	15.3	6.0	19.4
1000°C	15.6	35.1	50.9	91.5
1100°C	63.9	79.4	100.0	100.0
1200°C	64.1	99.4	99.4	99.2
1300°C	75.7	98.4	98.8	99.3
Material M (as-received = 4.8 volume % monoclinic)				
900°C	5.0	16.0	9.3	3.2
1000°C	3.4	9.8	5.3	1.0
1100°C	4.0	1.4	11.1	24.1
1200°C	17.8	21.3	34.8	39.2
1300°C	34.0	34.4	37.5	47.0

* Estimated error is $\pm$ 5 volume %

ordered magnesium or yttrium zirconate phase. These phases would not necessarily have peaks in the same angular range in the diffractogram as the unordered phases. In this work, only the angular range between 25 and 35° 2θ was examined.

The critical time, t_c, can be defined as that time at 1000°C where the material would have transformed to 100% monoclinic. This time is ~4300 hours for material C, ~850 hours for material K, and <50 hours for material G. The times calculated for materials M and J were infinity. From this analysis, it is evident that the yttria stabilized materials are more resistant to phase change than are the magnesia stabilized materials.

The modulus of elasticity (MOE) of the coupon materials was determined by a pulse echo ultrasonic technique. The values are presented in Table 4, and the data is presented graphically in Figure 3. The MOE of a material is dependent on several factors, one of which is the porosity of the material. The density of the coupons changed with heat treatment, mainly due to a change in the volume. Microscopy showed that porosity was formed at the grain boundaries, as was another (unidentified) phase. There is also some evidence that the sonic MOE of pure single crystal monoclinic zirconia is greater than that of the tetragonal or cubic phase.* Thus, the behavior of the sonic MOE would be complicated, decreasing as the density decreases and increasing as the volume percent monoclinic phase increases. This

*Private communication with D. Lewis.

Table 4. SONIC MODULUS OF ELASTICITY OF HEAT TREATED COUPONS*

	MOE (GPa)			
	50 hr	100 hr	250 hr	500 hr
Material C (as-received = 227 GPa)				
900°C	206	206	206	202
1000°C	217	209	208	212
1100°C	214	202	204	163
1200°C	205	194	195	193
1300°C	-	173	159	135
Material G (as-received = 149 GPa)				
900°C	155	152	150	151
1000°C	174	168	161	156
1100°C	156	128	115	115
1200°C	124	96	106	-
1300°C	-	110	-	-
Material J (as-received = 189 GPa)				
900°C	186	185	182	184
1000°C	189	186	185	183
1100°C	188	184	185	185
1200°C	188	190	186	185
1300°C	-	197	186	199
Material K (as-received = 215 GPa)				
900°C	206	204	206	205
1000°C	209	207	205	207
1100°C	207	204	204	211
1200°C	203	190	195	183
1300°C	-	201	192	188
Material M (as-received = 198 GPa)				
900°C	206	207	199	205
1000°C	203	198	203	203
1100°C	198	202	199	204
1200°C	205	207	205	210
1300°C	-	212	214	216

* Estimated error is $\pm$ 2%

complicated behavior is seen both in Table 4 and in Figure 3, which show the sonic MOE of the five coupon materials as a function of time and temperature.

The micro-hardness of three of the as-received coupon materials was determined. These values were measured with a Vickers indenter using several different loads on a Leitz micro-hardness tester according to ASTM Standard E 384-73. The results are presented in Table 5. The hardest material of those examined was material M, while that with the lowest hardness was material C. As would be expected, the hardness of these materials decreases with increasing indentation load.

Table 5. HARDNESS OF SELECTED COUPON MATERIALS

	H_v (GPa)	H_v (GPa)	H_v (GPa)
Material	500 g load	1000 g load	2000 g load
C	10.55	10.29	9.78
J	11.02	10.07	9.82
M	13.84	13.05	12.82

One of the properties that was initially to be used as a measure of the degradation of the material with time-at-temperature was the fracture toughness measured by the indentation crack length technique.[1] As-received coupons were polished and indented using a Vickers indenter with loads ranging from 5 to 25 kg. The toughness of the magnesia stabilized materials, C, G, and K, could not be determined using this technique. The grain size of materials C and K was too large, and the crack patterns were poor and unmeasurable, even at very high loads (see Figure 4). Material G was too porous to use this technique, as was material J, the yttria stabilized FSZ. Material M, that with the smallest grain size, was the only material that gave measurable cracks with which to calculate the fracture toughness. Because the results on the as-received samples were so poor, the attempt to measure toughness by indentation crack length was abandoned.

Microstructural analysis was performed on the polished samples. The magnesia stabilized materials showed an increase in porosity with time-at-temperature, as well as the formation of another (unidentified) phase at the grain boundaries. The two yttria stabilized materials, M and J, showed little change after heat treatments. Figure 5 shows the microstructural changes that occurred in materials K and M with time-at-temperature. After the heat treatments and before the samples were polished, the surfaces of the coupons were examined optically. Figure 6 shows heat treated surfaces of several coupons. The texture seen on the surface is relief from the transformed monoclinic precipitates.

Chemical analysis was performed on selected coupons to determine the loss of the stabilizer from the heat treatments, as well as the impurities present. The results are presented in Table 6. The analysis shows few changes in chemistry with heat treatment except a loss of Mg in material K.

The testing of coupon materials indicated that the anticipated loss of density due to increased amount of monoclinic phase and change in the microstructure did indeed occur. Accordingly, the second part of the program, analysis of time-at-temperature effects on mechanical properties, was initiated.

ROOM TEMPERATURE TESTING OF BEND SPECIMENS

Billets of various commercial and developmental zirconia materials from manufacturers were obtained. Table 7 presents the materials and suppliers. Five of these materials were MgO stabilized TTZs, one was a MgO partially stabilized zirconia (PSZ), seven were yttria TZPs, one was a Y_2O_3 stabilized PSZ, and two were yttria fully stabilized zirconias (FSZ). One of the MgO stabilized materials, H, was a newer vintage of another of the MgO stabilized materials, G. Bend specimens, 52 × 3 × 2 mm, were machined from the billets. Properties, such as density, sonic MOE, phase content, etc. were determined on the bars.

Bars of eleven types of zirconia (A, D, E, H, I, L, O, P, Q, R, and S) were heat treated in a laboratory furnace in air at 1000°C for 100 or 500 hours. (The other materials were tested only in the as-received state due to the small number of specimens available.) The heat treatments consisted of a four hour heat to temperature, followed by a hold at temperature. The furnaces were allowed to cool naturally, which took approximately 16 hours. The bend specimens were supported on knife

1. LAWN, B.R., EVANS, A.G., and MARSHALL, D.B. *Elastic/Plastic Indentation Damage in Ceramics: The Median/Crack System.* J. Amer. Cer. Soc., v. 63, no. 9-10, 1980, p. 547-81.

Table 6. CHEMICAL ANALYSIS OF COUPONS*

	wt% Al			wt% Si			wt% Ti		
	AR**	500hr 1000°C	500hr 1000°C	AR	500hr 1000°C	500hr 1000°C	AR	500hr 1000°C	500hr 1000°C
Material									
C	0.15	0.06	0.01	0	0	0	0.07	0.07	0.07
G	0.11	0.17	0.19	0.06	0	0.04	0.04	1.87	0.04
J	0.36	0.42	0.49	0.43	0.44	0.44	0.05	0.06	0.06
K	0.09	0.07	0.12	0.02	0	0	0.04	0.04	0.04
M	0.54	0.69	0.95	0.72	0.68	0.67	0.09	0.11	0.10

	wt% Cr			wt% Fe			wt% Zn		
	AR**	500hr 1000°C	500hr 1000°C	AR	500hr 1000°C	500hr 1000°C	AR	500hr 1000°C	500hr 1000°C
Material									
C	0	0	0.01	0	0	0	0.04	0.05	0.02
G	0.03	0.01	0.01	0.01	0	0	0.04	0	0
J	0.01	0	0	0.02	0	0	0.02	0	0
K	0.02	0	0	0.01	0	0	0.02	0	0
M	0.08	0	0	0.01	0	0	0.03	0.05	0.03

	wt% Mg			wt% Ca			wt% Y		
	AR**	500hr 1000°C	500hr 1000°C	AR	500hr 1000°C	500hr 1000°C	AR	500hr 1000°C	500hr 1000°C
Material									
C	1.88	1.89	1.95	0.01	0.02	0.06	0.05	0.06	0.02
G	1.48	1.46	1.24	0.07	0	0.08	0.08	0.06	0.06
J	0.03	0.03	0.03	0.68	0.75	0.75	7.1	7.38	7.47
K	2.29	1.79	1.76	0.02	0.09	0.07	0.03	0.12	0.11
M	0.01	0.01	0.01	0.03	0.05	0.04	6.7	6.77	6.64

* Error is $\pm$ 0.05 wt%

** AR = as-received, 0 indicates none detected, - indicates not analyzed.

edges made of oxidized silicon carbide. Although the bend specimens did not stick to the knife edges (i.e., the zirconia did not react with the silicon carbide), care was taken to place the part of the bend specimen that was in contact with the knife edge outside of the inner span during flexural testing. A silicon carbide plate was above the specimens during the heat treatment to protect them against the possibility of falling debris from the insulating brick of the furnace.

After the heat treatments, the properties listed above were measured to determine the changes with time-at-temperature. Table 8 gives the density of the bend specimens, both as-received and after heat treatments. Figure 7 shows in graphical form the change in density of the materials with time-at-temperature. It is seen from the graph that the density of the magnesia stabilized materials decreases, while that of the yttria stabilized materials remains the same after heat treatment. The change in density of the magnesia stabilized materials is most likely linked to the change in phase content; i.e., the density decreases due to the spontaneous transformation of tetragonal precipitates to the monoclinic phase, which has a slightly lower density (5.826 g/cm^3 for pure ZrO_2) than does the tetragonal form (5.859 g/cm^3 for pure ZrO_2), as well as the formation of porosity at the grain boundaries (see Figure 5).

Table 7. MATERIALS USED FOR MECHANICAL PROPERTIES EVALUATION

Material	Code	Stabilizer	Supplier	Suppliers Designation
A	PSZ	Y_2O_3	AC Sparkplug	Sensor Material (1982)
B	TZP	Y_2O_3	Naval Research Labs	None (1982)
D	TTZ	MgO	Nilsen, USA	TS Grade (1982)
E	TTZ	MgO	Nilsen, USA	MS Grade (1982)
F	FSZ	Y_2O_3	Ceradyne	None (hot pressed) (1982)
G	TTZ	MgO	Coors Porcelain Co.	ZDM (1981)
H	TTZ	MgO	Coors Porcelain Co.	ZDM (1983)
I	TZP	Y_2O_3	Coors Porcelain Co.	TZP (1984)
J	FSZ	Y_2O_3	Coors Porcelain Co.	ZDY (1981)
L	PSZ	MgO	American Feldmuehle Corp.	ZT-35 (1982)
N	TZP	Y_2O_3	NGK Sparkplug	Unknown
O	TZP	Y_2O_3	NGK Sparkplug	Z-191 (1984)
P	TZP	Y_2O_3	Toshiba Ceramics Co.	Unknown (1983)
Q	TZP	Y_2O_3	Toray Co.	Unknown (hot pressed) (1983)
R	TZP	Y_2O_3	Toray Co.	Unknown (Sintered) (1983)
S	TTZ	MgO	Corning Glass Works	Zircoa 2120 (1982)

Table 8. DENSITY OF THE BEND BAR MATERIALS BEFORE AND AFTER HEAT TREATMENTS AT 1000°C*

Material	ρ (g/cm^3) As-Received	ρ (g/cm^3) 100 hr	ρ (g/cm^3) 500 hr
A	5.667(14)	5.628(25)	5.668(12)
B	5.774(20)	5.785(18)	5.763(20)
D	5.660(18)	5.643(11)	5.629(16)
E	5.646(16)	5.632(13)	5.553(22)
F	5.599(38)	-	-
G	5.294(13)	-	-
H	5.649(21)	5.548(12)	5.537(14)
I	5.939(38)	5.986(30)	5.979(7)
J	5.534(22)	-	-
L	5.506(14)	5.512(12)	5.450(11)
N	5.771(3)	-	-
O	5.770(9)	-	-
P	5.928(17)	5.937(22)	5.920(21)
Q	5.950(8)	5.943(9)	5.956(4)
R	5.897(9)	-	5.714(34)
S	5.576(88)	5.469(78)	5.472(94)

* All densities by physical measurements, except that of material N which was done by immersion.

The volume percent monoclinic phase of the sixteen zirconia materials before and after heat treatment is given in Table 9, and the change in monoclinic content with time-at-temperature for seven of the materials is presented in Figure 8. Material A, the yttria partially stabilized material, is the only material that has fairly constant monoclinic phase content. The others show substantial increases in monoclinic phase content. Interestingly, one of the materials that shows a large increase in monoclinic phase content is the sintered TZP materials from Toray, material R. The reason for this behavior is unknown. A more thorough study of TZP materials would need to be done to determine the causes of this phenomenon. Three of the four toughened zirconias, materials D, H and S, show an approximately linear increase of monoclinic phase. Material L, which was not initially toughened, showed a slight change after 100 hours, followed by a sharp increase in monoclinic content after 500 hours. Material E also showed a slight change followed by a large increase in monoclinic phase content. The interpretation in both cases is that materials D, H, and S were ideally aged as-received, and further heat treatment caused growth of the tetragonal precipitates beyond the critical size for spontaneous transformation. Material L, on the other hand, was not aged at all, Material E was not ideally aged, and the 100 hour heat treatment was not enough to cause the precipitates to grow to the critical size; the 500 hour heat treatment, however, was sufficient.

Table 9. MONOCLINIC PHASE CONTENT OF BEND SPECIMENS BEFORE AND AFTER HEAT TREATMENTS*

Material	Vol% Monoclinic As-Received	Vol% Monoclinic 100 hrs, 1000°C	Vol% Monoclinic 500 hrs, 1000°C
A	35.2	34.0	29.0
B	0	0	0
D	27.7	57.7	80.4
E	23.9	34.8	79.1
F	0	-	-
G	66.2	-	-
H	14.0	62.3	93.2
I	0	0	0
J	0	-	-
L	6.4	14.7	70.3
N	7.0	-	-
O	-	-	0
P	0	0	0
Q	0	0	0
R	3.8	-	61.1
S	35.9	69.6	76.0

* Estimated error is $\pm$ 5%

The sonic modulus of elasticity was measured on bend specimen materials before and after heat treatments (Table 10). Figures 9a and 9b show the changes in the sonic modulus as a function of time-at-temperature for eleven of the zirconia materials. It is seen that the bars exhibit less complicated behavior than the coupons did. In most cases, there was little change in the sonic modulus of the bend specimens with time-at-temperature, although that of a few materials did increase with heat treatment.

Chemical analysis was performed on pieces of the bend specimen materials to determine if any changes in chemistry, especially a loss of stabilizer, had occurred from the heat treatments. The results, presented in Table 11, show that there were no unexpected elements in the materials and that no changes occurred from the heat

Table 10. SONIC MODULUS OF ELASTICITY OF BEND SPECIMEN MATERIALS

Material	MOE(GPa)* As-Received	100 hrs, 1000°C	500 hrs, 1000°C
A	213	214	215
B	202	202	202
D	227	213	210
E	208	208	208
F	180	-	-
G	149	-	-
H	199	188	203
I	211	212	213
J	189	-	-
L	215	196	193
N	198	-	-
P	209	210	209
Q	215	214	213
R	213	-	218
S	194	197	203

* No standard deviations given as MOE was measured on only two samples of each material; estimated error is ± 2%

treatments. The amount of aluminum found in the as-received sample of material I is very high and probably incorrect. The yttria stabilized materials in general have a larger amount of silica than do the magnesia stabilized materials. This larger amount of silica could adversely affect the high temperature mechanical properties.

The microstructure of the bend specimens was examined before and after heat treatment. Figure 10 shows the microstructures of the as-received and heat treated samples. The photomicrographs at the top are unetched, while those at the bottom have been etched. The changes in microstructures were due to an increase in porosity, especially at the grain boundaries, and the formation of another phase at the grain boundaries. The changes observed in the microstructure of the bend specimens were not as severe as those of the coupons.

The micro-hardness of the bend specimens was measured before and after heat treatments, using a method described earlier in this section. The results are presented in Table 12 and Figure 11. From these it is seen that the hardness of magnesia stabilized TTZ materials as-received is about 9 GPa, while that of the yttria stabilized TZPs is about 11 GPa. The hardness of the TTZs decreases as a function of time-at-temperature, while that of the TZPs remains essentially constant.

The strength and toughness of these zirconia materials are two of the most important properties used as specifications by the engine designers. As the effect of time-at-temperature on the mechanical properties had not been determined, no conclusions could be drawn about the expected lifetime of components made of these materials; nor was the data available to engine designers to enable them to make design changes that would accommodate the lower strengths and toughnesses that the materials of the components would exhibit after long times at moderate temperature.

Since using the standard indentation crack length measurements technique had proven unfeasible when tried on the coupons, it was decided to use a new method[2] in

2. CHANTIKUL, P., ANSTIS, G.R., LAWN, B.R., and MARSHALL, D.B. *A Critical Evaluation of Indentation Techniques for Measuring Fracture Toughness: II.* J. Amer. Cer. Soc., v. 64, no. 9, 1981, p. 539-43.

Table 11. CHEMICAL ANALYSIS OF BEND SPECIMEN MATERIALS*

Material	wt% Al		wt% Si		wt% Ti	
	AR**	500 hr 1000°C	AR**	500 hr 1000°C	AR**	500 hr 1000°C
A	1.83	2.0	0.02	0	0.05	0.07
B	0.10	0.22	0.05	0.05	0.07	0.08
D	0.03	0	0	0.03	0.08	0.08
E	0.10	0.04	0.05	0.04	0.13	0.11
F	<0.01	-	0	-	0.08	-
G	0.05	-	0.02	-	0.04	-
H	0.05	0	0	0	0.04	0.04
I	0.68	0.18	0.09	0.09	0.08	0.09
J	0.36	-	0.43	-	0.05	-
L	0.03	0.03	0	0.04	0.04	0.04
N	0.54	-	0.72	-	0.09	-
O	0.43	0.44	0.52	0.34	0.03	0.03
P	0.10	0.08	0.17	0.10	0.04	0.04
Q	0.52	0.52	0	0	0.01	0.01
R	0.66	0.68	0.08	0	0.01	0.01
S	0.06	0.02	0.01	0	0.03	0.03

Material	wt% Cr		wt% Fe		wt% Zn	
	AR**	500 hr 1000°C	AR**	500 hr 1000°C	AR**	500hr 1000°C
A	0.02	0	0.06	0	0.06	0.04
B	0	0.01	0.07	0.08	-	-
D	0	0	0.04	0	0.08	0.07
E	0	0	0.08	0.05	-	-
F	0.01	-	0.02	-	0.03	-
G	0.01	-	0.02	-	0.02	-
H	0	0.01	0	0	0.0	0.02
I	0.02	0.01	0.03	0.07	-	-
J	0.01	-	0.02	-	0.02	-
L	0	0.01	0	0	0.01	0.03
N	0.01	-	0.01	-	0.03	-
O	0.01	0	0.16	0.08	0.17	-
P	0	0	0.10	0.08	-	-
Q	0	0	0.08	0.06	-	-
R	0	0	0.08	0.10	-	-
S	0.02	0	0.07	0	0.54	0.11

Material	wt% Mg		wt% Ca		wt% Y	
	AR**	500 hr 1000°C	AR**	500 hr 1000°C	AR**	500 hr 1000°C
A	0	0	0	0	6.1	6.1
B	0.02	0.01	0.05	0.03	6.5	6.4
D	1.98	1.95	0	0.01	0.04	0.01
E	1.94	1.86	0.04	0.02	0	0
F	0.01	-	0	-	11.1	-
G	1.55	-	0.01	-	0.06	-
H	1.71	1.71	0	0	0.01	0.01
I	0.01	0.01	0	0	4.2	4.4
J	0.03	-	0.68	-	7.1	-
L	2.09	2.11	0.02	0.02	0.03	0.02
N	0.01	-	0.03	-	6.7	-
O	0.01	0.01	0	0	4.0	4.2
P	0.01	0.01	0	0.05	4.3	4.0
Q	0.01	0.01	0	0	3.5	3.5
R	0.02	0.02	0.03	0.02	3.8	3.8
S	1.65	1.51	0.13	0.15	0.36	0.41

* Error is ± 0.05 wt %
** AR = as-received, o indicates none detected, - indicates not analyzed.

Table 12. VICKER'S HARDNESS OF BEND SPECIMEN MATERIALS BEFORE AND AFTER HEAT TREATMENTS

Material	H_v (GPa) 2000g load As-Received	H_v (GPa) 2000g load 100 hr, 1000°C	H_v (GPa) 2000g load 500 hr, 1000°C
A	10.71(16)	10.82(16)	10.89(16)
B	10.93(21)	11.02(14)	10.93(18)
D	9.12(28)	8.48(13)	8.67(8)
E	9.69(20)	8.81(34)	8.54(27)
F	*	-	-
G	*	-	-
H	8.99(13)	7.72(14)	7.37(16)
I	12.08(16)	12.13(10)	12.00(14)
J	*	-	-
L	9.32(15)	8.94(12)	7.51(17)
N	11.42(11)	-	-
O	-	-	-
P	11.56(15)	11.46(26)	11.63(13)
Q	12.55(19)	11.98(32)	12.31(8)
R	11.34(18)	-	10.11(12)
S	9.00(14)	8.28(11)	7.27(8)

* Unable to measure hardness as the sample spalled.

which the bend specimens are indented and then stressed to failure in four point loading. The toughness can then be calculated by:

$$K = n(E/H)^{1/8}(\sigma_f P^{1/3})^{3/4}$$

where P is the indentation load, E is the modulus of elasticity, H is the hardness, n is a dimensionless constant, and σ_f is the failure strength.

Each bend specimen was broken twice: once from a controlled identation flaw and once from the as-machined surface. The indentations were made at a load of P = 100 N in air, and were subsequently covered with a drop of silicon oil to minimize fatigue effects in the failure mechanics. The bending strengths, σ_f, were evaluated from the breaking loads using simple beam theory.

The results of the breaking tests for all bend specimens are given in Tables 13 and 14, and shown in Figures 12 and 13 as a function of time-at-temperature. In Figures 12 and 13, the individual data points represent mean values of measured strengths. It is clear from these figures that the different zirconias respond to heat treatment in different ways. Generally, the transformation toughened materials show a greater tendency to a degradation in the properties. Materials D, E, H, and S fall into this category. The results indicate that these magnesia stabilized materials become severely overaged with time-at-temperature. Material L, on the other hand, actually increases in strength for the first 100 hours exposure, and decreases thereafter. The interpretation in this instance is that this magnesia stabilized material had not been initially toughened; the heat treatment applied in the experiments thus takes the materials up to, and subsequently beyond, the fully aged state.

Table 13. FLEXURAL STRENGTH AND WEIBULL ANALYSIS OF BEND SPECIMEN MATERIALS*

Material	As-Received n	σ_f (MPa)	σ_o (MPa)	m	100 hrs, 1000°C n	σ_f (MPa)	σ_o (MPa)	m	500 hrs, 1000°C n	σ_f (MPa)	σ_o (MPa)	m
A	8	309	324	10.2	12	314	342	5.6	12	274	303	4.3
B	2	708	**	**	3	659	**	**	2	624	**	**
D	10	588	609	14.1	13	385	409	7.8	9	392	405	15.6
E	14	640	665	13.4	8	493	505	21.4	9	288	307	7.4
F	4	207	**	**	-	-	-	-	-	-	-	-
G	13	186	190	21.4	-	-	-	-	-	-	-	-
H	12	534	596	4.2	12	320	327	24.6	11	240	252	9.9
I	14	921	1010	4.5	15	920	1026	2.4	16	998	1154	2.9
J	10	242	250	16.0	-	-	-	-	-	-	-	-
L	10	445	483	5.9	13	592	624	9.5	12	314	328	11.4
N	5	758	827	13.5	-	-	-	-	-	-	-	-
O	-	-	-	-	-	-	-	-	-	-	-	-
P	9	518	544	10.2	8	560	597	7.5	7	457	488	6.8
Q	3	1159	**	**	-	-	-	-	3	237	**	**
R	1	954	**	**	-	-	-	-	2	212	**	**
S	20	511	543	7.7	15	312	324	13.6	11	327	341	11.6

* No standard deviations given, too few data points.
** No Weibull analysis done, too few data points.

Material A, the yttria partially stabilized zirconia, shows only a very small change in strength and toughness over the time range covered; this is also seen in the TZP materials, B, I and P. The apparent stability here is attributable to the fact that a considerably higher temperature is generally required to cause aging in yttria stabilized materials than in otherwise equivalent magnesia stabilized materials. However, materials Q and R show a dramatic decrease in the flexure strength, from ~1000 MPa as-received to 225 MPa after 500 hours at 1000°C. The reasons for the degradation of these TZP materials as opposed to the others is as yet unknown.

The heat treatment of magnesia stabilized zirconia for relatively short times at moderate temperatures leads to grain growth of metastable tetragonal precipitates and spontaneous transformation to the monoclinic phase. This results in a decrease in density due to the increase in monoclinic phase content, as well as changes in the microstructure. These changes lead to a degradation in the flexure strength. More importantly, the transformation of the tetragonal precipitates eliminates the main toughening mechanism in these materials, and thus reduces the toughness substantially.

Fracture surfaces of the bend specimens are shown in Figure 14. In most samples, the fracture origin was a processing defect or machining damage. No changes in the fracture origins was observed in those samples that had been heat treated. The origins in some samples, especially the TTZs which have very large grains, were almost impossible to determine.

Table 14. FRACTURE TOUGHNESS OF THE BEND SPECIMEN MATERIALS*

	As-Received			100 hr, 1000°C			500 hr, 1000°C		
Material	n	P (N)	K_{Ic} (MPa $m^{1/2}$)	n	P (N)	K_{Ic} (MPa $m^{1/2}$)	n	P (N)	K_{Ic} (MPa $m^{1/2}$)
A	-	-	-	-	-	-	8	20	4.10
	6	100	4.10	12	100	3.93	3	100	3.84
	-	-	-	-	-	-	2	150	3.80
	-	-	-	2	200	4.09	-	-	-
B	2	100	5.03	3	100	4.63	3	100	4.88
D	-	-	-	-	-	-	3	50	5.87
	4	100	7.88	12	100	6.52	4	100	6.06
	-	-	-	-	-	-	3	150	6.40
E	9	100	10.40	7	100	8.87	7	100	5.61
H	4	100	10.19	5	100	6.12	3	100	4.51
	4	150	10.69	6	150	6.23	3	150	5.32
	4	250	11.57	-	-	-	3	250	5.96
I	14	100	6.81	17	100	6.83	17	100	8.38
J	7	20	3.01	-	-	-	-	-	-
L	4	20	5.00	-	-	-	1	20	5.49
	5	50	5.31	-	-	-	-	-	-
	5	100	5.26	11	100	9.44	3	100	6.66
	4	150	5.08	-	-	-	3	150	6.90
	-	-	-	2	200	8.96	3	200	6.94
	-	-	-	-	-	-	2	250	7.22
O	-	-	-	-	-	-	2	100	8.68
P	1	100	8.19	-	-	-	-	-	-
	8	150	7.04	8	150	6.84	6	150	6.73
R	1	100	11.63	-	-	-	-	-	-
S	1	20	5.54	-	-	-	-	-	-
	-	-	-	1	30	4.53	-	-	-
	-	-	-	-	-	-	3	50	5.15
	8	100	8.73	3	100	5.36	3	100	5.58
	2	150	10.51	3	150	5.47	3	150	5.49

* No standard deviations given, too few data points

HIGH TEMPERATURE TESTING OF BEND SPECIMENS

Bend specimens were also tested in stepped temperature stress rupture (STSR) and stress rupture (SR).* The materials tested are listed in Table 15. The STSR tests were performed before the SR tests, as STSR is a rapid, easy method of determining whether the materials exhibit any sensitivity to a particular stress/temperature regime. Conventional SR was then performed to confirm the results. Due to the small number of furnaces available and large number of samples, the SR runs were terminated after 500 hours. Since only a small number of samples were available of each type of material, the analyses should be considered tentative.

*I would like to thank George Quinn of the Ceramics Research Division for some of the analyses of the STSR and SR data

Table 15. MATERIALS EXAMINED IN SR AND STSR

Material	Stabilizer	Manufacturer	Designation
A	Y_2O_3	AC Sparkplug	Sensor Material
D	MgO	Nilsen, USA	TS Grade
F	Y_2O_3	Ceradyne	Unknown
G	MgO	Coors Porcelain Co.	ZDM (1981)
H	MgO	Coors Porcelain Co.	ZDM (1983)
I	Y_2O_3	Coors Porcelain Co.	TZP
J	Y_2O_3	Coors Porcelain Co.	ZDY
L	MgO	American Feldmuehle	ZT-35
N	Y_2O_3	NGK Sparkplug	Unknown
S	MgO	Corning Glass Works	Zircoa 2120

The temperature range for the STSR runs for all nine materials studied was 800 to 1200°C. In STSR, the specimen is heated to the lower temperature, then the load is applied. After 24 hours, the temperature is rapidly increased 100°C without changing the load. The temperature is increased by 100°C after every 24 hour period until the specimen fails or the upper temperature limit is reached.[3] In SR, the load is applied after the specimen has been heated to a given temperature. Neither the temperature nor the load is changed until the specimen fails or the experiment is ended after a given time.

Figures 15a and 15j show the results of the STSR tests, while Table 16 gives the results of the SR. Material A, an yttria partially stabilized zirconia, exhibited a 35% strength loss between room temperature and 800°C as seen from the STSR results (Figure 15a). The load carrying capability at 1200°C was approximately a third of the room temperature capability. There was no evidence of slow crack growth in the specimens at temperatures up to 1200°C. Creep was observed in the specimens subjected to temperatures greater than 1100°C. The activation energy for the creep was determined to be 151 Kcal/mole from the SR experiments.

The MgO stabilized TTZ, material D, showed a strength loss of 32 to 49% between room temperature and 800°C (Figure 15b). This value agrees well with that given in Nilsen literature for this material. Static fatigue was found to be a significant problem at 1200°C; the failure is via creep fracture. The activation energy for creep was found to be 73 Kcal/mole from the SR experiments, a relatively low value, implying little resistance to creep.

Material F, an yttria fully stabilized zirconia, showed significant strength loss (~50%) at 800°C relative to the room temperature strength, 207 MPa (Figure 15c). Due to the small number of samples, there is insufficient data to draw any conclusions from the STSR tests, and no SR tests were performed.

The older vintage Coors magnesia stabilized material, G, showed a partial strength loss at 800°C of about 35% relative to the room temperature strength of

3. QUINN, G.D. and KATZ, R.N. *Stepped Temperature Stress-Rupture Testing of Silicon Based Ceramics*. J. Amer. Cer. Soc., v. 57, no. 11, 1978, p. 1057-58.

Table 16. RESULTS OF THE STRESS RUPTURE TESTS

Material	Stress (MPa)	Temperature (°C)	Time to Failure (hrs)	Strain (%)	Retained Strength* (MPa)
A	100	1000	>500	0.01	-
	100	1100	312.6**	3.13	-
	100	1200	1.6**	1.01	-
D	200	900	>500	0.04	400
	200	1000	>500	0.23	343
	200	1100	125.2**	1.03	-
	200	1200	26.4	0.96	-
F	No SR Done				
G	No SR Done				
H	200	900	>500	0	324
	200	1000	>500	0.58	221
	200	1100	73.5	1.60	-
I	175	1000	>500	0.66	5.77
	175	1100	(8.6 sec)	-	-
	175	1100	(2.8 sec)	-	-
	175	1200	(14.2 min)	-	-
	175	1200	(5.2 sec)	-	-
J	No SR done				
L	200	900	>500	0.09	561
	200	1000	>500	0.42	-
	200	1100	(4.8 min)	-	-
	200	1200	Failed on Loading	-	-
	200	1200	(9.0 min)	-	-
N	No SR Done				
S	200	1000	500	1.19	-
	200	1100	Failed on Loading		-
	200	1200	Failed on Loading		-

* Retained Strength was not measured on all samples.

** Did not fail; tripped microswitch and ended run.

186 MPa (Figure 15d). Static fatigue was found to be a problem at 1200°C with the failure mechanism being creep fracture. No SR tests were done on this material. The newer vintage, material H, showed a significant strength loss at 800°C of 50-60% of the room temperature value of 534 MPa (Figure 15e). Again, static fatigue was a problem at 1200°C with the failure mechanism being creep fracture. The SR tests revealed that creep is significant at 1000 and 1100°C and that it may occur at lower temperatures. The activation energy for creep was found to be 96 Kcal/mole.

Material I, the Coors TZP material, showed a loss in strength of ~60% compared to the room temperature strength of 921 MPa (Figure 15f). The load carrying capability of this material at 1200°C is approximately 20% of the room temperature capability. Approximately 0.7% creep was observed in the sample tested in SR at 175 MPa at 1000°C. Creep activation energy analysis from the SR data could not be done as there was insufficient data due to many of the samples breaking on loading or very shortly (seconds) after loading.

Material J, the Coors fully stabilized zirconia, showed 45% strength loss relative to the room temperature strength of 242 MPa (Figure 15g). Static fatigue

was a serious problem at any temperature above 800°C. No specimens survived more than one hour at 1000°C. No creep was observed at any temperature. No SR tests were performed.

The American Feldmuehle magnesia partially stabilized material, L, had a strength loss of 50% at 800°C relative to the room temperature value of 445 MPa (Figure 15h). However, the load carrying capability at 1200°C was almost 50% of the room temperature capability. Static fatigue was not found to be a problem, but creep was severe at 1200°C (all 1200°C tests ended when the bowed sample tripped the microswitch). Insufficient data was obtained from the SR tests to obtain the activation energy for creep.

The only Japanese TZP material examined in STSR and SR, material N, exhibited a strength loss of 49% relative to the room temperature strength of 779 MPa (Figure 15i). Static fatigue occurred at all temperatures between 800 and 1100°C. Slow crack growth was found at 1000°C. Creep was noted in specimens that reached 1000°C in STSR; this is somewhat lower in temperature than was found for the other zirconias. No SR tests were performed on this material.

Material S, a magnesia stabilized TTZ, showed a reduction of 53% in strength at 800°C relative to that at room temperature, 527 MPa (Figure 15j). Time dependent failure at 1100 and 1200°C due to creep fracture was observed. This material exhibited very poor resistance to creep at 1100 and 1200°C. Insufficient data was available to calculate the activation energy for creep.

In summary, all eleven zirconia materials tested exhibited a strength loss of about 40-60% from room temperature to 800°C. The STSR failures between 800 and 1200°C are due to two reasons: a reduction in fast fracture strength with temperature, or time dependent phenomena including creep fracture and slow crack growth. The specimens had very little strength at 1200°C, and all creep badly at that temperature. Some of the materials examined (such as N, F and J) may have no load carrying capability at 1200°C. No conclusions can be drawn from the yttria stabilized TZP materials. The magnesia stabilized TTZ materials (D, G, H, L and S) are resistant to static fatigue until 1100-1200°C, whereupon creep resistance is poor and failure via creep fracture occurs. Creep likely occurs as well at 1000°C in the magnesia stabilized materials.

ZIRCONIA TOUGHENED ALUMINA

Since there was strong evidence that magnesia stabilized zirconia was not stable at the expected operating temperature of the low-heat-rejection diesel and little was known about the response of yttria stabilized TZP materials to time-at-temperature, a project was undertaken at the University of Michigan to develop a candidate material with the good mechanical properties of zirconia that would be more resistant to degradation with heat treatment. The materials examined were zirconia toughened alumina (ZTA) consisting of zirconia/hafnia particles dispersed in an alumina/chromia matrix and zirconia toughened mullite (ZTM). Samples of these materials were sent to AMMRC for evaluation. The compositions of these materials are presented in Table 17. All four ZTA materials have 10 volume % dispersed phase, with the amount of chromia in the alumina being 10 or 20 mole %.

In the ZTA materials, the chromia was added to the alumina to reduce the thermal conductivity, while the hafnia was added to the zirconia to increase the stable

Table 17. COMPOSITIONS OF THE ZIRCONIA TOUGHENED ALUMINAS

Code	Mole% chromia in Aluminia	Mole% hafnia In Zirconia	Volume % dispersed Phase
U1	10	10	10
U2	10	20	10
U3	20	10	10
U4	20	20	10

transformation temperature. It was found that compositions with ~15 mole % chromia in the alumina and ~15 volume % dispersed phase had a thermal conductivity equivalent to toughened zirconia at temperatures of about 600 to 700°C.[4]

These six materials were machined into bend specimens and heat treated as were the TTZ and TZP materials in the earlier section. Due to the small number of samples supplied by the University of Michigan, only materials U1 and U4 were heat treated for 100 hours at 1000°C. Samples of all six materials were heat treated for 500 hours at 1000°C. Various properties were measured, both before and after the heat treatments. Table 18 gives the measured densities of the bend specimens. As would be expected, the density of the ZTA materials is much lower than that of the zirconia materials, ~4.3 g/cm^3 (the density of pure alumina is 3.97 g/cm^3), while the ZTM materials had a density of ~3.4 g/cm^3 (the density of pure mullite is ~3.2 g/cm^3). After heat treatment, the densities changed very little, with the maximum change of -0.5% being observed in material U6.

Table 18. DENSITIES OF THE ZTA AND ZTM MATERIALS BEFORE AND AFTER HEAT TREATMENTS

Sample	ρ (g/cm^3) As-Received	ρ (g/cm^3) 100 hrs, 1000°C	ρ (g/cm^3) 500 hrs, 1000°C
U1	4.328(16)	4.318(16)	4.321(26)
U2	4.367(37)	-	4.379(27)
U3	4.398(17)	-	4.408(10)
U4	4.296(15)	4.291(12)	4.290(4)
U5	3.390(48)	-	3.406(6)
U6	3.421(31)	-	3.403(29)

The phase content of these materials was examined to determine if there was any change upon heat treatment. The ZTA materials, U1 through U4, consisted of alumina/chromia solid solution and monoclinic zirconia. The two zirconia toughened mullite materials, U5 and U6, consisted of mullite and monoclinic zirconia. Zircon was found in the heat treated U5 material as well as in both the as-received and heat treated U6 material. Zircon is formed from the reaction of the zirconia with the silica in the mullite, leaving free alumina.

4. TIEN, T.Y. *Transformation Toughened Ceramics - A Potential Material for Light Diesel Engine Applications* Final Report, AMMRC Contract DAAG46-82-C-0080, AMMRC DOE Interagency Agreement EC-76-A-1707-002, AMMRC TR 84-26, 1984.

The sonic modulus of elasticity of the ZTA and ZTM samples was determined as described in an earlier section. The results of the tests are given in Table 19. The results of the MOE tests for materials U2 and U3 were anomalous. The MOE values of the as-received samples fell into two distinct populations, one with a high MOE (~350 GPa) and one with a low MOE (~245 GPa). The heat treated samples also exhibited MOEs that fell into two populations; the high MOE (~350 GPa) was the same as that of the as-received samples, but the low MOE value was substantially greater (~320 GPa) than that of the as-received value. No reason for this behavior could be found when the density and phase content were examined. However, when photomicrographs of the samples were examined, it was seen that the microstructures of the high and low MOE samples differed only slightly (see Figure 16). The difference in the microstructure of the U2 as-received and 500 hour at 1000°C heat treated samples is much more pronounced, but these two samples had essentially the same sonic modulus of elasticity. The reasons for the effects of the microstructure on the sonic MOE are unknown.

Table 19. SONIC MODULUS OF THE ZIRCONIA TOUGHENED ALUMINA AND MULLITE

Material	AR		100 hr, 1000°C		500 hr, 1000°C	
	n	MOE (GPa)	n	MOE (GPa)	n	MOE (GPa)
U1	10	363(2)	4	364(1)	4	363(1)
U2 hi	7	351(2)		-	3	350(0)
med		-		-	1	322
low	7	241(9)		-		-
U3 hi	8	352(2)		-	2	350(4)
med		-		-	2	324(2)
low	5	248(9)		-		-
U4	7	361(1)	2	263(3)	4	362(1)
U5	2	182(16)		-	4	175(1)
U6	2	169(5)		-	4	158(8)

Chemical analysis results of the zirconia toughened materials are presented in Table 20. As was expected, the major constituents of the materials were alumina, chromia, and silica. Any other element was found only in trace amounts.

The microstructure of the ZTA and ZTM materials was examined by optical microscopy. Figure 16 shows, as in Figure 10, photomicrographs of polished and etched samples, respectively. In the polished, unetched micrographs of materials U1 through U4, the dark grey or black areas are porosity, the medium grey is alumina, and the light grey is zirconia. The microstructures of the U5 and U6 samples are very difficult to determine. The polished surfaces were very reflective under the optical microscope.

The Vicker's hardness of the ZTA and ZTM materials was measured. The results are presented in Table 21. The value reported is the average of ten hits on each sample. Because of the few samples available, the U2 and U3 samples with low, medium and high MOE could not all be measured. The samples that spalled did so even at 100 g load.

The flexural strength and fracture toughness of the ZTA and ZTM materials was measured as-received and after heat treatment of 100 or 500 hours at 1000°C, just as the TTZ and TZP materials. The results are reported in Table 22. These values in

Table 20. CHEMICAL ANALYSIS OF THE ZIRCONIA TOUGHENED ALUMINA AND MULLITE

	wt% Al			wt% Si			wt% Ti		
	AR	100hr 1000°C	500hr 1000°C	AR	100 hr 1000°C	500 hr 1000°C	AR	100hr 1000°C	500hr 1000°C
U1	38.0	38.0	38.0	0.13	0.12	0.12	0.09	0.03	0.02
U2	34.2	-	35.2	0.11	-	0.10	0.01	-	0.01
U3	35.9	-	34.6	0.11	-	0.10	0.01	-	0.01
U4	40.3	38.6	39.6	0.11	0.13	0.11	0.01	0.01	0.01
U5	26.2	-	26.4	10.1	-	10.2	0.01	-	0.02
U6	22.2	-	22.3	10.3	-	10.4	0.01	-	0.01

	wt% Cr			wt% Fe			wt% Zr		
	AR	100hr 1000°C	500hr 1000°C	AR	100 hr 1000°C	500 hr 1000°C	AR	100hr 1000°C	500hr 1000°C
U1	7.5	7.3	7.5	0.15	0.10	0.02	6.9	6.8	6.9
U2	14.3	-	14.9	0.05	-	0.03	7.4	-	7.8
U3	14.9	-	14.4	0.01	-	0.03	7.9	-	7.4
U4	7.8	7.9	7.9	0.06	0.07	0.07	7.9	7.7	8.2
U5	0	-	0.03	0.01	-	0.03	14.2	-	14.2
U6	5.0	-	5.0	0.16	-	0.09	13.8	-	13.9

	wt% Mg			wt% Ca			wt% Y		
	AR	100hr 1000°C	500hr 1000°C	AR	100 hr 1000°C	500 hr 1000°C	AR	100hr 1000°C	500hr 1000°C
U1	0.02	0.02	0.01	0.05	0.05	0.03	0.03	0	0
U2	0.01	-	0.01	0.04	-	0.03	0	-	0
U3	0.01	-	0.01	0.02	-	0.02	0	-	0
U4	0.02	0.02	0.02	0.02	0.03	0.03	0	0	0
U5	0.01	-	0.01	0.03	-	0	0	-	0
U6	0.01	-	0.01	0	-	0	0	-	0

Table 21. VICKER'S HARDNESS OF THE ZTA AND ZTM MATERIALS

	H_v (GPa) 2000g Load		
Material	As-Received	100 hr, 1000°C	500 hr, 1000°C
U1	16.64(67)	16.09(33)	15.97(53)
U2 hi	15.97(34)	-	Spalled
U2 low	Spalled	-	-
U3 hi	Spalled	-	13.95(40)
U3 med	-	-	13.82(40)
U4	15.95(41)	15.51(41)	15.96(36)
U5	9.15(20)	-	8.13(22)
U6	6.26(18)	-	6.68(33)

most cases represent averaged values of several specimens, although in a few cases only one value was obtained. Due to the small number of specimens, not all properties were determined for each composition and no standard deviations will be presented. The ZTA materials with a high sonic MOE have an as-received flexure strength of ~425 MPa; this strength does not seem to decrease with time-at-temperature. The as-received fracture toughness of the ZTA materials is ~4.9 MPa $m^{1/2}$, which decreases slightly after 500 hours at 1000°C. The U2 and U3 samples with the medium and low MOE also had a lower strength and toughness than did those with the high MOE.

Table 22. FLEXURE STRENGTH AND FRACTURE TOUGHNESS OF THE ZTA AND ATM MATERIALS*

Material	As-Received σ_f (MPa)	As-Received K_{Ic}** (MPa $m^{1/2}$)	100 hr, 1000°C σ_f (MPa)	100 hr, 1000°C K_{Ic} (MPa $m^{1/2}$)	500 hr, 1000°C σ_f (MPa)	500 hr, 1000°C K_{Ic} (MPa $m^{1/2}$)
U1	436	4.86	371	4.85	450	4.56
U2 hi	457	4.97	-	-	410	4.93
U2 med	-	-	-	-	286	-
U2 low	122	3.52	-	-	-	-
U3 hi	386	4.98	-	-	413	3.94
U3 med	-	-	-	-	373	3.47
U3 low	-	-	-	-	-	-
U4	-	5.29	398	4.95	456	4.70
U5	260	-	-	-	296	-
U6	282	-	-	-	292	-

* No standard deviations reported, too few data.
** Fracture toughness measured via indentation strength technique, 100 N load.

The high temperature STSR and SR tests were performed on the ZTA materials. The bend specimens of the ZTM materials were too short to use with the available fixtures, so no results are available for these. The results of the STSR tests are shown in Figures 17a through 17d, and Table 23 gives the SR results.

Table 23. STRESS RUPTURE RESULTS OF THE ZTA MATERIALS

Material	Stress (MPa)	Temperature (°C)	Time to Failure (hrs)	Strain (%)	Retained Strength* (MPa)
U1	100	900	>500	<<0.05	511
	100	1000	>500	0.16	325
	100	1100	>500	0.45	258
	100	1200	127*	1.69	223
U2 hi	150	1100	262	0.68	-
hi	150	1200	0.9	0.43	-
low	150	900	(1 min)	<<0.05	-
U3 hi	100	900	on loading	<<0.05	-
low	75	1000	>500	0.32	-
hi	75	1000	>500	0.17	331
U4	100	900	>500	<<0.05	431
	100	1000	>500	0.08	380
	100	1100	>500	0.55	270
	100	1200	1/5	0.69	-

* Sample did not fail. Microswitch tripped and ended run.

The fast fracture strength of material U1 at 800°C (~200 MPa) is less than half that at room temperature (436 MPa); no samples survived 24 hours at 1200°C. The SR samples, loaded to 100 MPa, all survived 500 hours, except that one tested at 1200°C. This latter sample might have survived 500 hours, but the creep at 1200°C was severe enough to cause the microswitch to trip and end the run after 127 hours. The activation energy for creep calculated from the SR tests was 42.4 Kcal/mole, a low value, implying very low resistance to creep. The retained strengths of the samples were all good. Interestingly, the retained strength of the SR sample tested at 900°C (511 MPa) was higher than the average of the as-received samples.

The U2 STSR samples with low sonic MOE had essentially no strength at 800°C. Those with high sonic MOE performed better; the strength at 800°C was about 250 MPa. Two high MOE samples, loaded to 150 MPa, were tested in SR; one at 1100°C and one at 1200°C. The creep activation energy calculated from these two samples is very high (207 Kcal/mole), and probably is not accurate. One low MOE sample survived 1 minute at 900°C when loaded to 150 MPa.

The high MOE samples of material U3 did not perform as well as the high MOE samples of material U2, but the U3 low MOE samples did better than those of U2. One low MOE sample of the U3 material, loaded to 75 MPa, survived to 1200°C; the rest failed on loading at 800°C. Two U3 samples, one low MOE and one high MOE, both loaded to 75 MPa, survived 500 hours in SR. The high MOE sample had retained strength of 331 MPa, which is almost as good as the as-received value. Due to the small number of samples, no creep activation energy could be calculated.

Material U4 performed much like U1 in STSR, with the fast fracture strength at 800°C being approximately 40% of the estimated as-received strength. No samples survived 24 hours at 1200°C. The SR samples were loaded to 100 MPa and tested at 900, 1000, 1100 and 1200°C. The three specimens tested at the lower temperatures all survived 500 hours, while the last failed after 1.5 hours at 1200°C. The calculated creep activation energy was 99 Kcal/mole. The retained strengths were all good.

In summary, the density, failure strength, fracture toughness, and sonic modulus of elasticity of the ZTA materials remain essentially constant with time-at-temperature. No conclusions can be drawn about the ZTM material due to the small number of samples provided, but indications are that this material is not as good as the ZTA material. The strengths of the ZTA materials with high sonic moduli after 500 hours at 1000°C are as good or better than those of magnesia stabilized TTZ after the same heat treatment, although the fracture toughnesses are slightly lower. The anomalous behavior of the ZTA specimens containing 20 mole % chromia has yet to be explained. These preliminary results on ZTA materials are encouraging and indicate that this material is a good possible candidate for diesel engine applications.

CONCLUSIONS

Examination of the effects of time-at-temperature on toughened oxide ceramics for heat engine applications has shown that, although the materials have great potential for use in the engine, several problems need to be overcome. Magnesia stabilized TTZ materials exhibit very good as-received mechanical properties. Exposure to the moderate temperatures as are expected in the low-heat-loss diesel for relatively short times causes changes in the microstructure with resulting degradation of mechanical properties. The changes are due to the spontaneous transformation of tetragonal precipitates as they reach a critical size from grain growth. The evidence for this conclusion is the increasing amount of monoclinic phase in the material with heat treatment. The strength and toughness of the magnesia stabilized TTZs after 500 hours (less than 10% of the expected lifetime of the engine) at 1000°C are reduced by one-third to one-half of the as-received values. The results of the SR and STSR show that these magnesia stabilized materials are resistant to static fatigue up to ~1100°C and that the creep resistance of these materials is low at higher temperatures.

The little data available on yttria stabilized materials indicates that these materials should be more resistant to the degradation of mechanical properties with time-at-temperature. The STSR results on the one TZP material studied, material N, were not encouraging. However, this material contains about 2 weight % silica, which is likely the cause of the poor high temperature properties. Preliminary results on other TZP materials indicate that the high temperature properties are much improved when the material contains little or no silica. Interestingly enough, the yttria stabilized PSZ, an oxygen sensor material, retained its strength and toughness throughout the heat treatments, and, after 500 hours at 1000°C, had as good or better properties than did the magnesia stabilized TTZ materials examined after the same heat treatment.

The preliminary results on the ZTA materials developed at the University of Michigan show that this material has a good potential for use in the diesel engines. Although the as-received strength is lower than that of the magnesia stabilized TTZs, they, like material A, retained their strength and toughness after heat treatment. As this material is still in early development, it would be expected that the mechanical properties will be improved by improved processing.

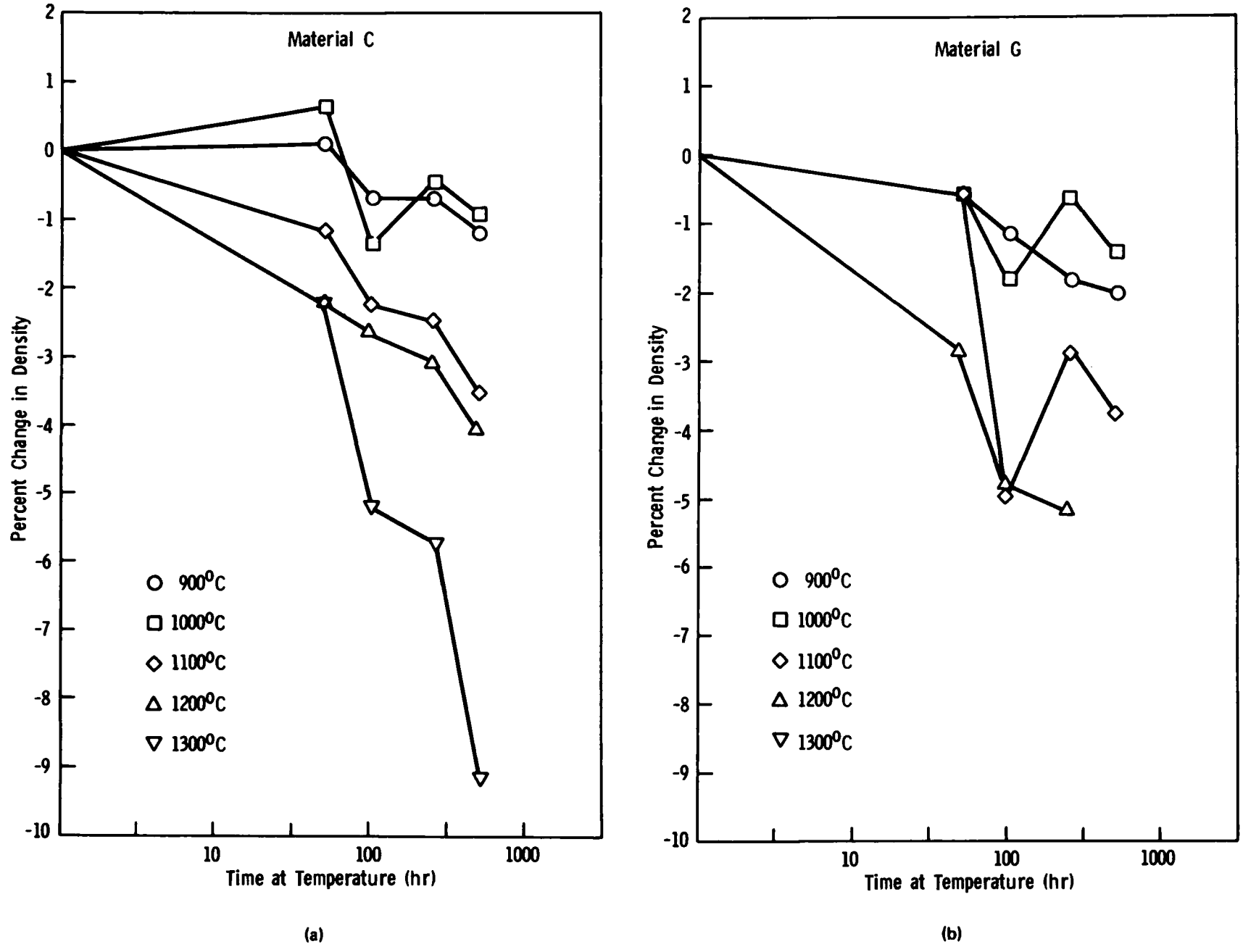
Material C
Material G
Percent Change in Density
Time at Temperature (hr)
900°C
1000°C
1100°C
1200°C
1300°C
2
1
0
-1
-2
-3
-4
-5
-6
-7
-8
-9
-10
10
100
1000
(a)
(b)

Figure 1.

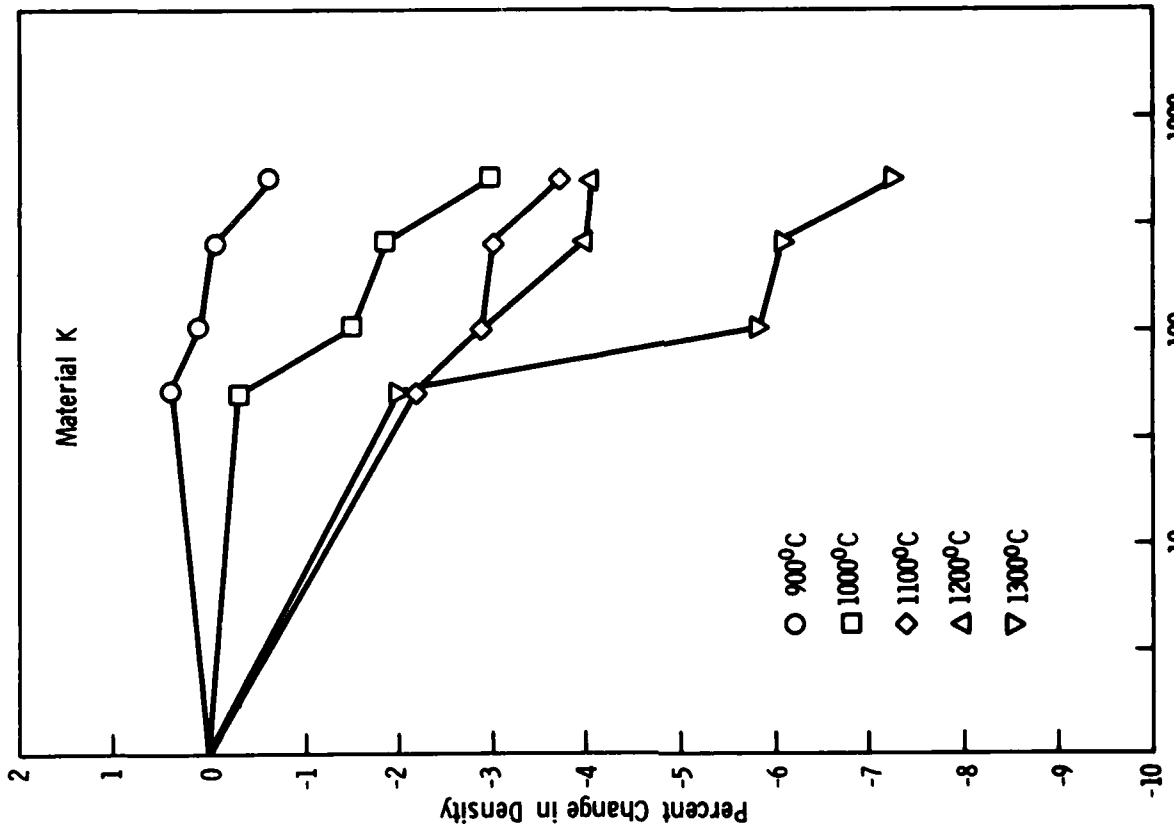

(d)

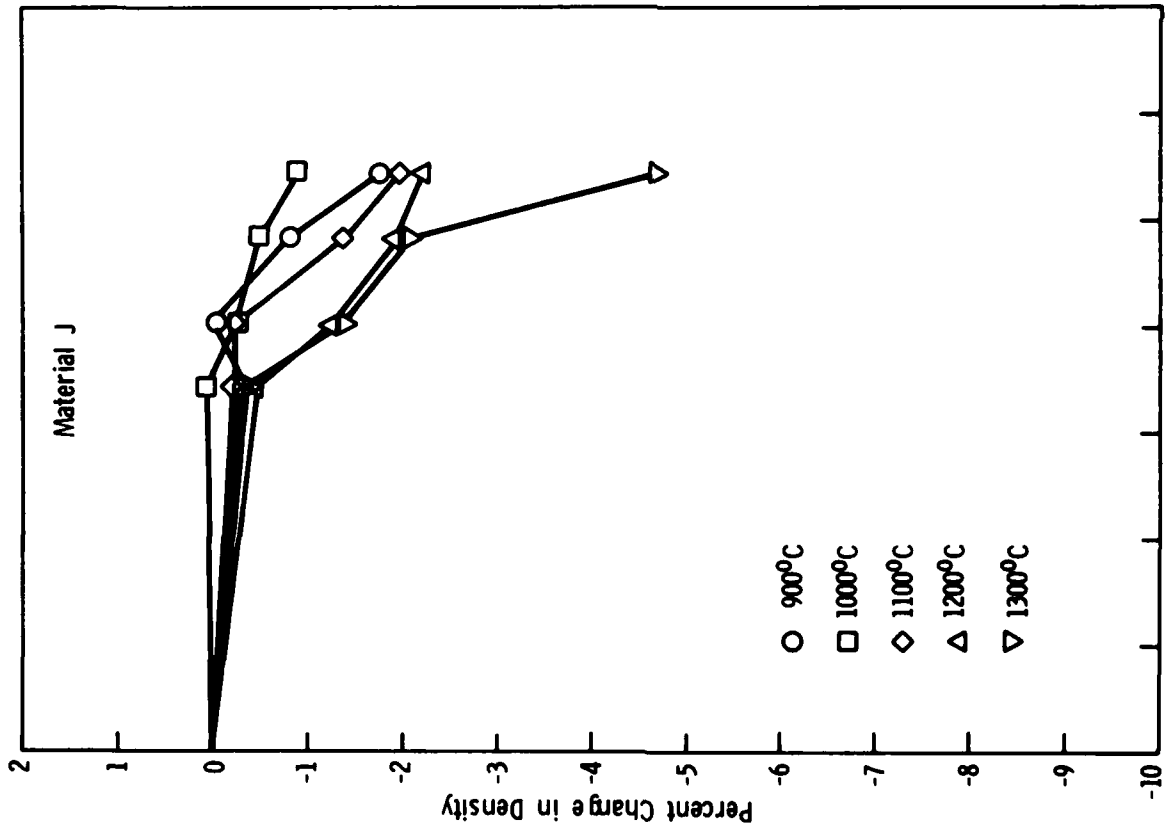

(c)

Figure 1. (cont'd)

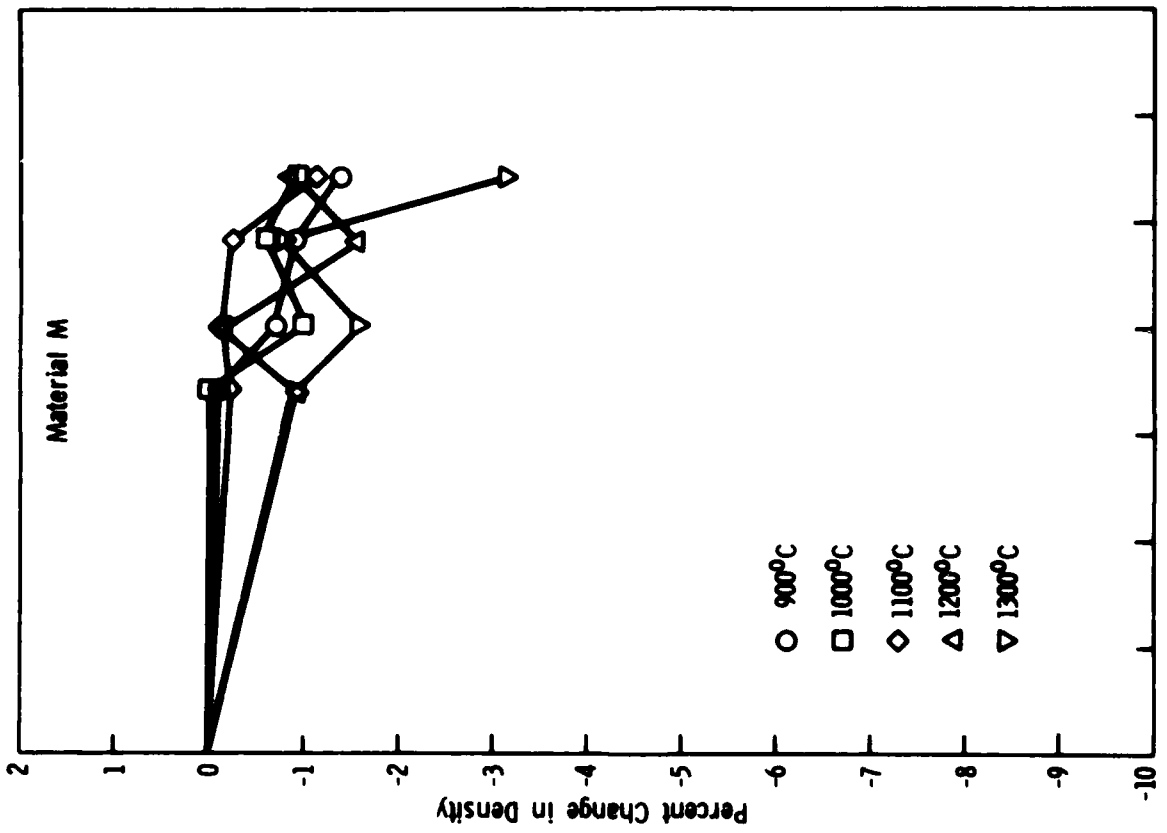

(e)

Figure 1. (cont'd)

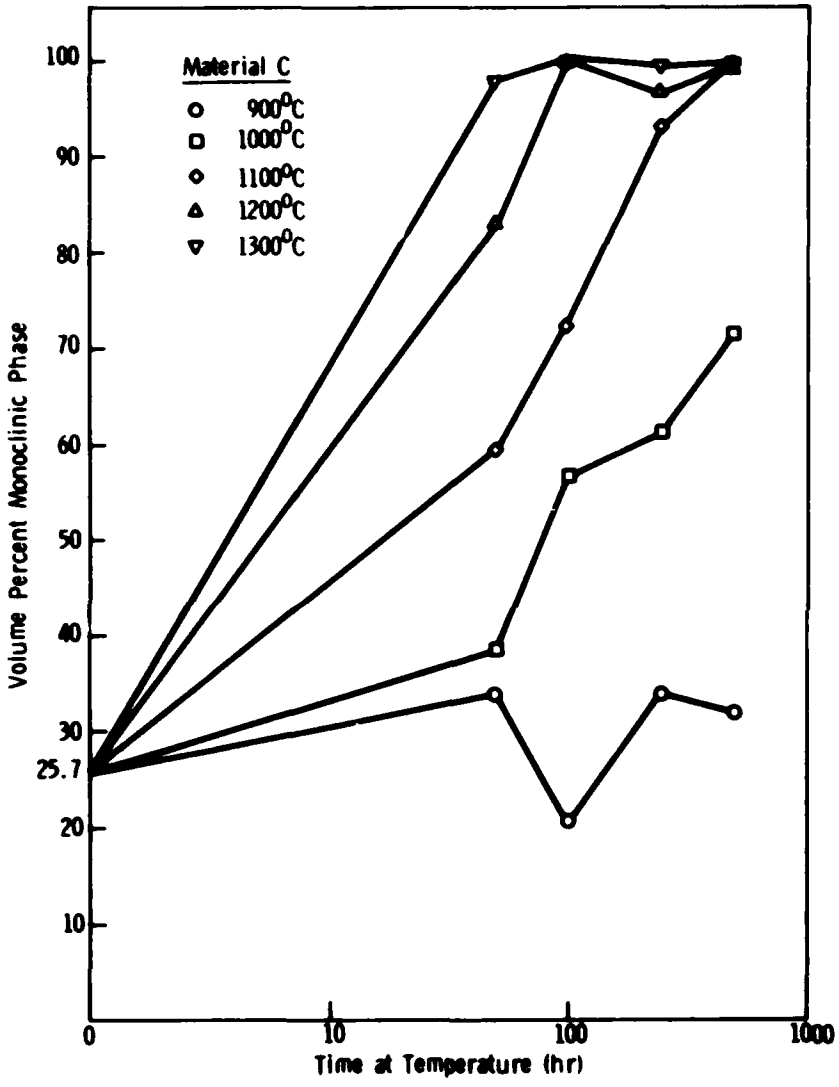
Material C
900°C
1000°C
1100°C
1200°C
1300°C
Volume Percent Monoclinic Phase
100
90
80
70
60
50
40
30
25.7
20
10
0
10
100
1000
Time at Temperature (hr)

(a)

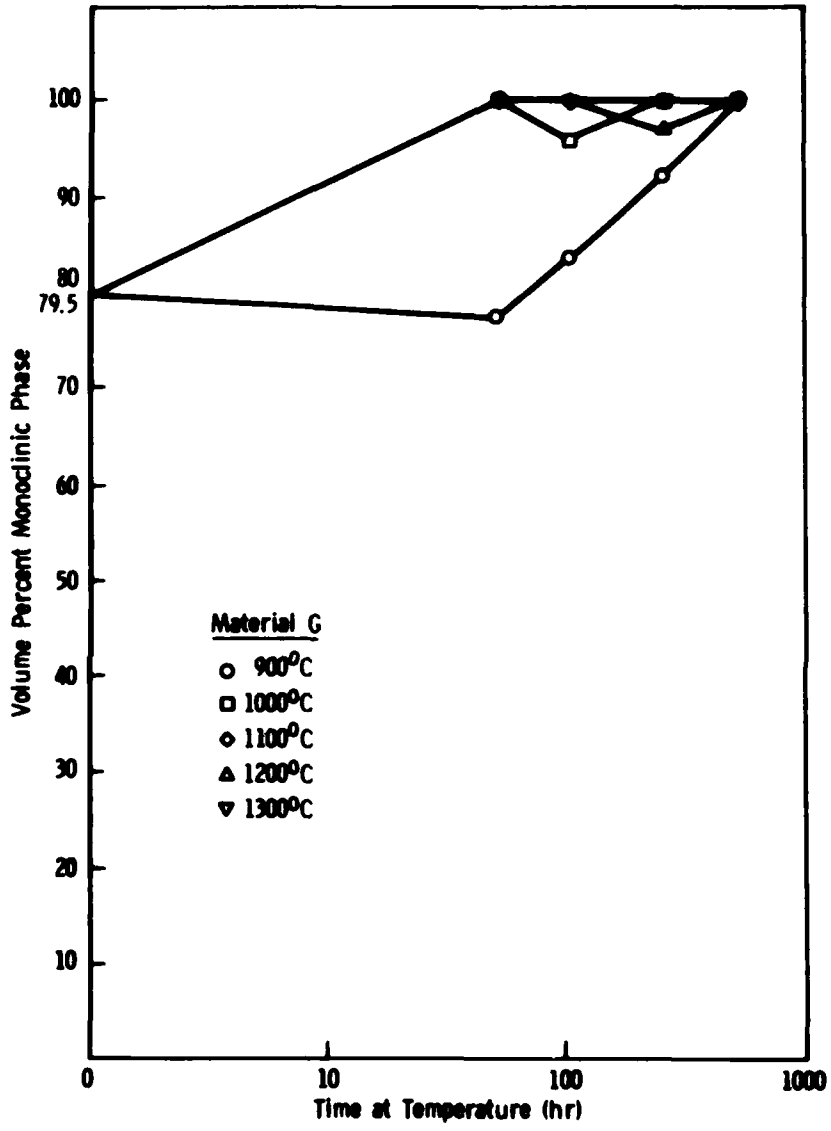
Material G
900°C
1000°C
1100°C
1200°C
1300°C
Volume Percent Monoclinic Phase
100
90
80
79.5
70
60
50
40
30
20
10
0
10
100
1000
Time at Temperature (hr)

(b)

Figure 2.

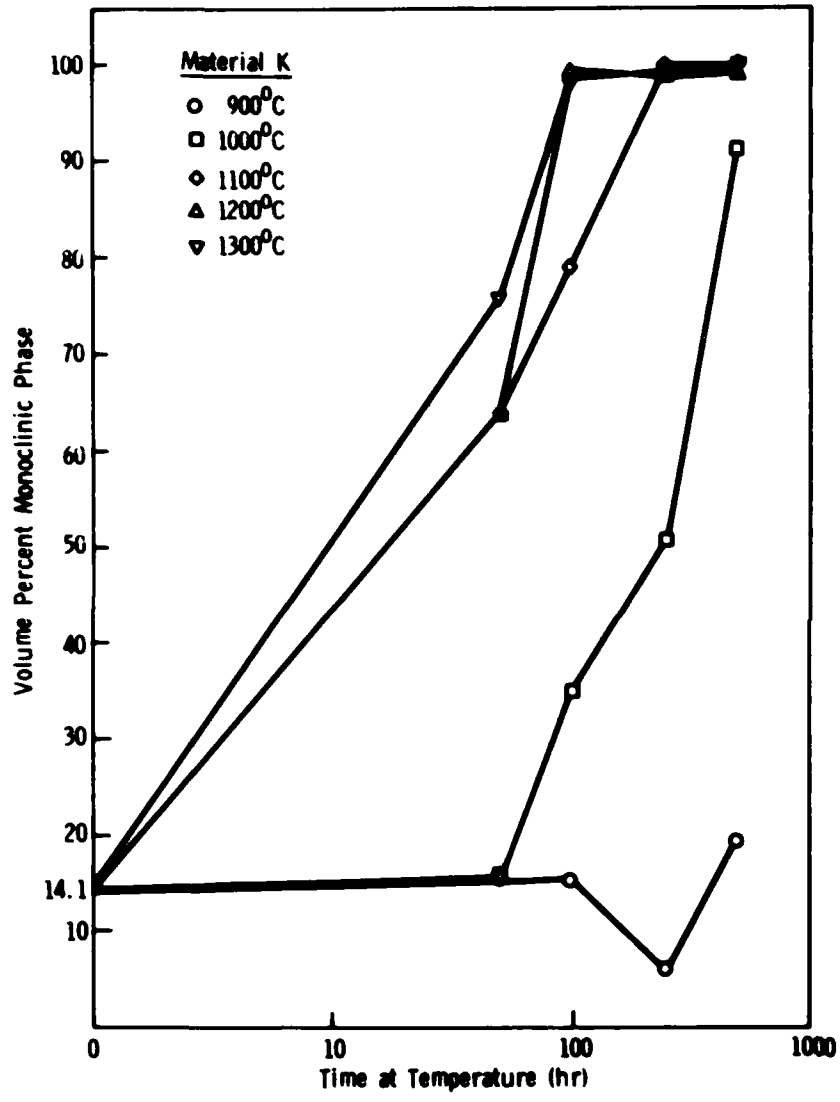

(c)

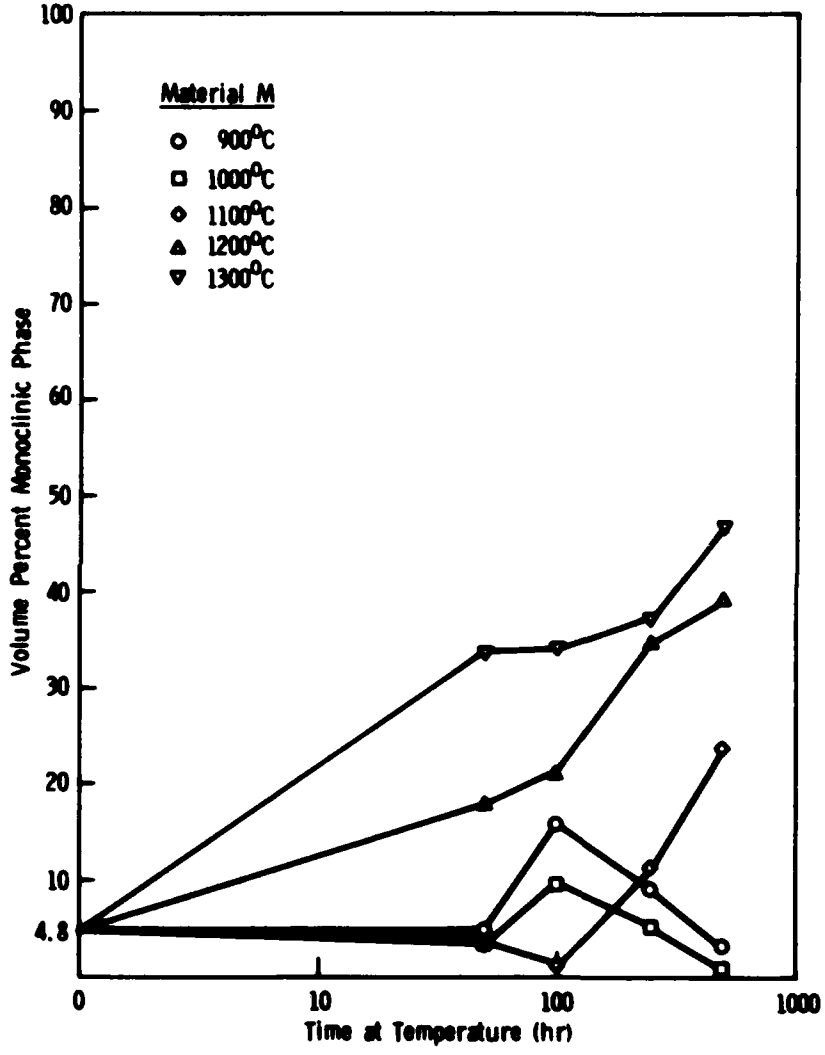

(d)

Figure 2. (cont'd)

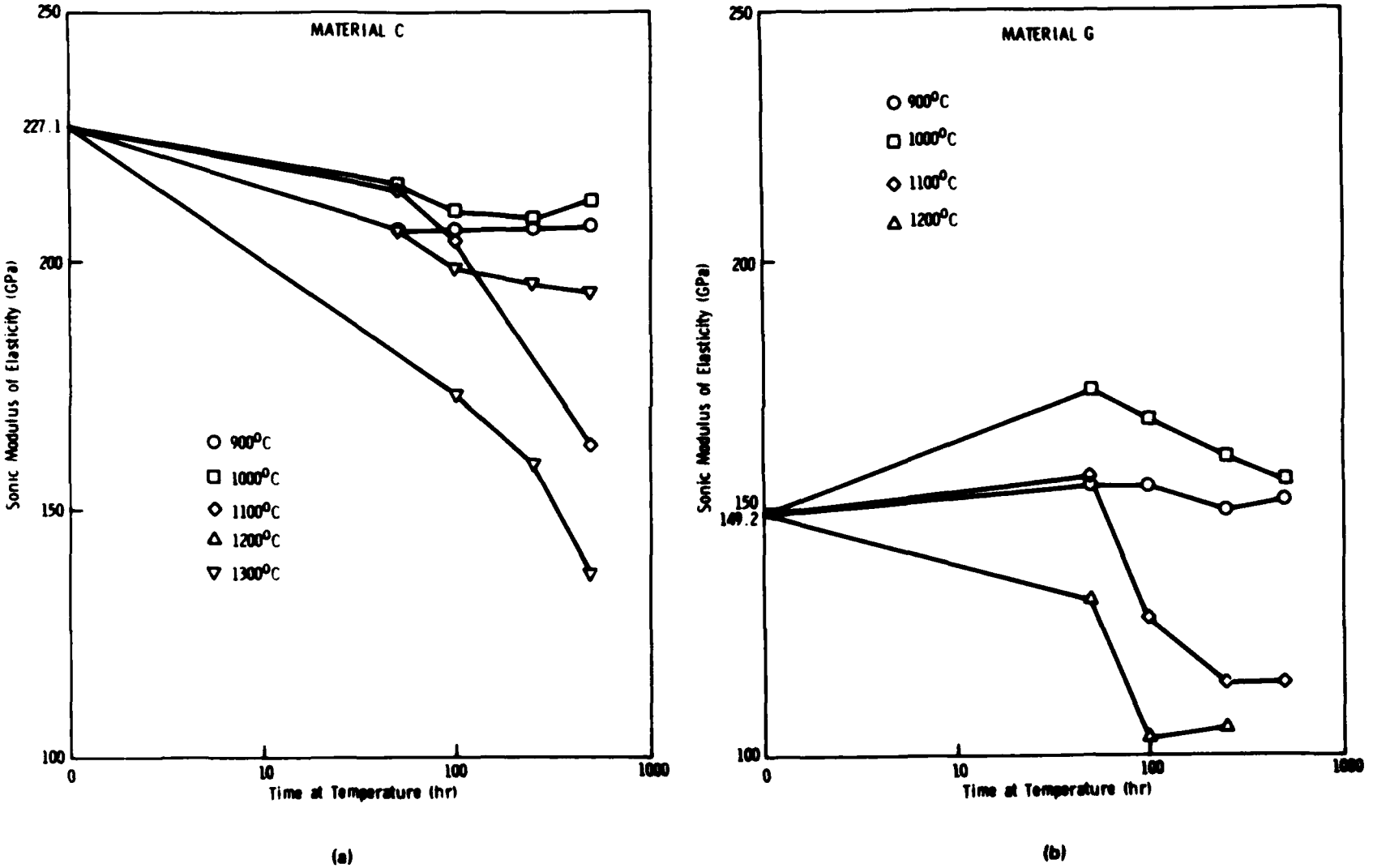
MATERIAL C
250
227.1
200
150
100
Sonic Modulus of Elasticity (GPa)
900°C
1000°C
1100°C
1200°C
1300°C
0
10
100
1000
Time at Temperature (hr)
(a)
MATERIAL G
250
200
150
149.2
100
Sonic Modulus of Elasticity (GPa)
900°C
1000°C
1100°C
1200°C
0
10
100
1000
Time at Temperature (hr)
(b)

Figure 3.

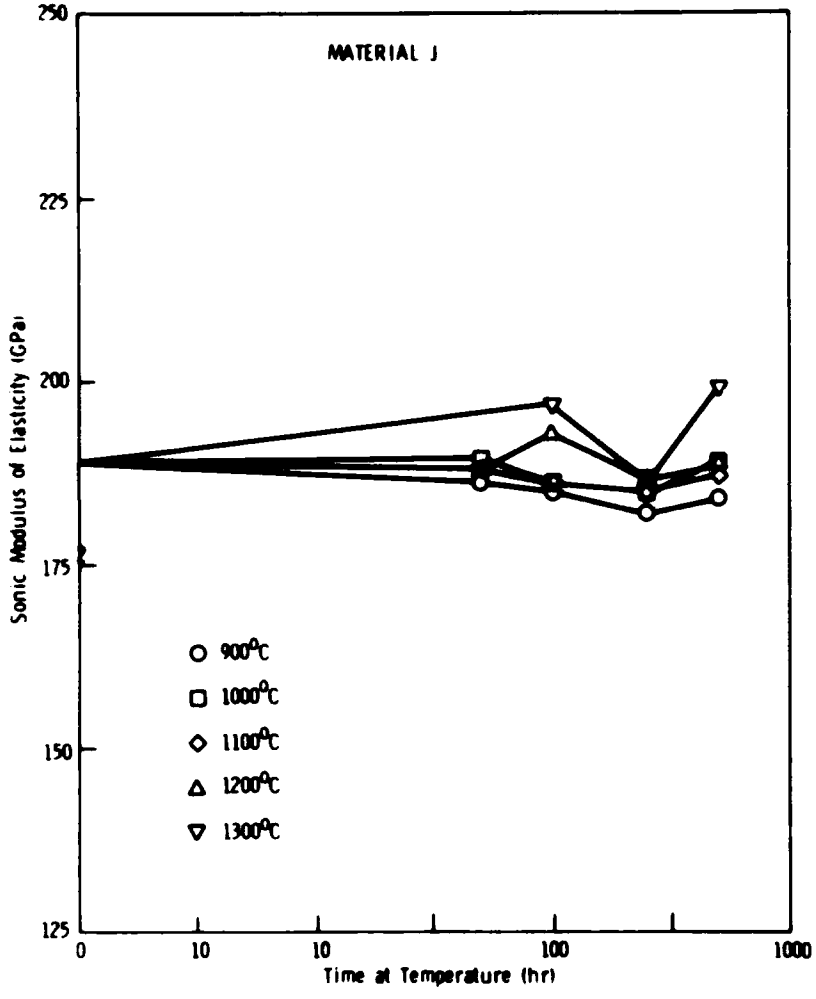

(c)

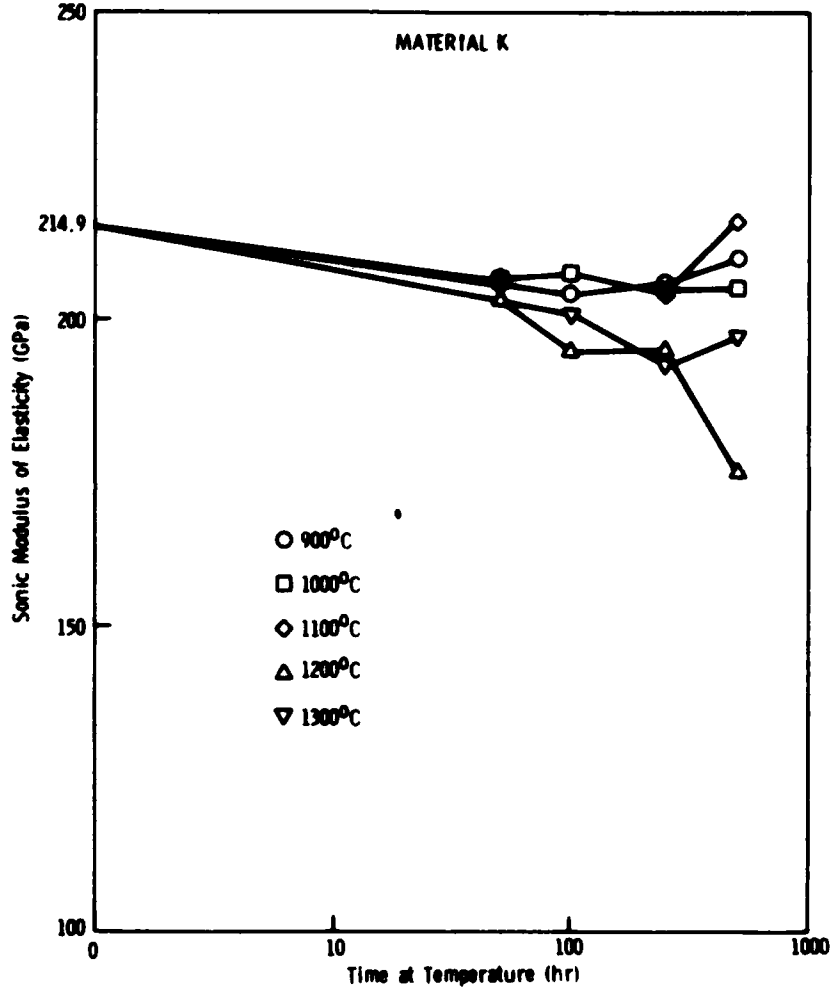

(d)

Figure 3. (cont'd)

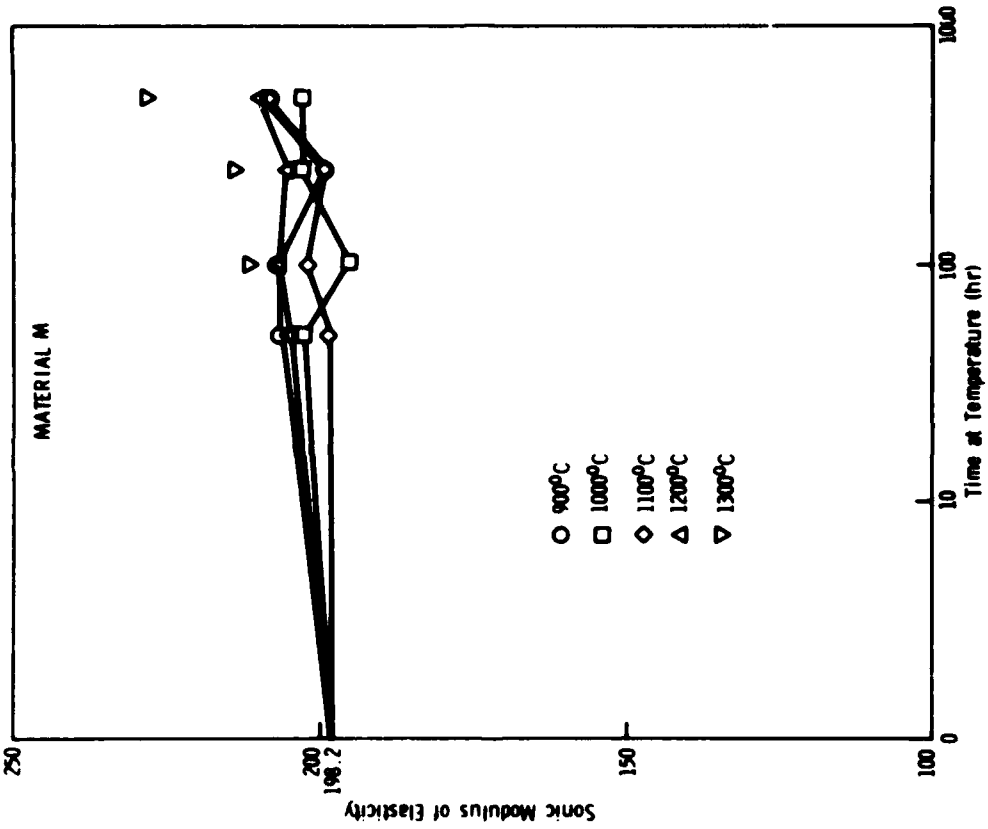

(e)

Figure 3. (cont'd)

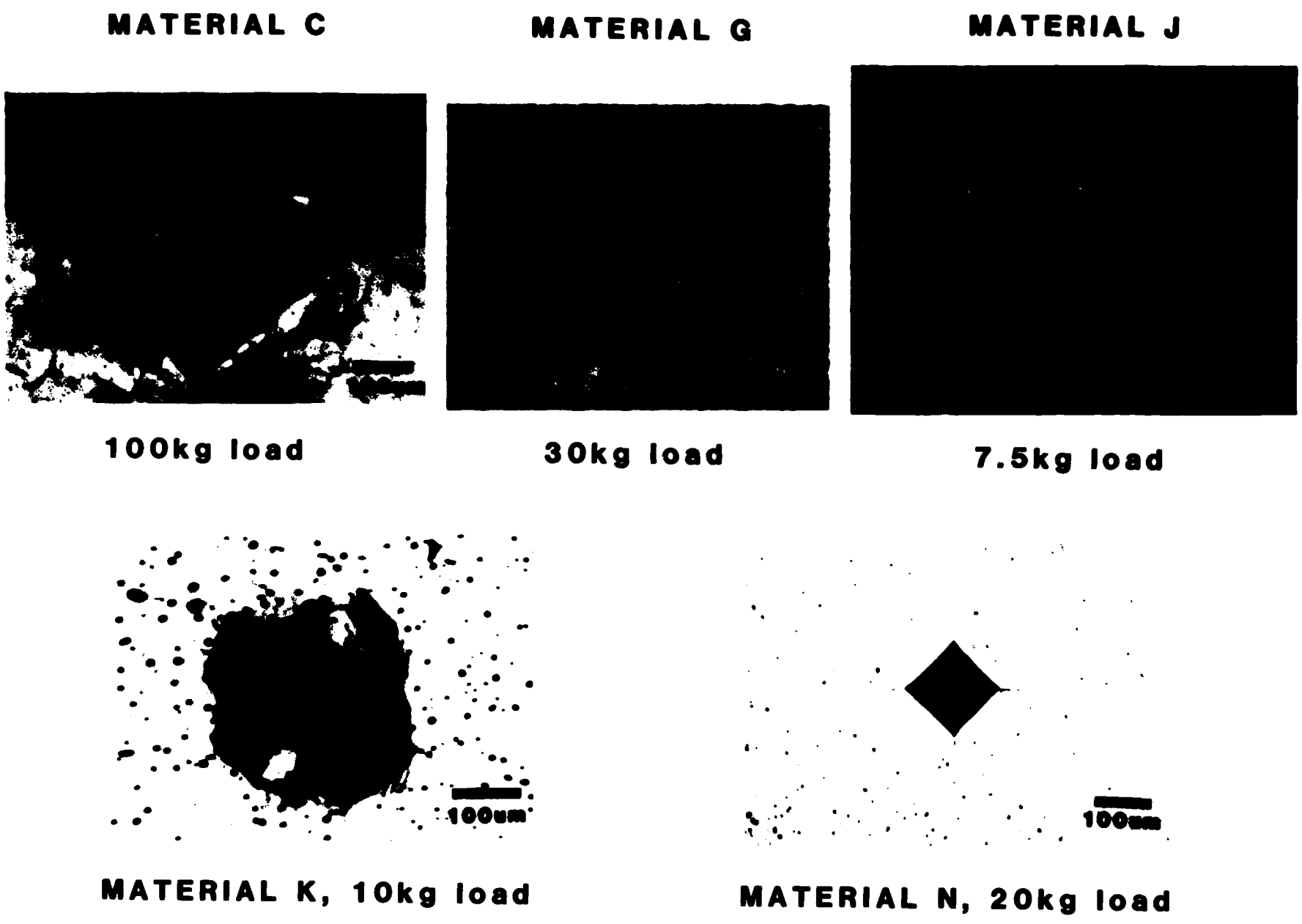
MATERIAL C
MATERIAL G
MATERIAL J
100kg load
30kg load
7.5kg load
100um
MATERIAL K, 10kg load
100um
MATERIAL N, 20kg load

Figure 4.

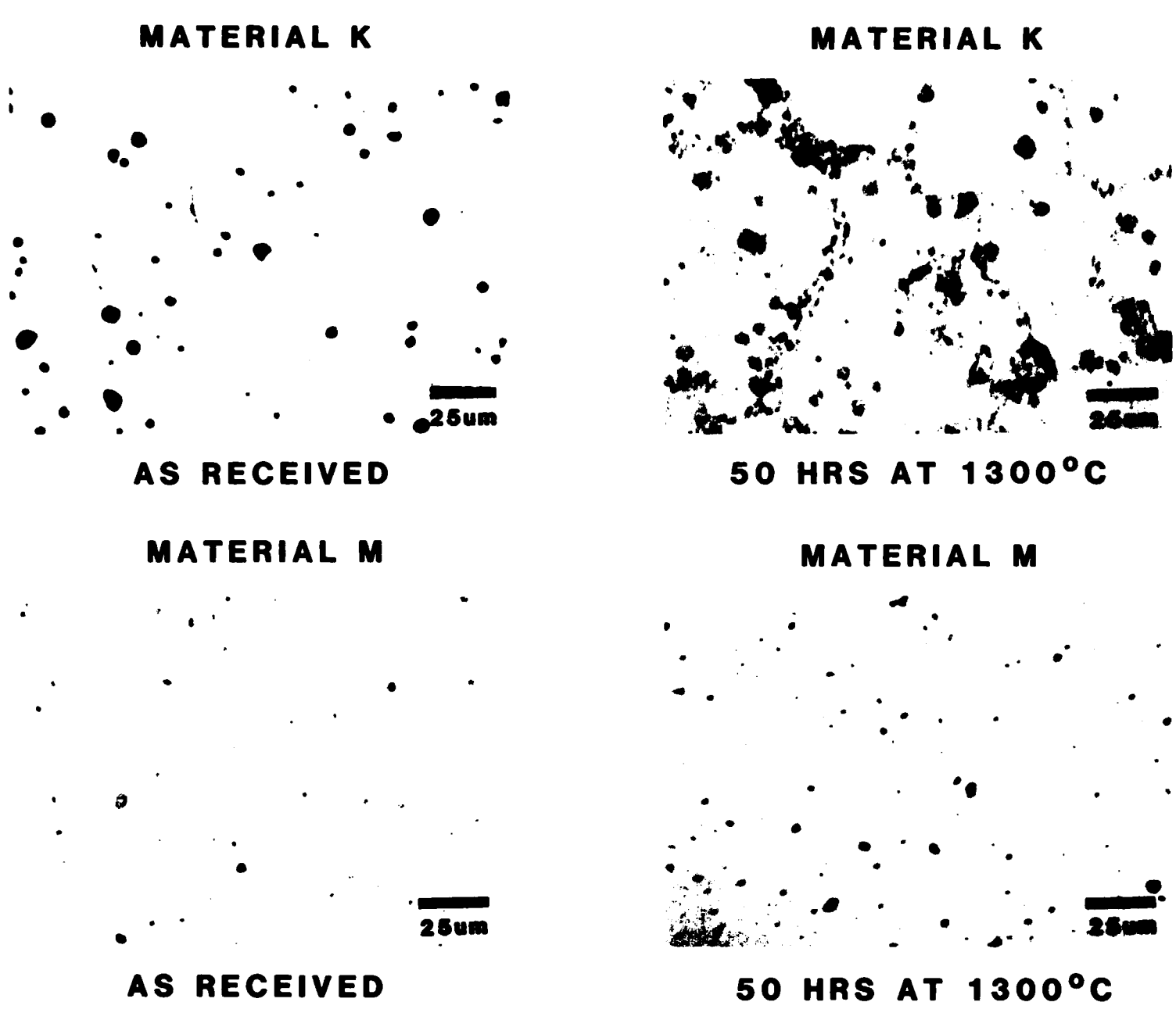
MATERIAL K
25um
AS RECEIVED
MATERIAL K
50 HRS AT 1300°C
MATERIAL M
25um
AS RECEIVED
MATERIAL M
50 HRS AT 1300°C

Figure 5.

MATERIAL D

100 HRS AT 1200°C

MATERIAL D

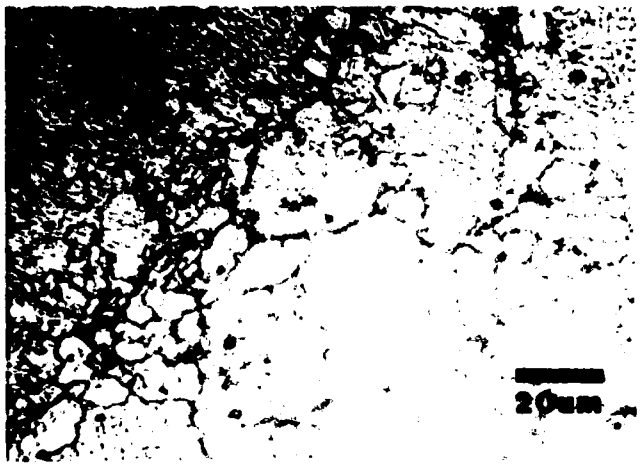

500 HRS AT 1200°C

(not available)

MATERIAL N

500 HRS AT 1300°C

Figure 6.

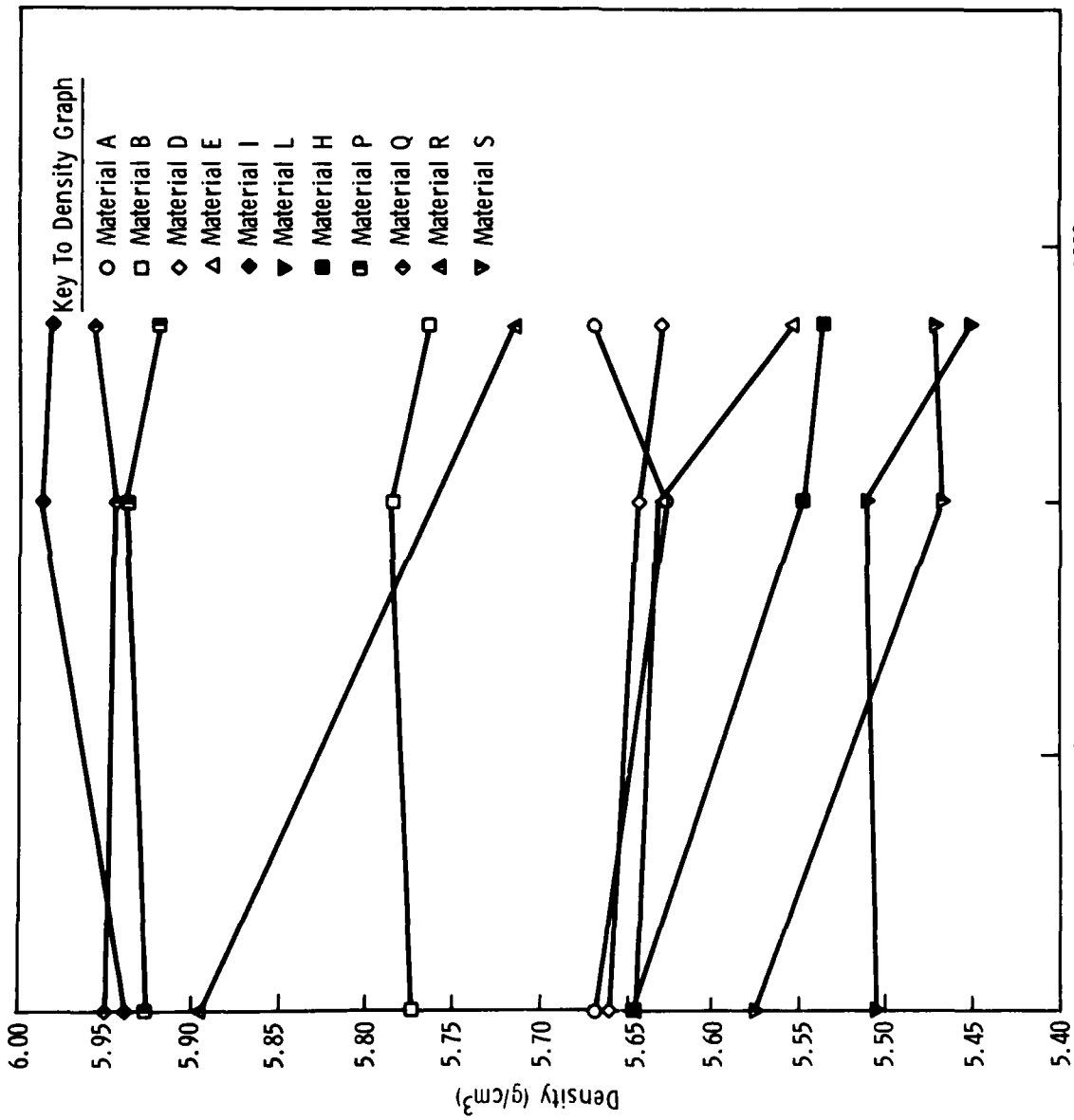
Key To Density Graph
Material A
Material B
Material D
Material E
Material I
Material L
Material H
Material P
Material Q
Material R
Material S
Density (g/cm³)
6.00
5.95
5.90
5.85
5.80
5.75
5.70
5.65
5.60
5.55
5.50
5.45
5.40
0
10
100
1000
Time at 1000°C (hr)

Figure 7.

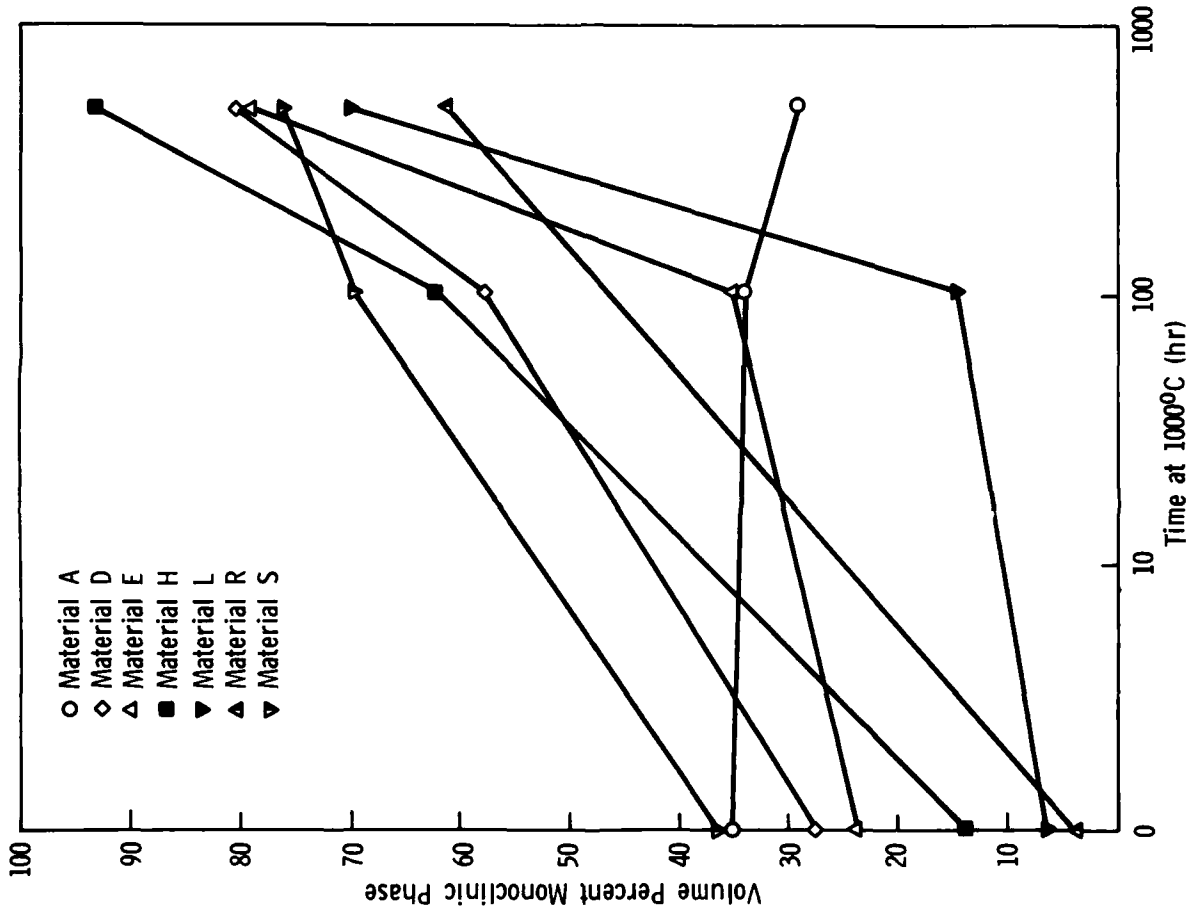
Volume Percent Monoclinic Phase
100
90
80
70
60
50
40
30
20
10
0
10
100
1000
Time at 1000°C (hr)
Material A
Material D
Material E
Material H
Material L
Material R
Material S

Figure 8.

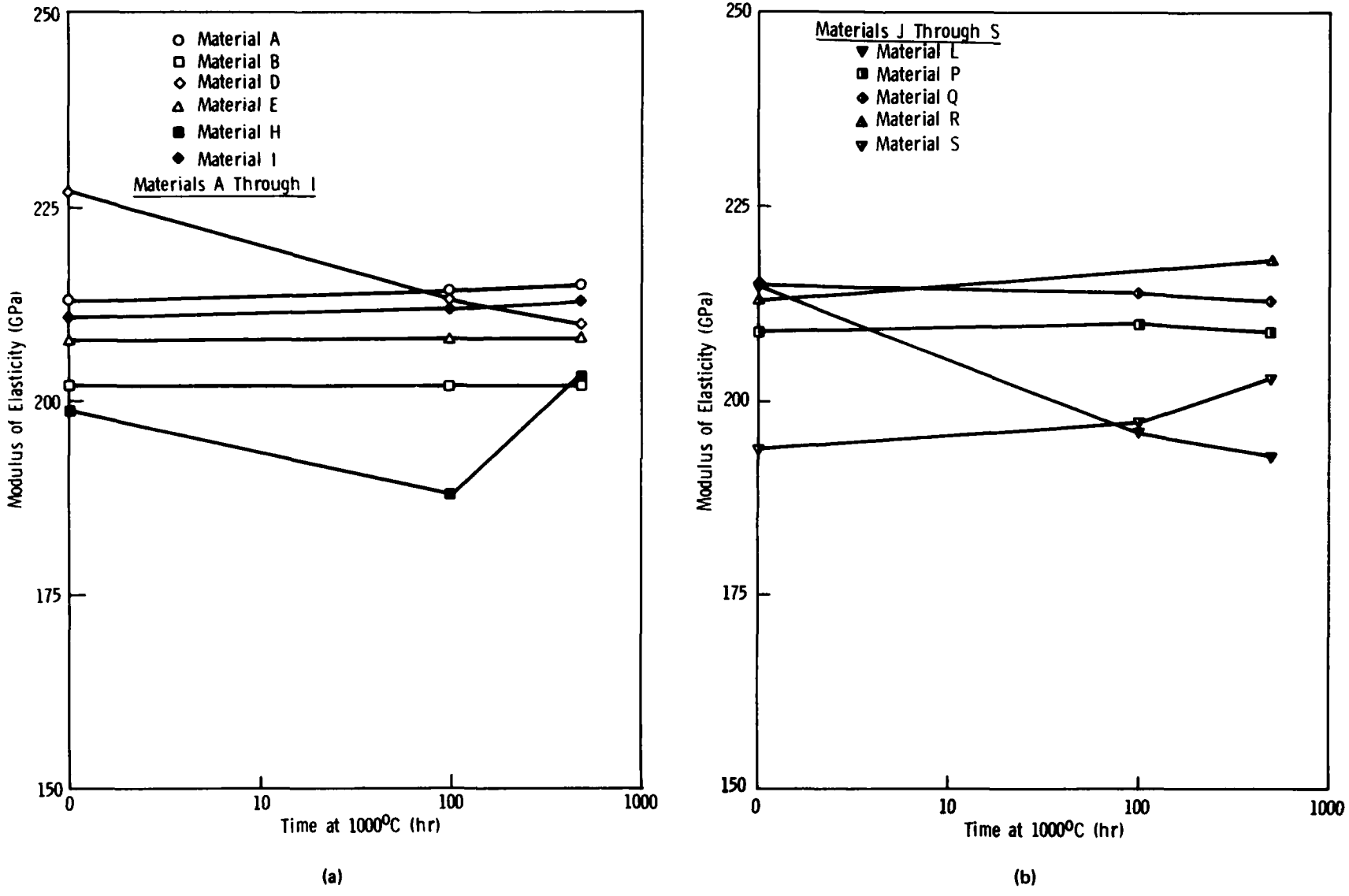
250
225
200
175
150
Modulus of Elasticity (GPa)
Material A
Material B
Material D
Material E
Material H
Material I
Materials A Through I
0
10
100
1000
Time at 1000°C (hr)
(a)
250
225
200
175
150
Modulus of Elasticity (GPa)
Materials J Through S
Material L
Material P
Material Q
Material R
Material S
0
10
100
1000
Time at 1000°C (hr)
(b)

Figure 9.

MATERIAL A

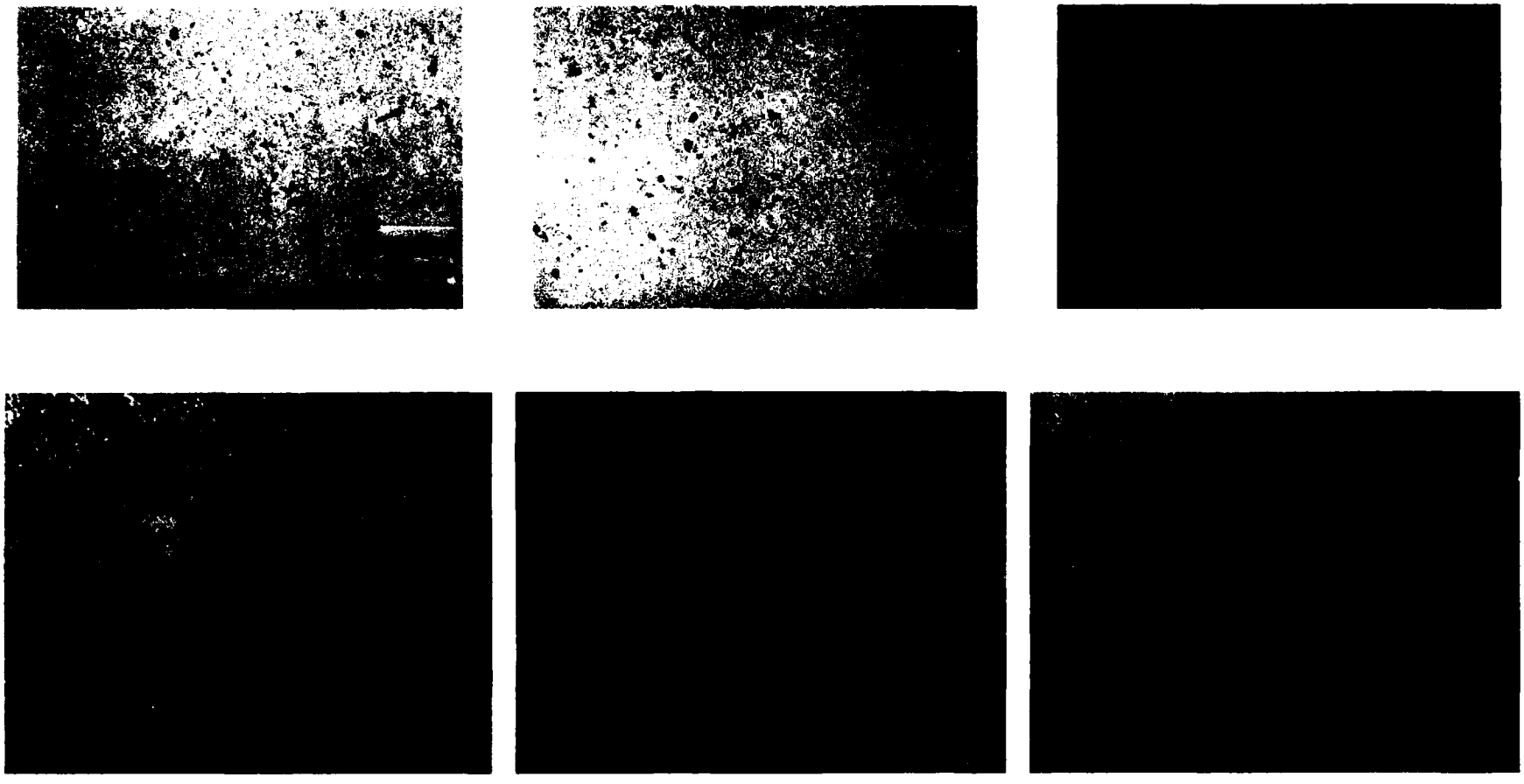

Figure 10.

MATERIAL B

(not available)

(not available)

20um

AS RECEIVED

100 HRS AT 1000°C

500 HRS AT 1000°C

Figure 10. (Cont'd)

MATERIAL D

(not available)

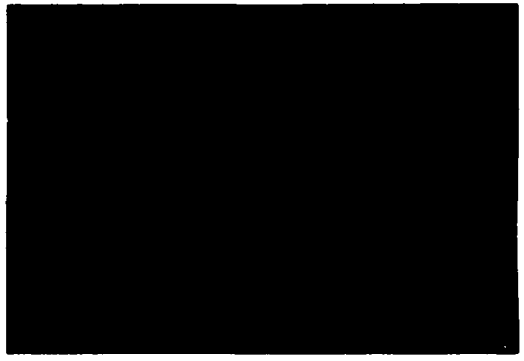

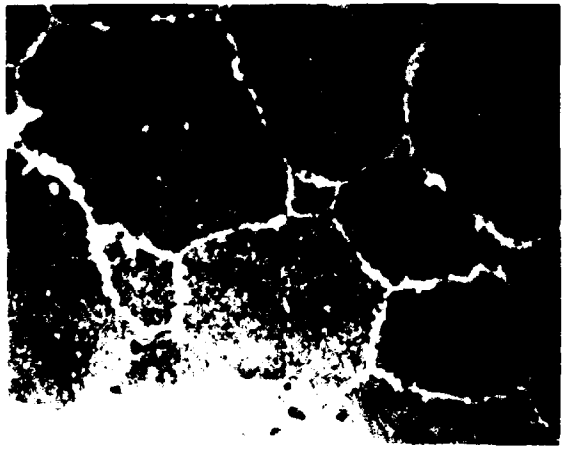

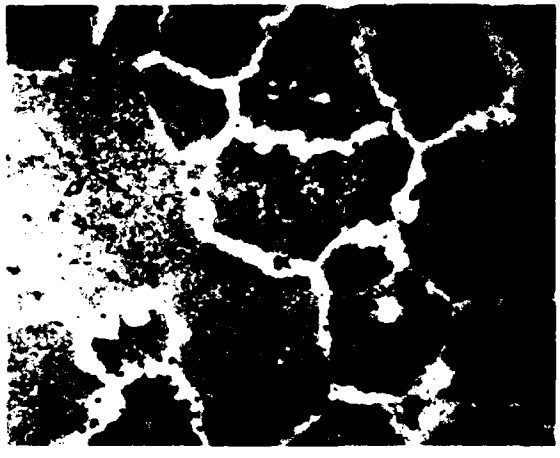

(not available)

AS RECEIVED

100 HRS AT 1000°C

500 HRS AT 1000°C

Figure 10. (Cont'd)

MATERIAL E

(not available) (not available) (not available)

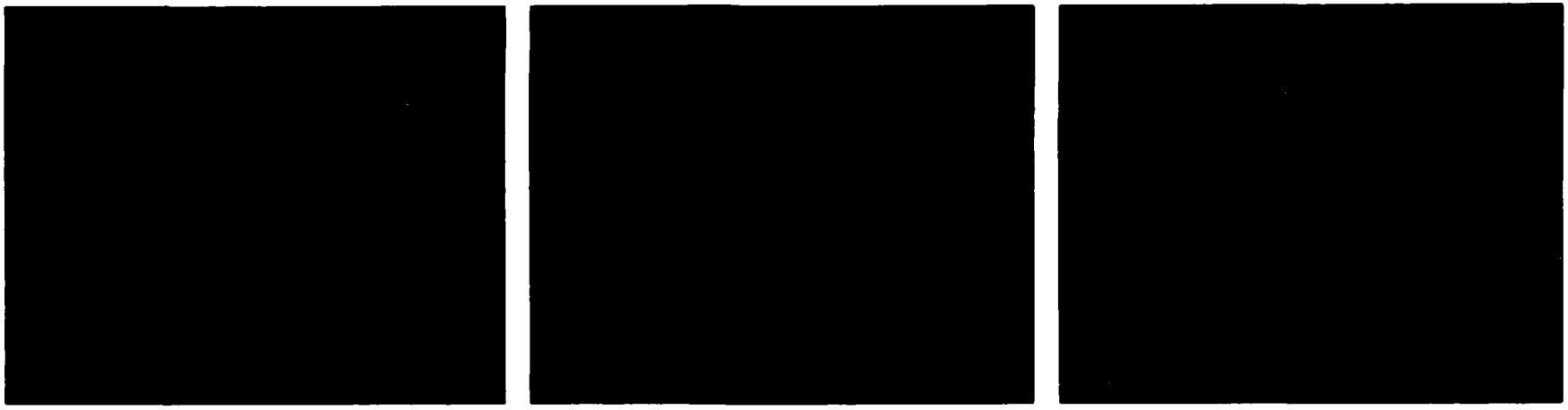

AS RECEIVED 100 HRS AT 1000°C 500 HRS AT 1000°C

Figure 10. (Cont'd)

MATERIAL F	MATERIAL G	MATERIAL J
		
AS RECEIVED	AS RECEIVED	AS RECEIVED
(not available)	(not available)	(not available)

Figure 10. (Cont'd)

MATERIAL H

(not available)

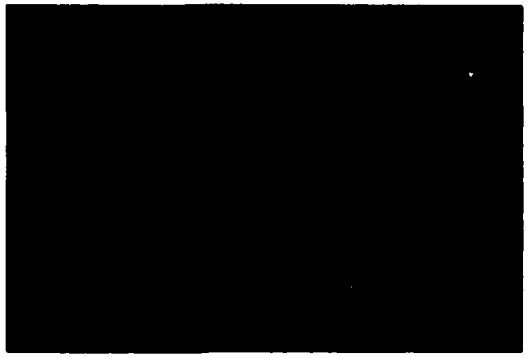

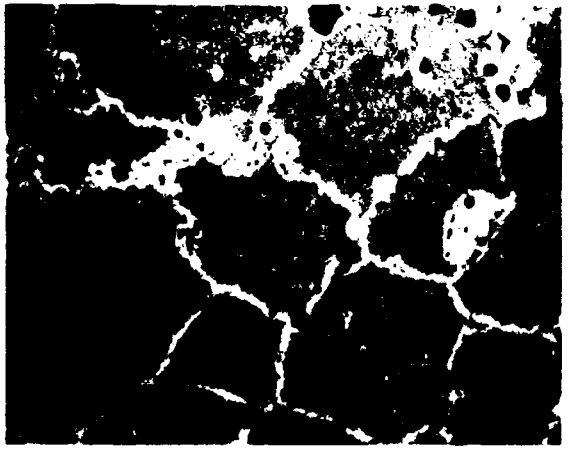

AS RECEIVED

100 HRS AT 1000°C

500 HRS AT 1000°C

Figure 10. (Cont'd)

MATERIAL I

(not available) (not available) (not available)

AS RECEIVED 100 HRS AT 1000°C 500 HRS AT 1000°C

Figure 10. (Cont'd)

MATERIAL L

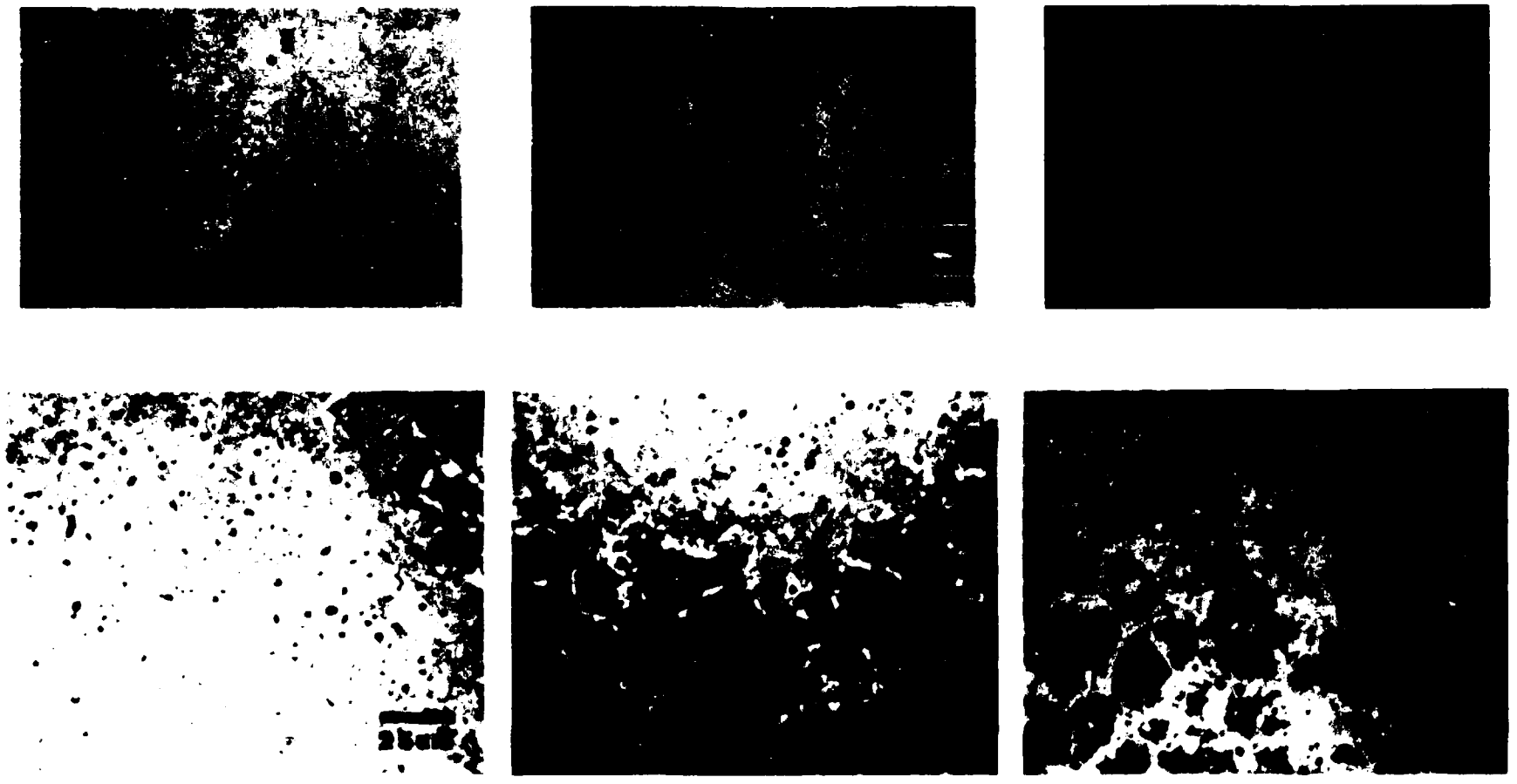

Figure 10. (Cont'd)

MATERIAL N,O

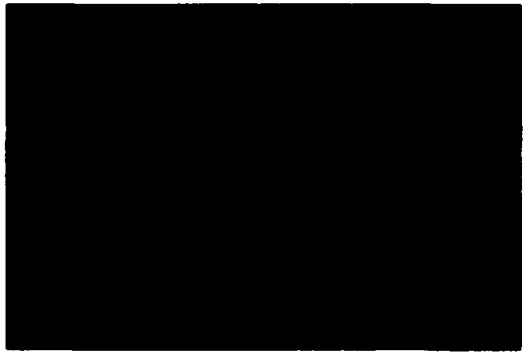

(not available)

(not available)

(not available)

(not available)

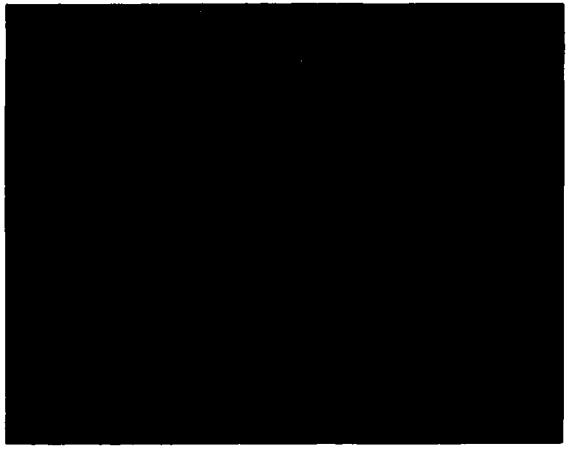

AS RECEIVED

100 HRS AT 1000°C

500 HRS AT 1000°C

Figure 10. (Cont'd)

MATERIAL P

(not available)

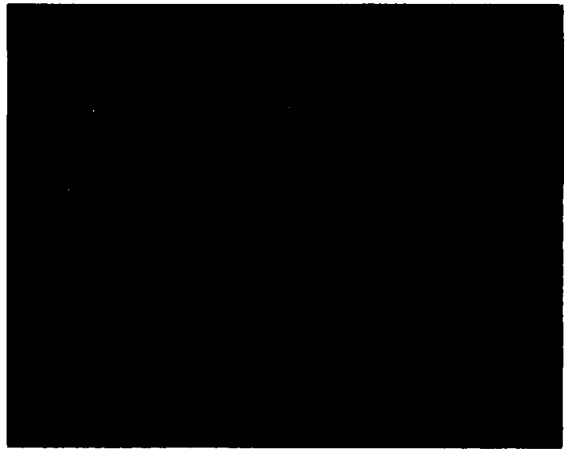

AS RECEIVED

100 HRS AT 1000°C

500 HRS AT 1000°C

Figure 10. (Cont'd)

MATERIAL Q

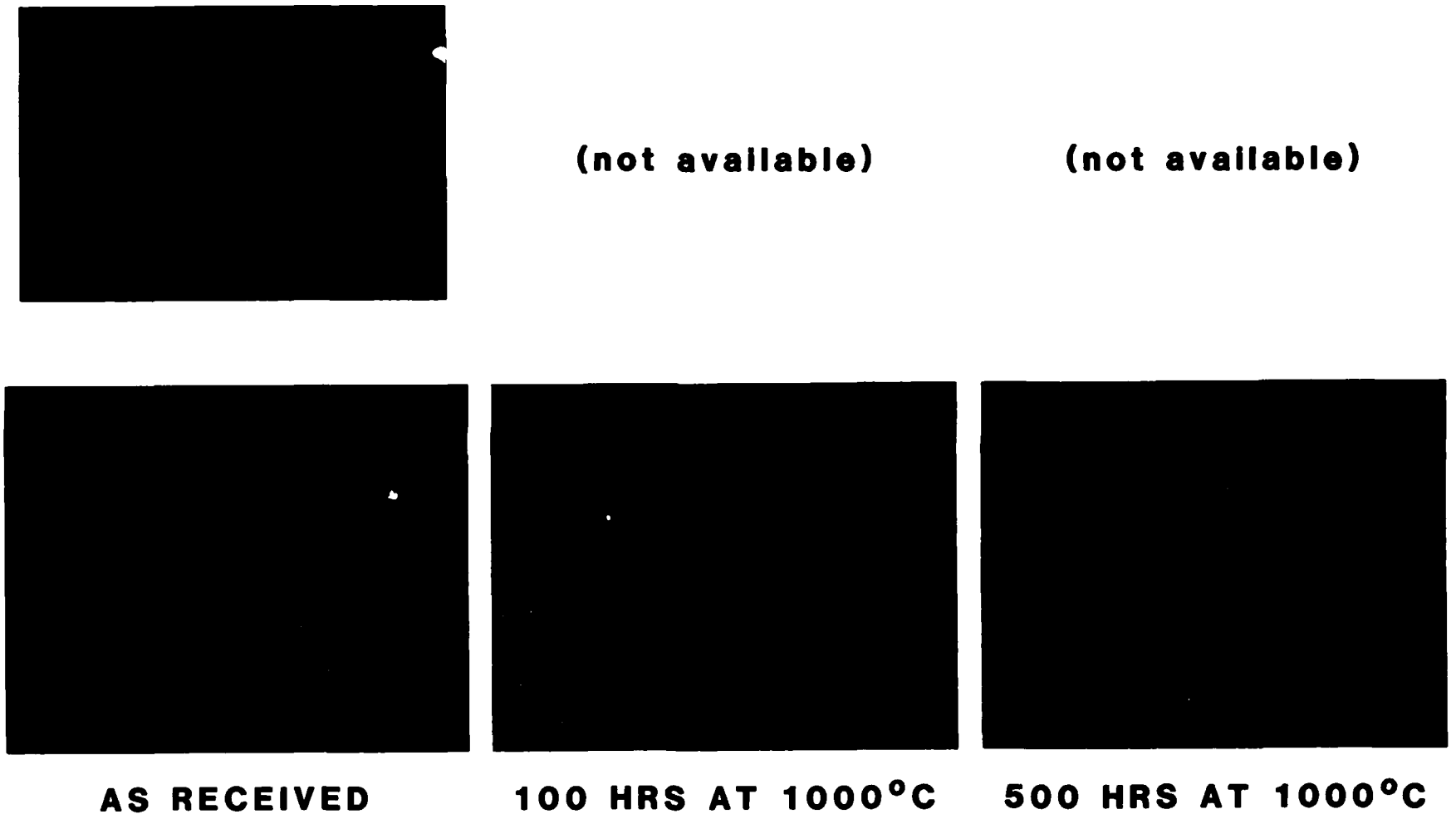

Figure 10. (Cont'd)

MATERIAL R

(not available)

(not available)

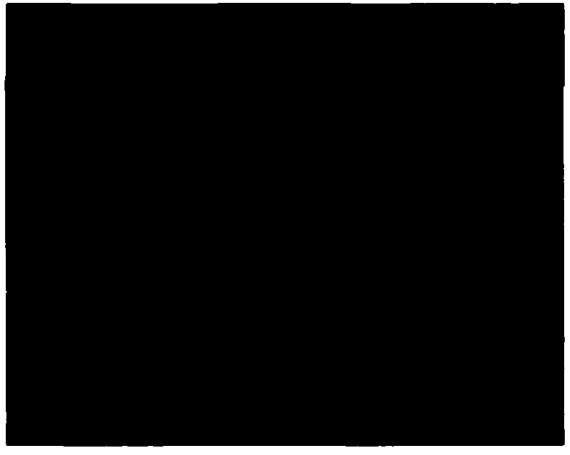

(not available)

AS RECEIVED

100 HRS AT 1000°C

500 HRS AT 1000°C

Figure 10. (Cont'd)

MATERIAL S

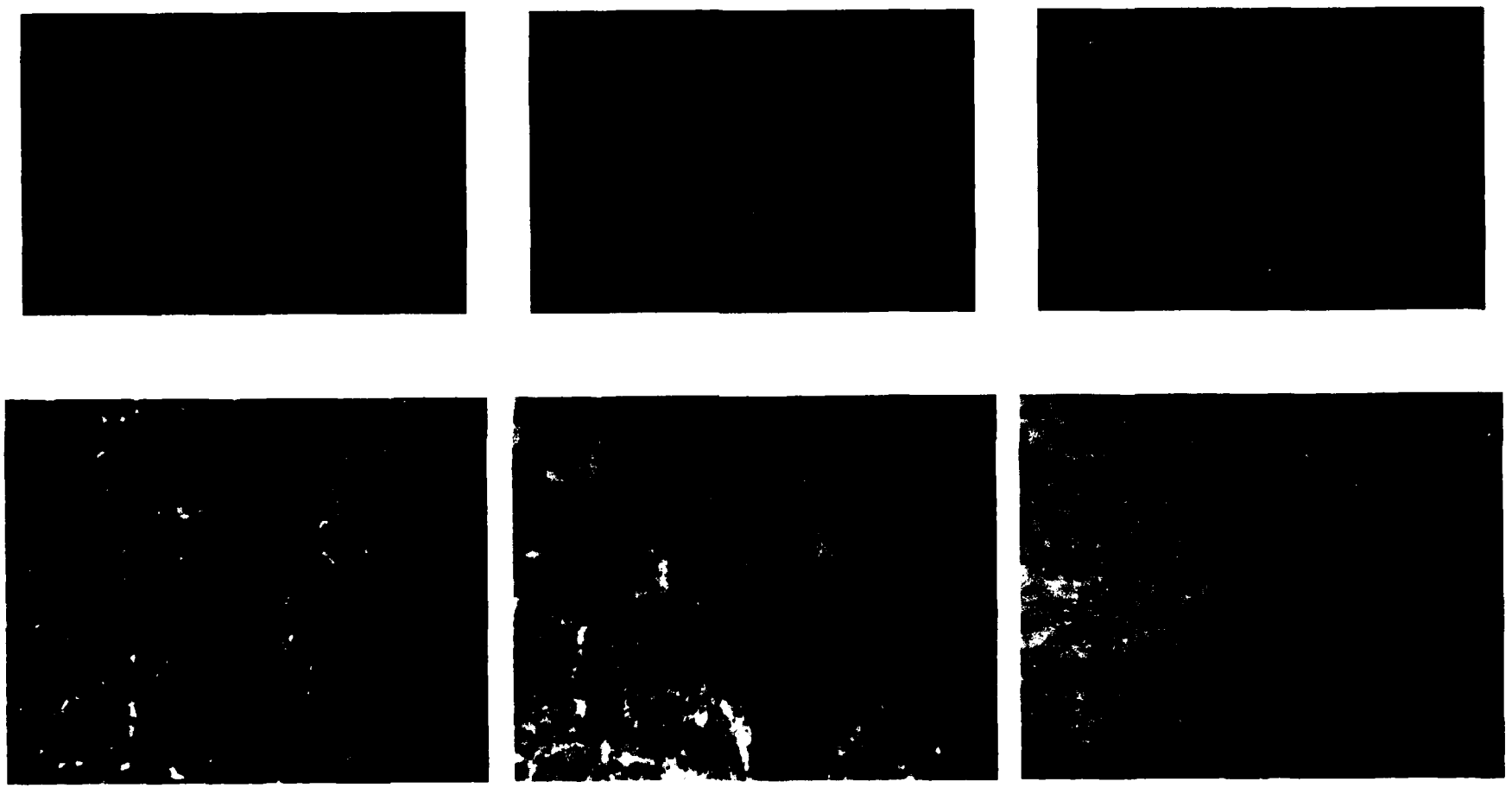

Figure 10. (Cont'd)

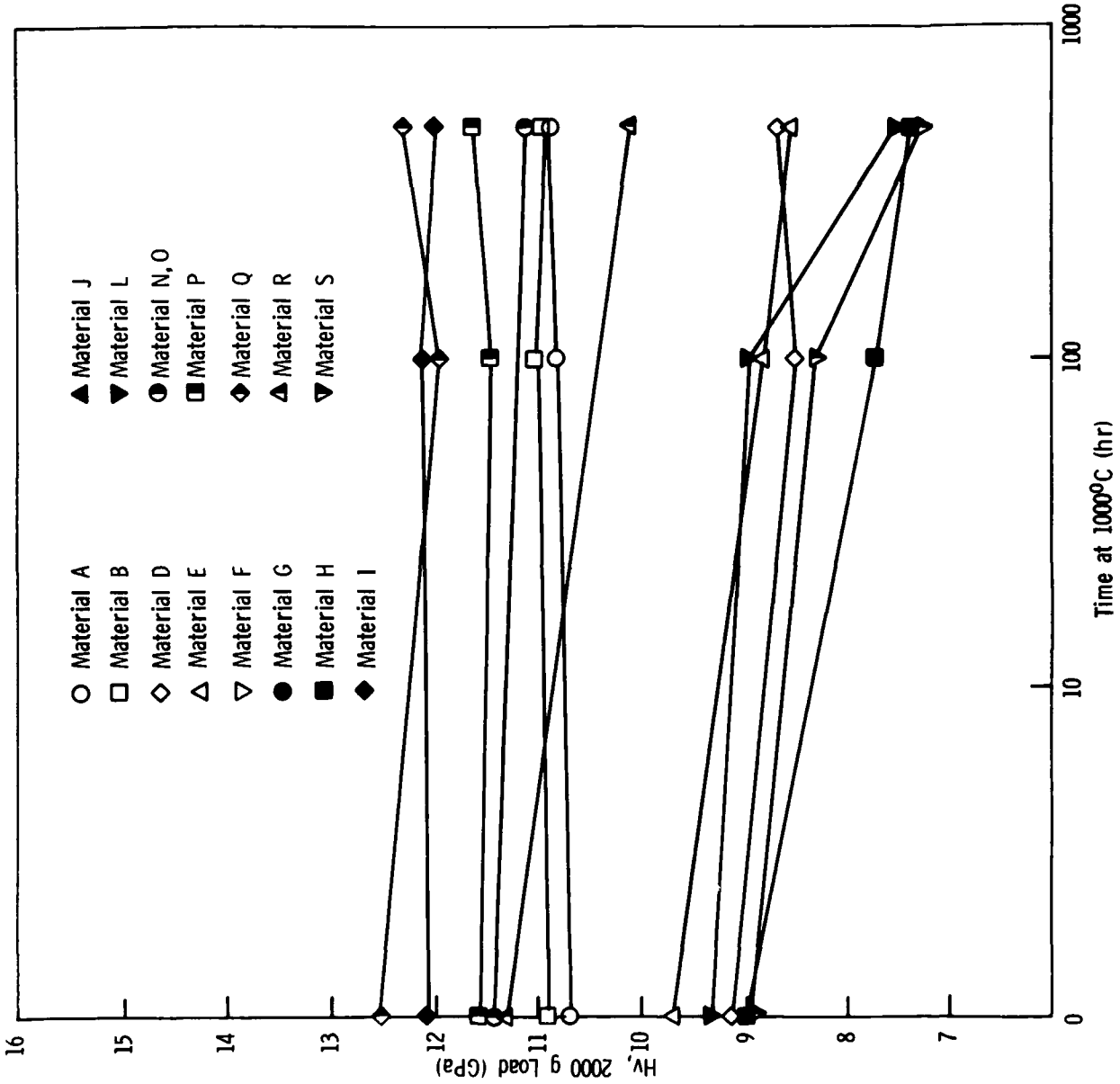
Material A
Material B
Material D
Material E
Material F
Material G
Material H
Material I
Material J
Material L
Material N,O
Material P
Material Q
Material R
Material S
HV, 2000 g Load (GPa)
16
15
14
13
12
11
10
9
8
7
0
10
100
1000
Time at 1000°C (hr)

Figure 11.

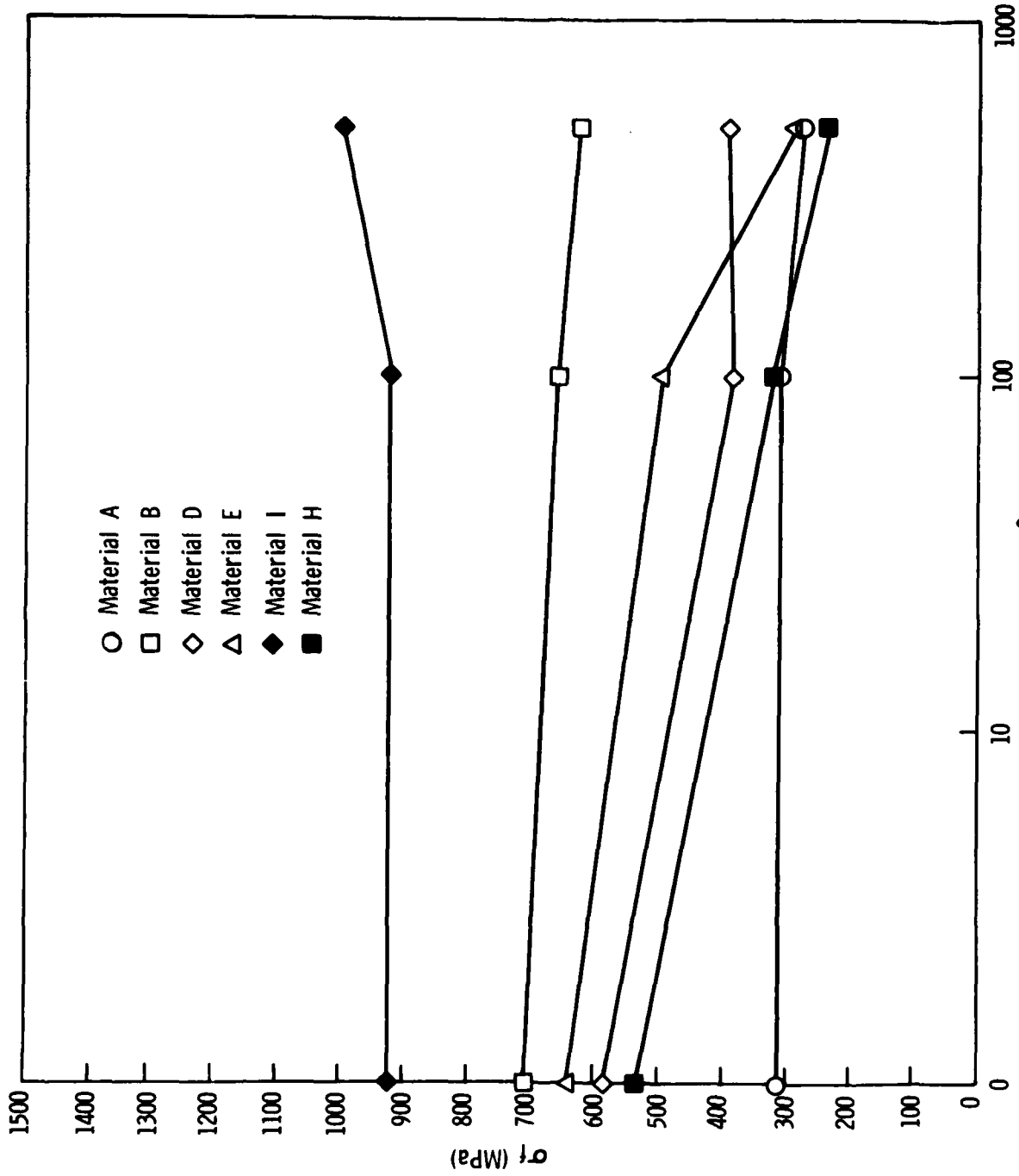
Material A
Material B
Material D
Material E
Material I
Material H
σf (MPa)
1500
1400
1300
1200
1100
1000
900
800
700
600
500
400
300
200
100
0
0
10
100
1000
Time at 1000°C (hr)

(a)

Figure 12.

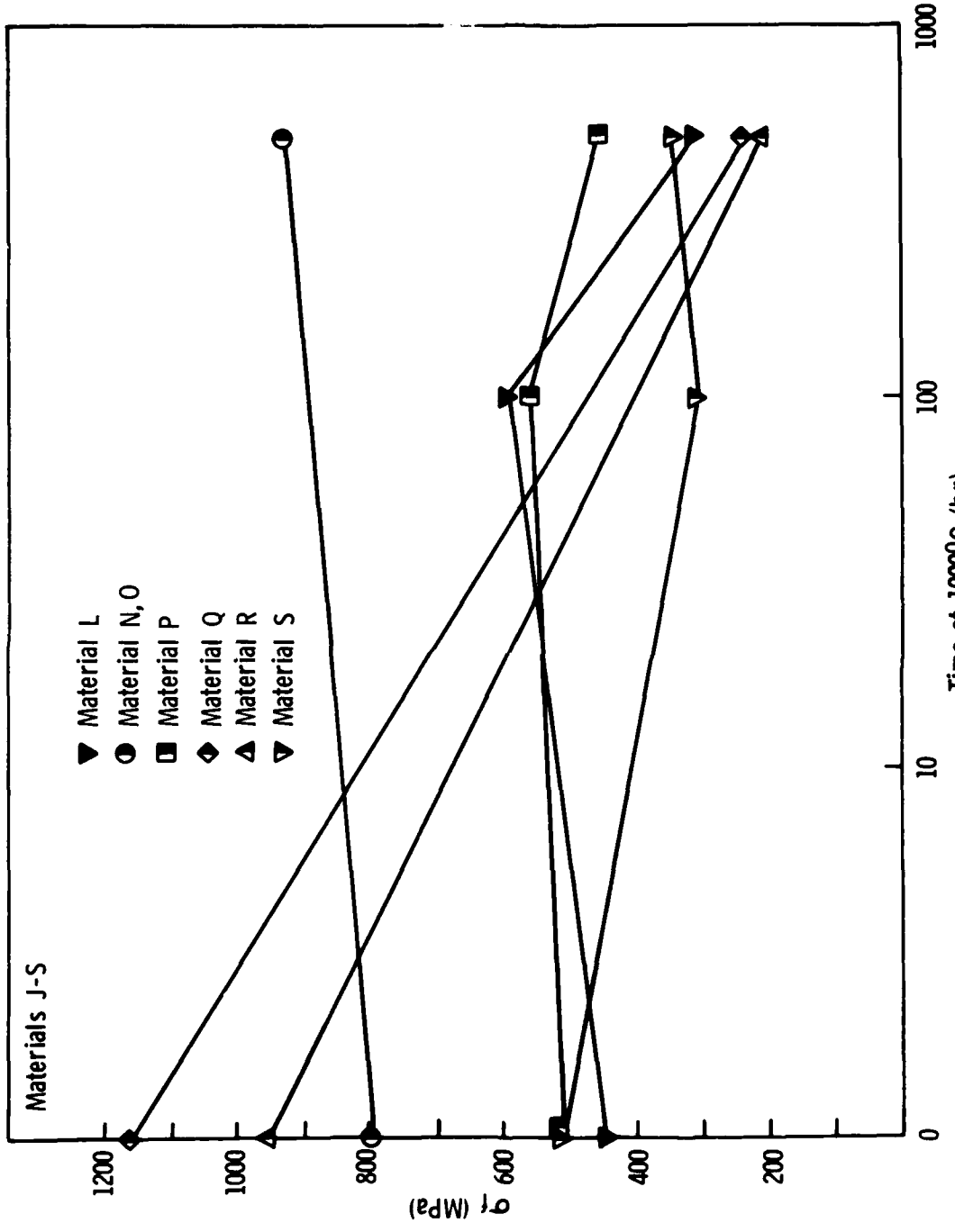
Materials J-S
Material L
Material N,O
Material P
Material Q
Material R
Material S
σf (MPa)
1200
1000
800
600
400
200
0
10
100
1000
Time at 1000°C (hr)

(b)

Figure 12.

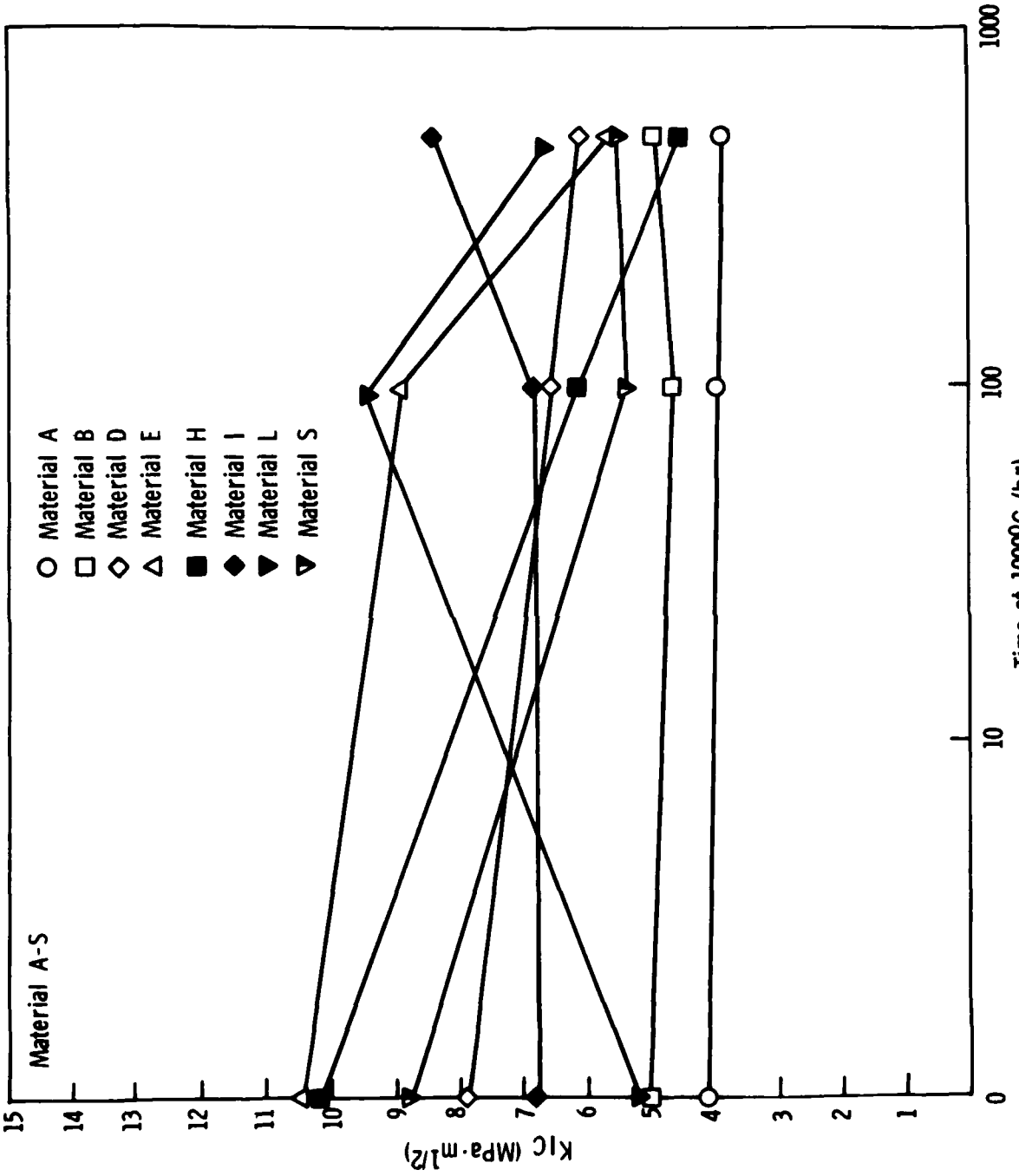
Material A-S
Material A
Material B
Material D
Material E
Material H
Material I
Material L
Material S
KIC (MPa·m1/2)
Time at 1000°C (hr)
15
14
13
12
11
10
9
8
7
6
5
4
3
2
1
0
10
100
1000

Figure 13.

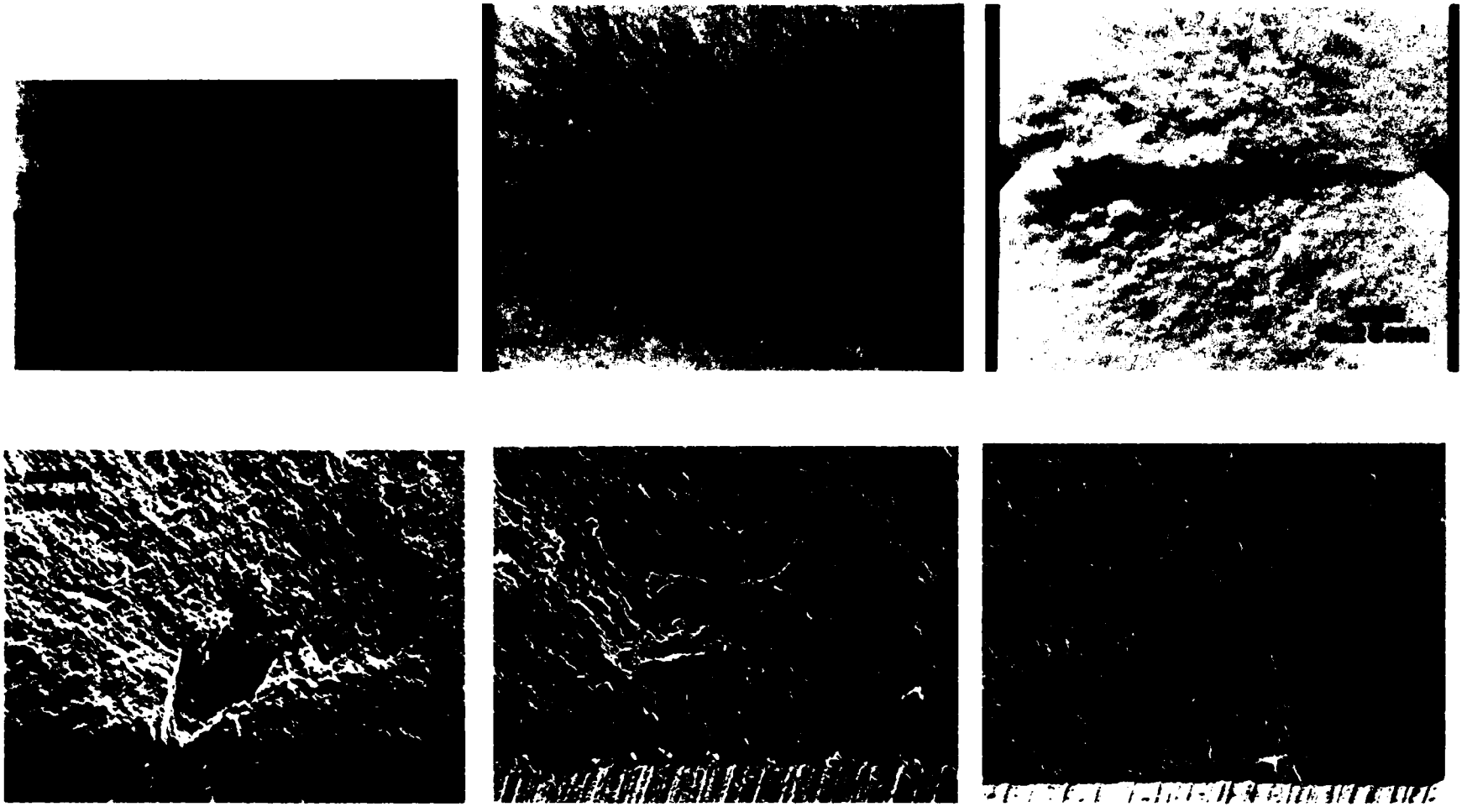

Figure 14.

MATERIAL B

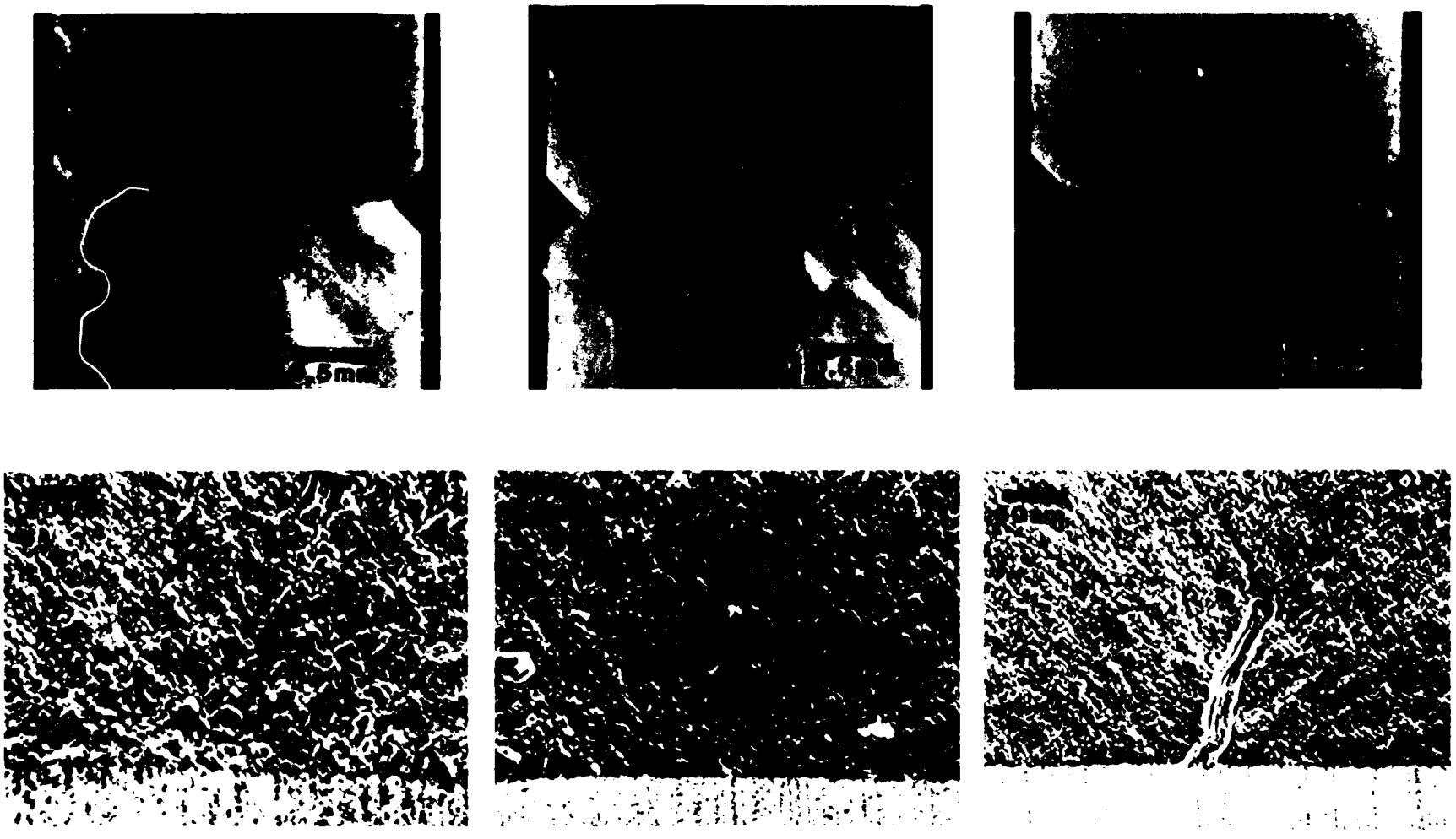

Figure 14. (Cont'd)

MATERIAL D

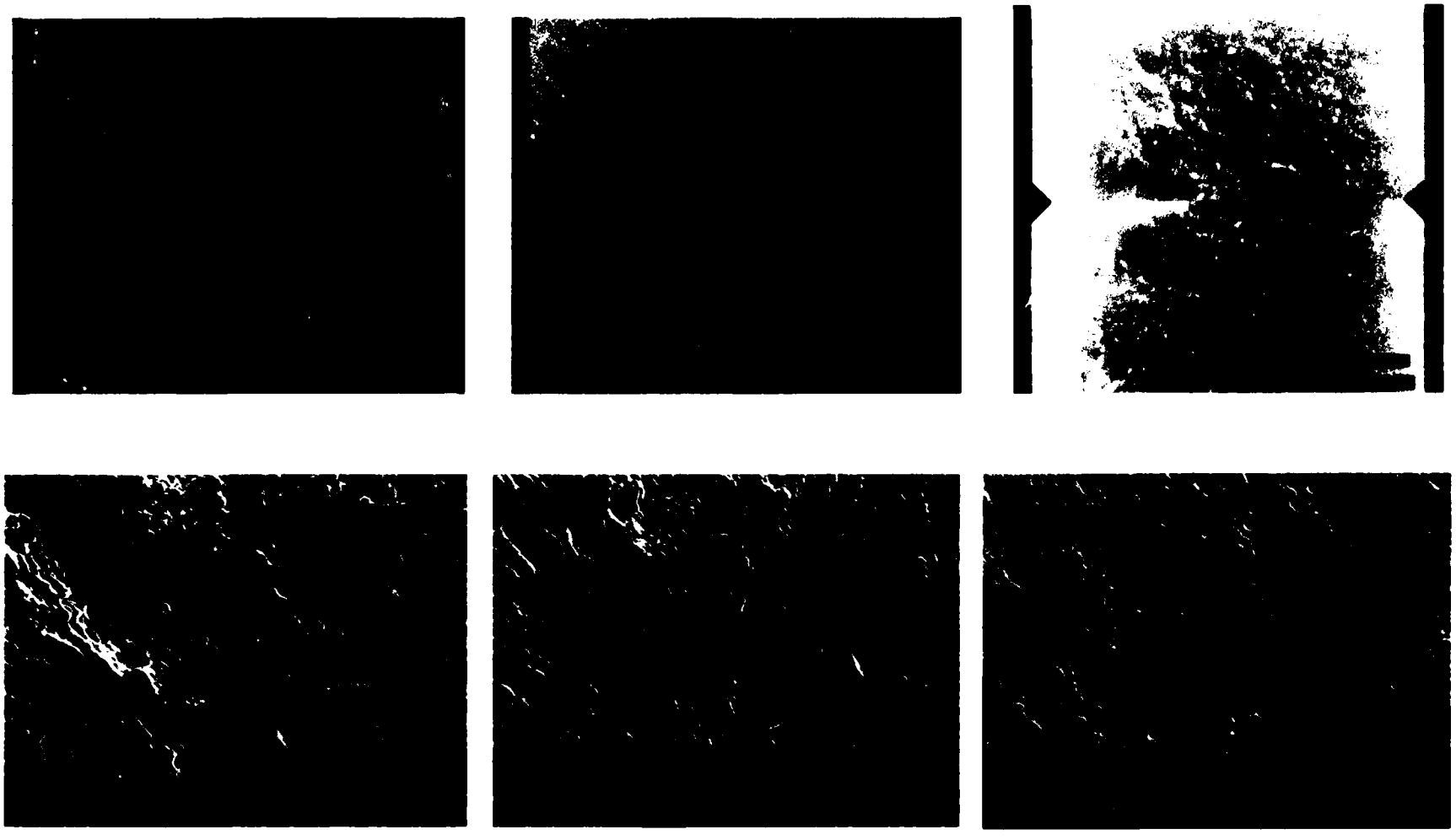

Figure 14. (Cont'd)

MATERIAL E

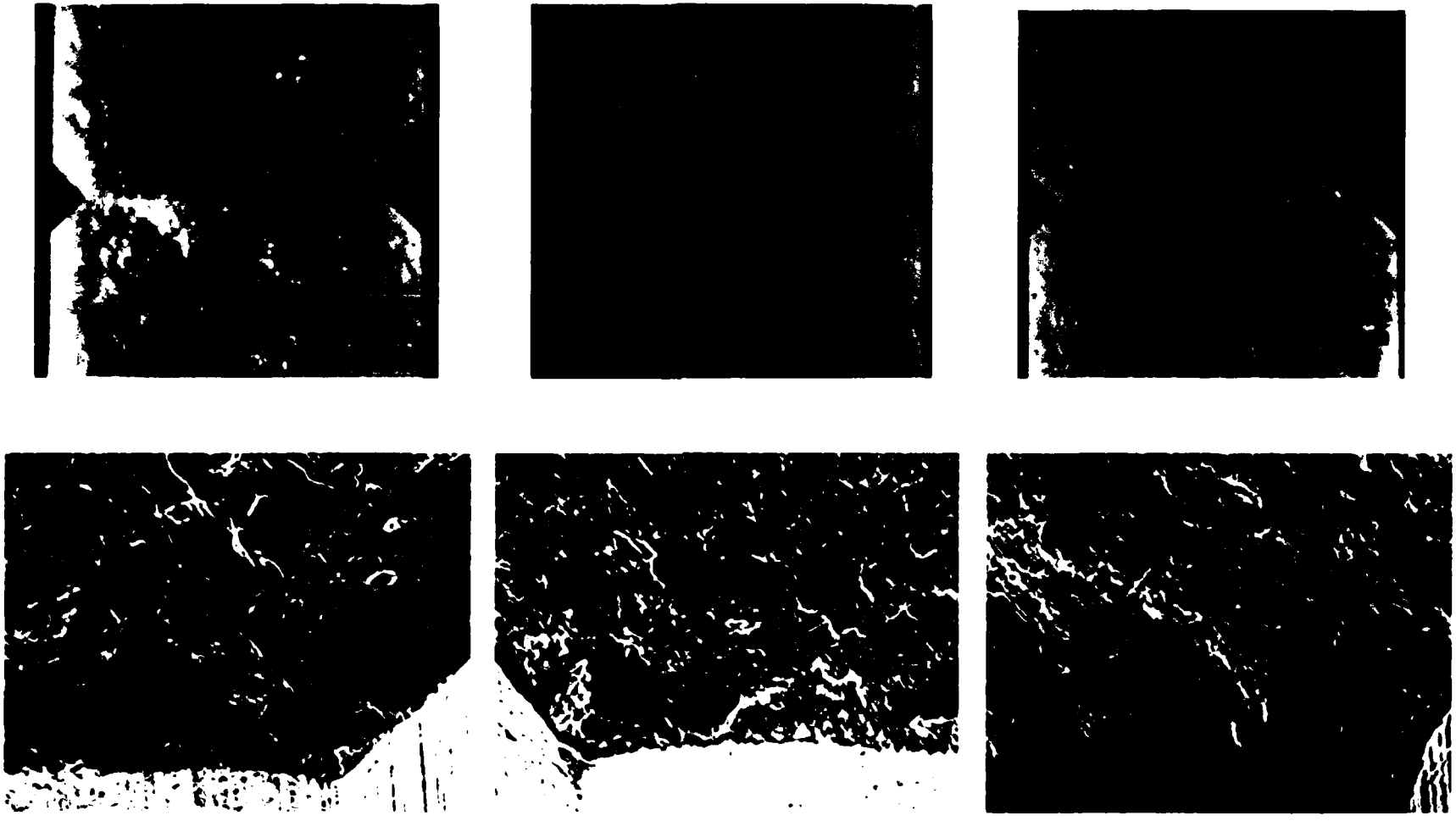

Figure 14. (Cont'd)

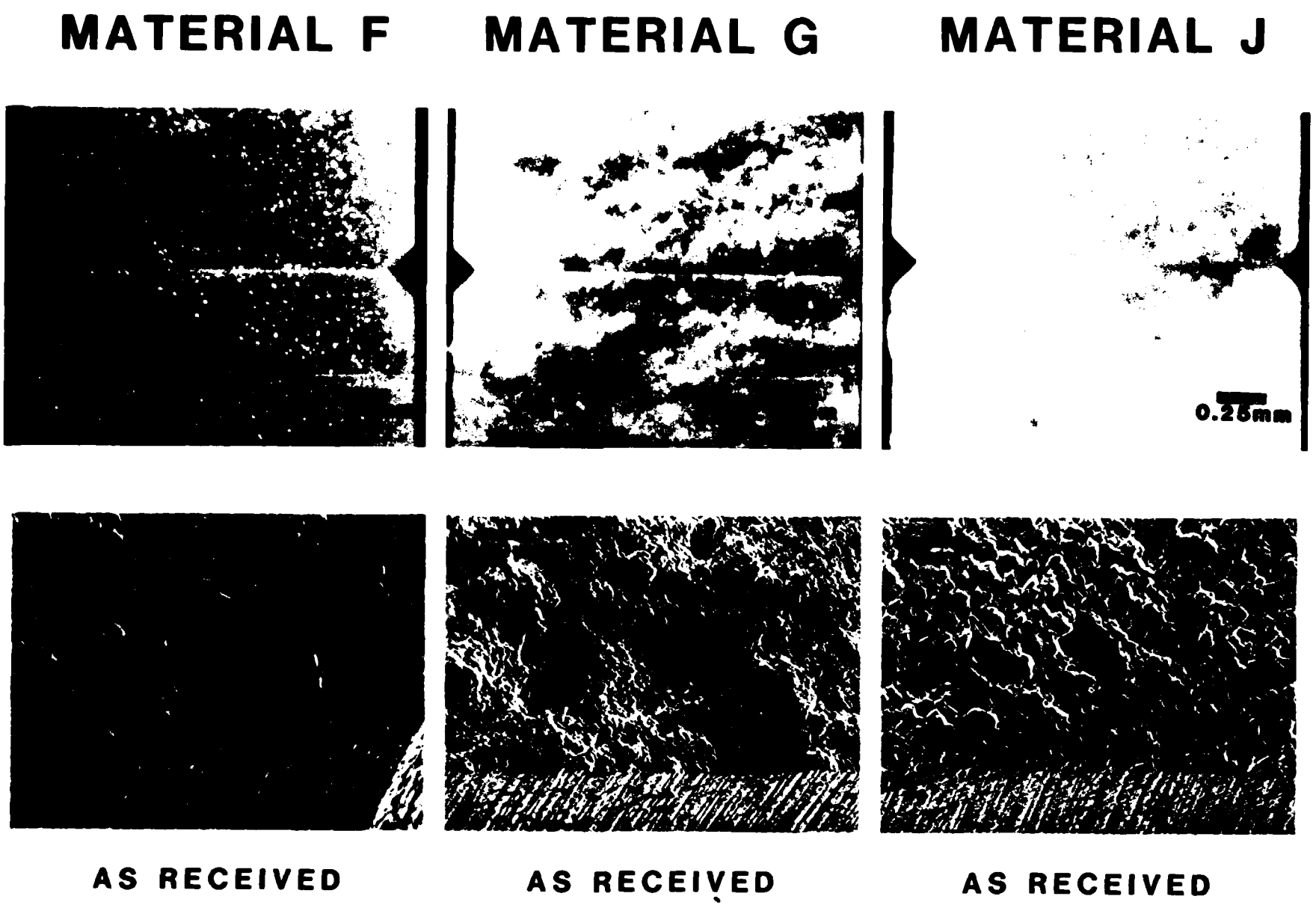

Figure 14. (Cont'd)

MATERIAL H

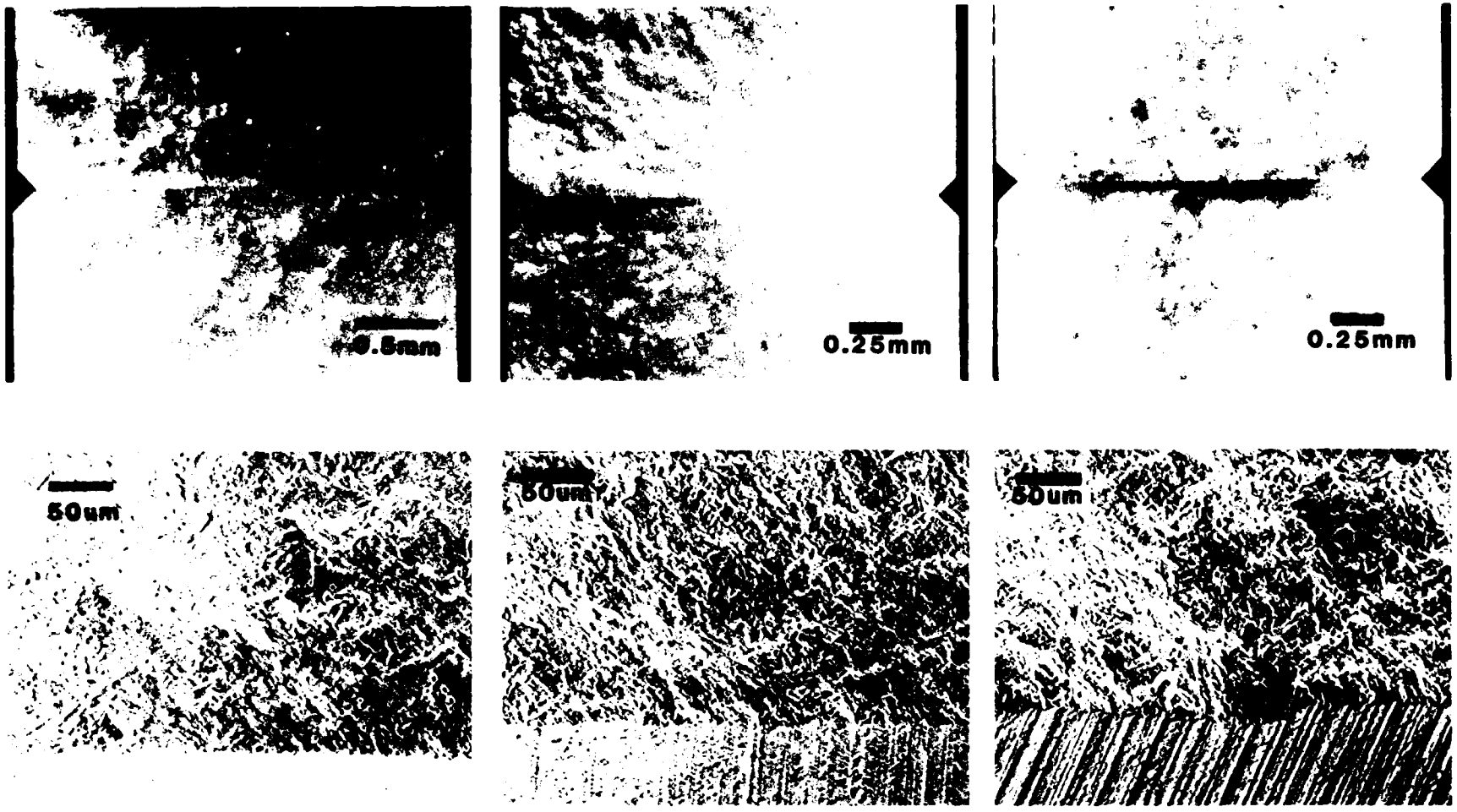

Figure 14. (Cont'd)

MATERIAL I

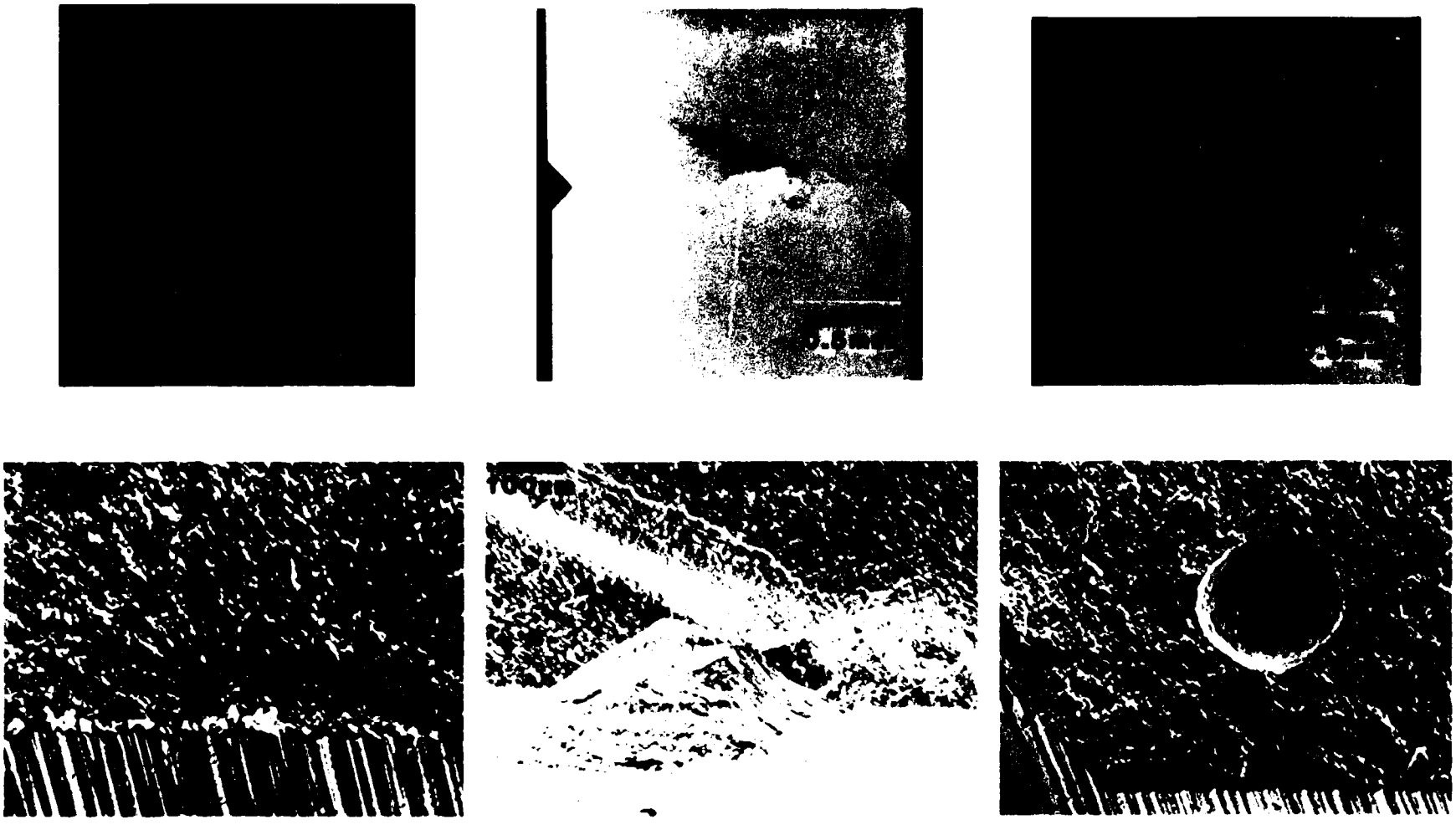

Figure 14. (Cont'd)

MATERIAL L

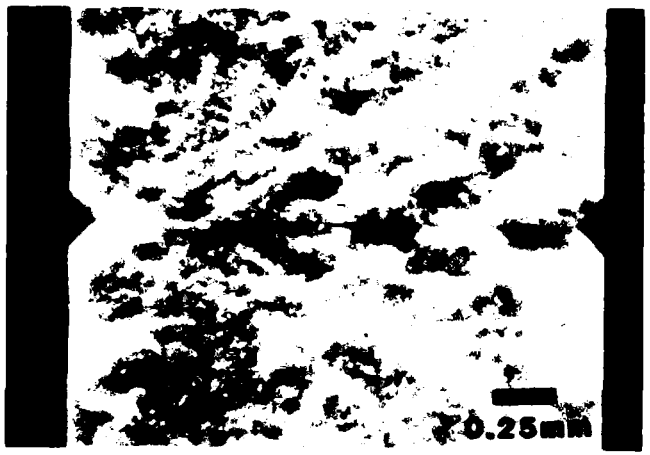

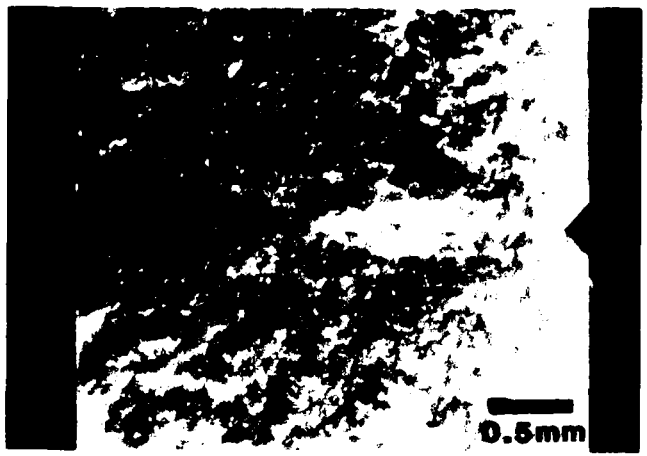

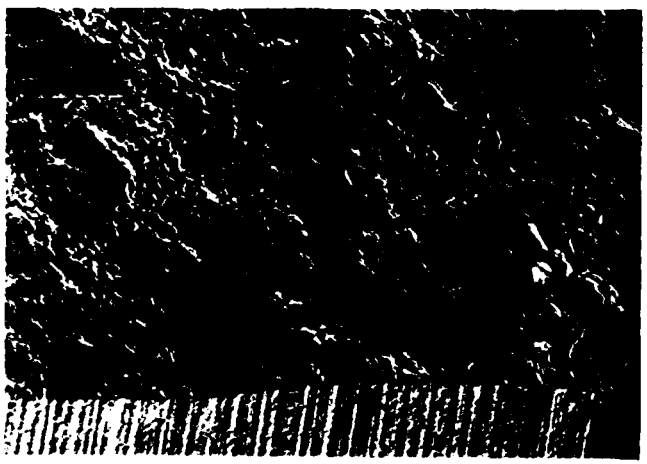

100 HRS AT 1000°C

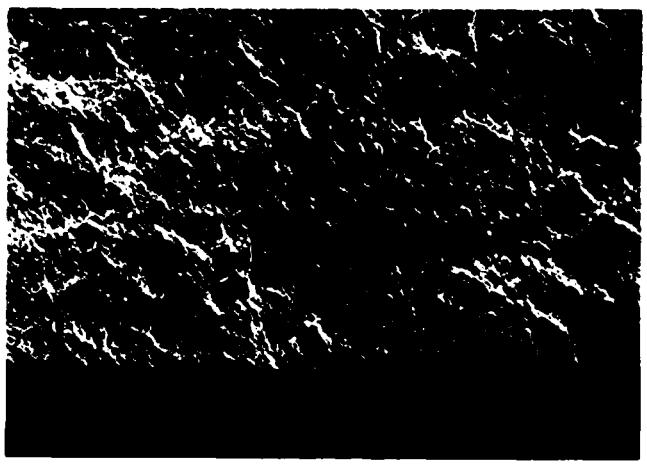

500 HRS AT 1000°C

Figure 14. (Cont'd)

MATERIAL L

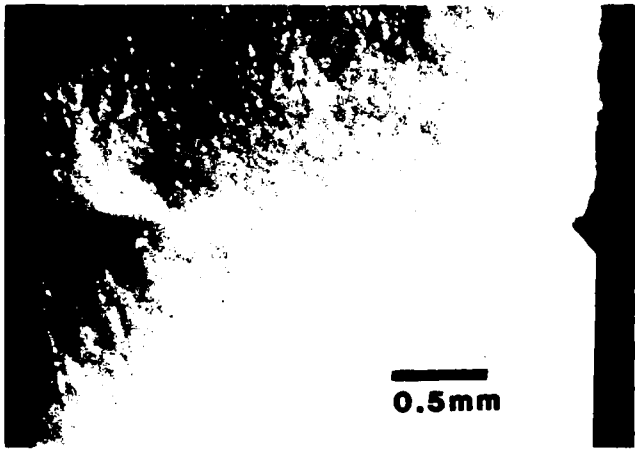

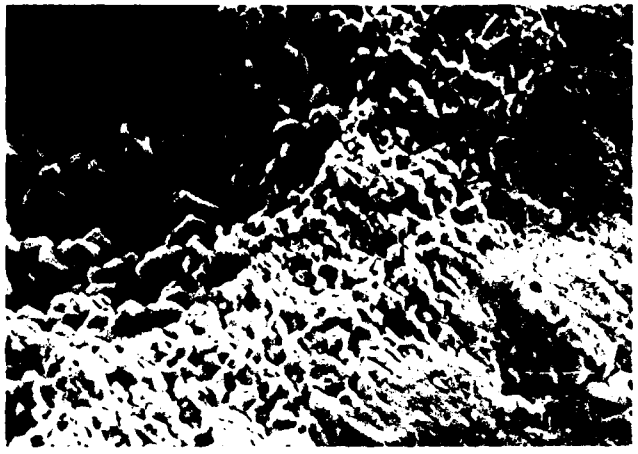

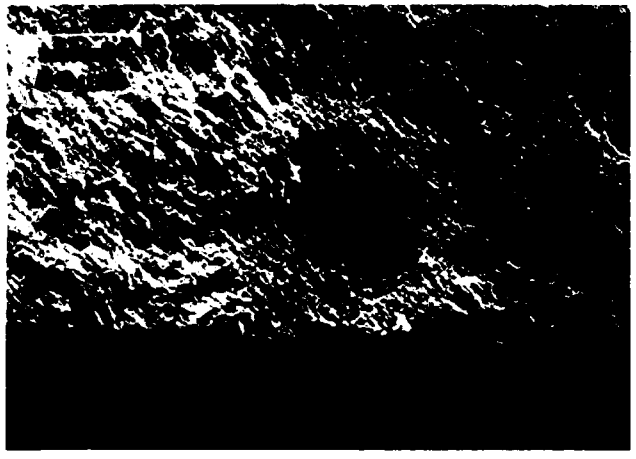

AS RECEIVED

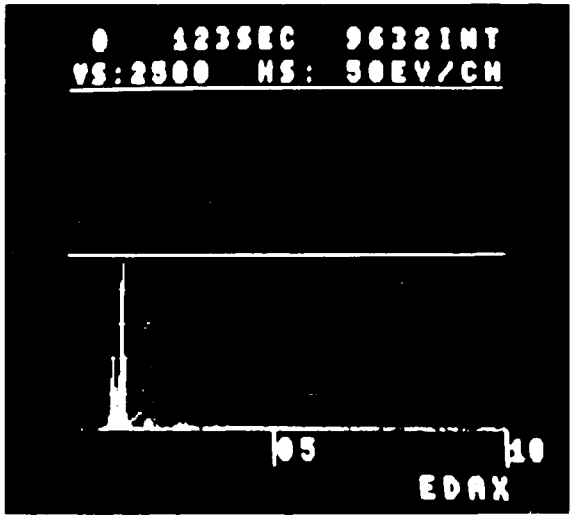

Figure 14. (Cont'd)

MATERIAL N,O

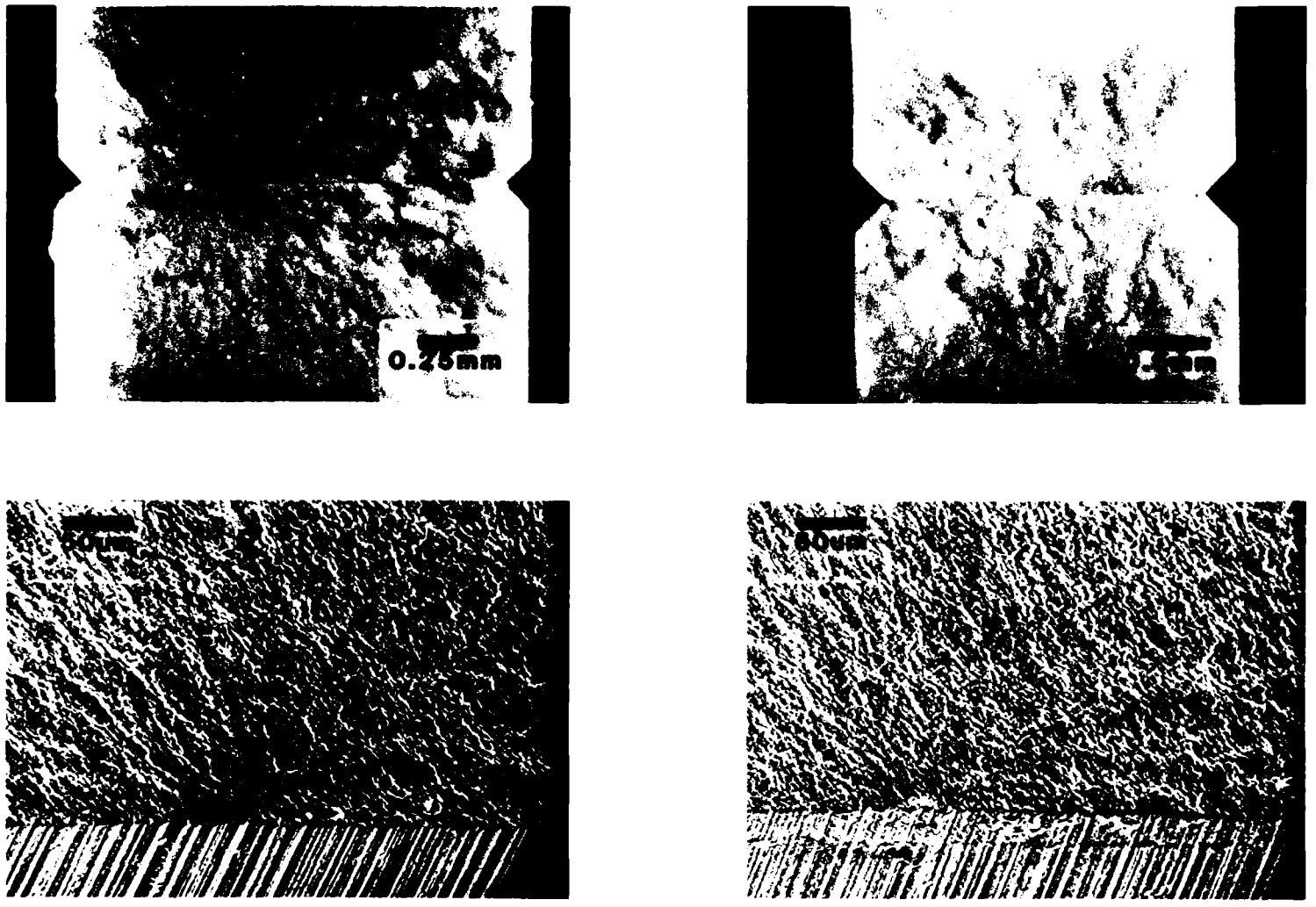

Figure 14. (Cont'd)

M. TERIAL P

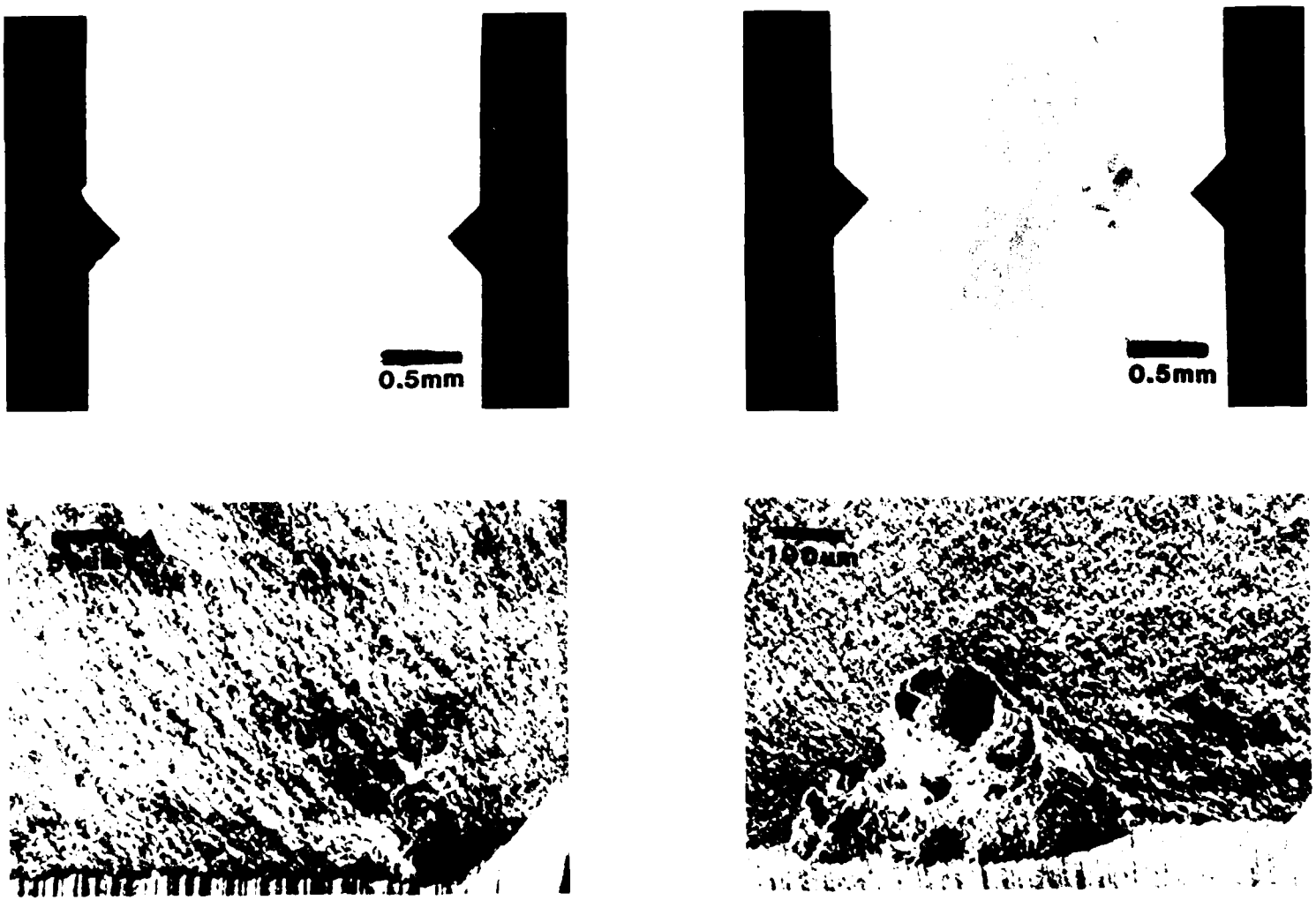

500 HRS AT 1000°C

Figure 14. (Cont'd)

MATERIAL P

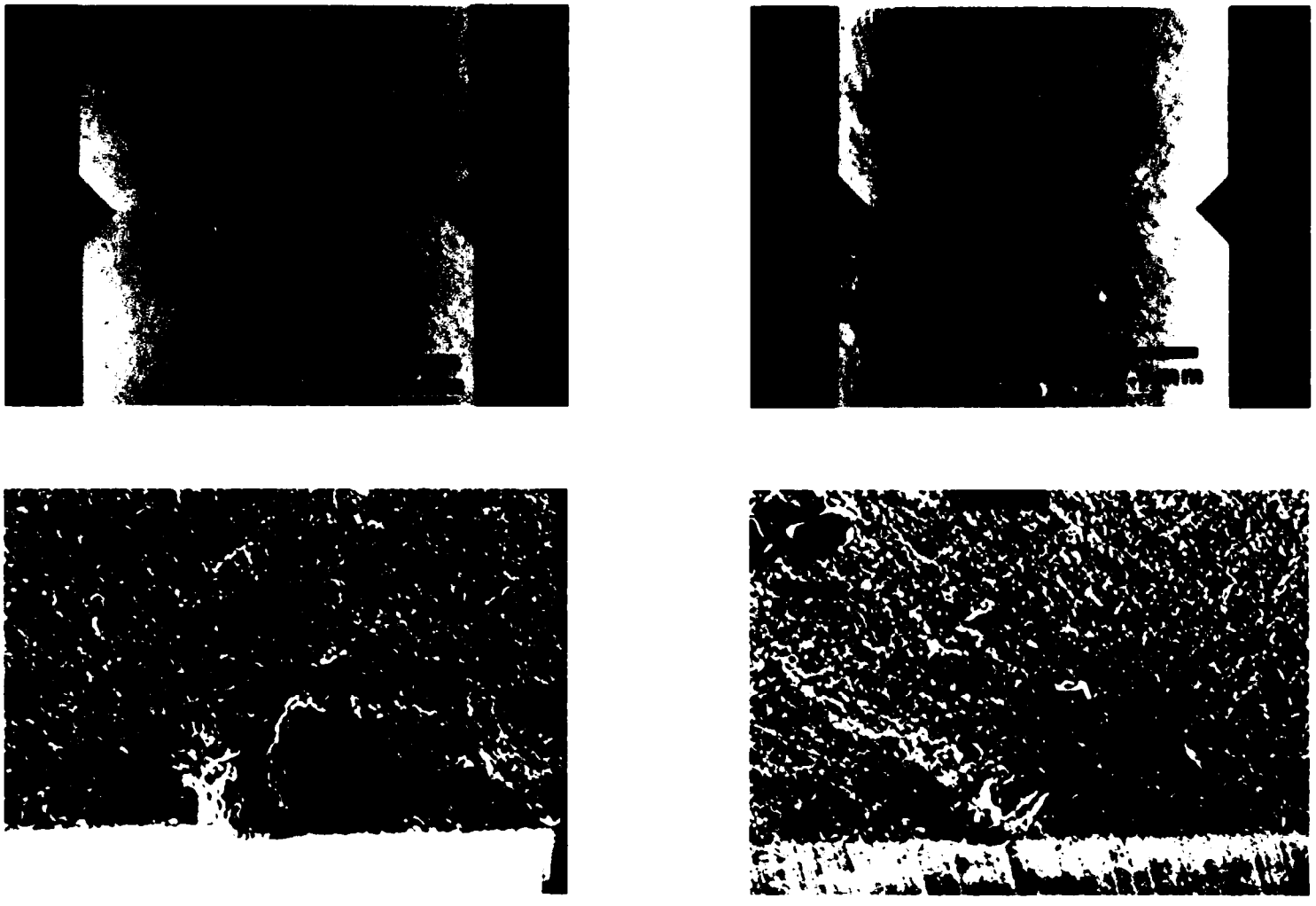

Figure 14. (Cont'd)

MATERIAL Q

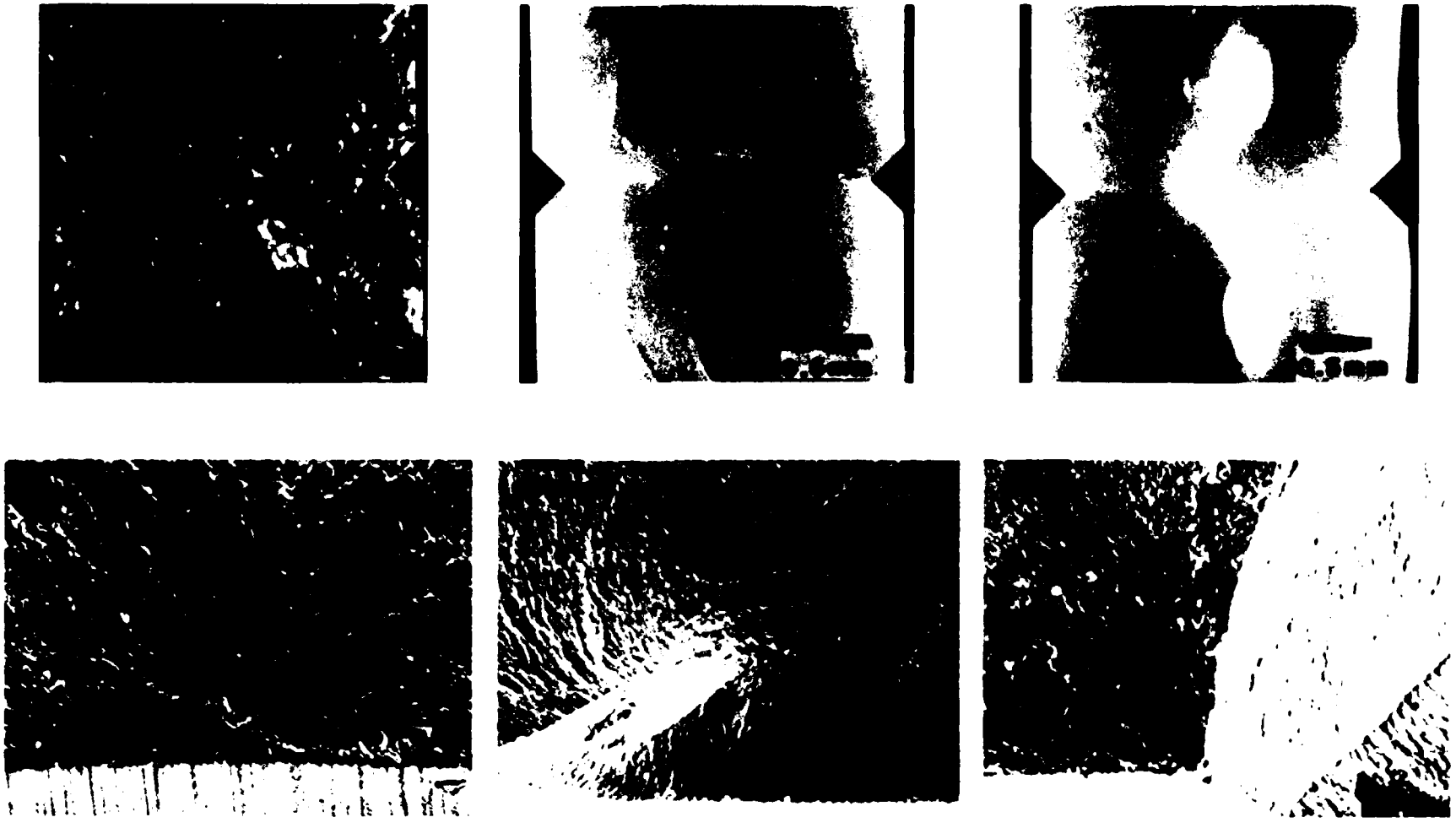

Figure 14. (Cont'd)

MATERIAL R

(not available)

AS RECEIVED

100 HRS AT 1000°C

Figure 14. (Cont'd)

MATERIAL S

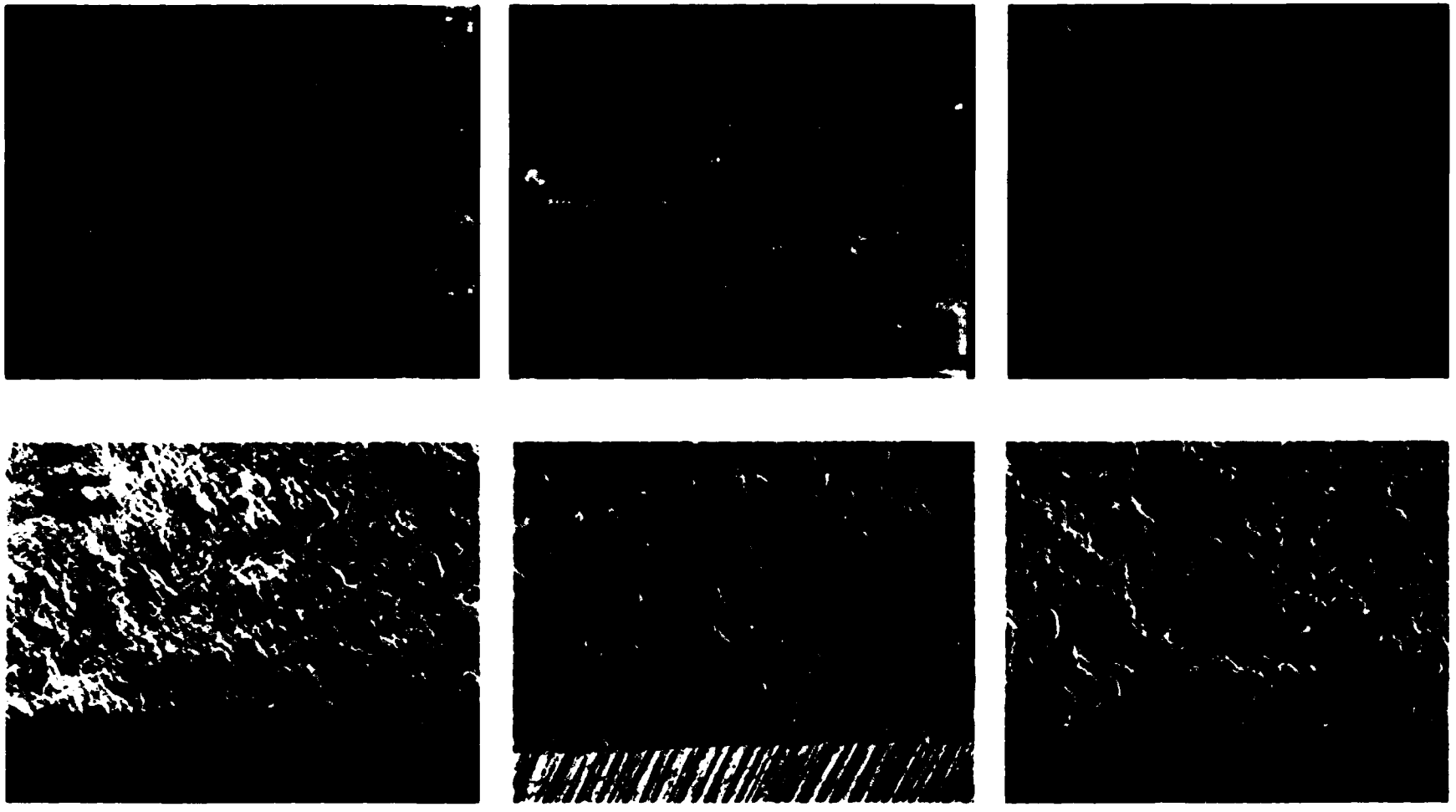

Figure 14. (Cont'd)

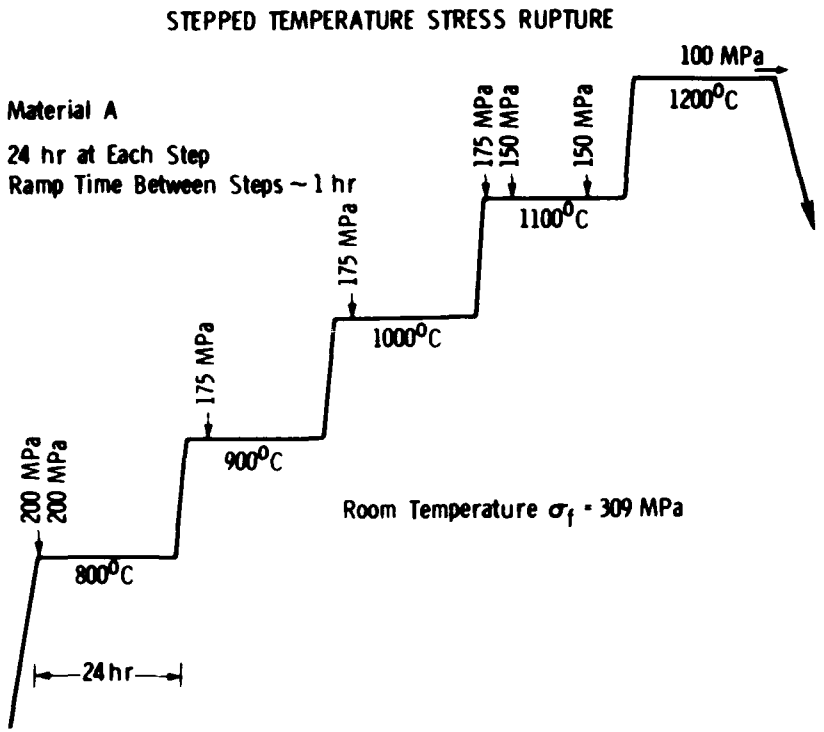
STEPPED TEMPERATURE STRESS RUPTURE
Material A
24 hr at Each Step
Ramp Time Between Steps ~ 1 hr
200 MPa
200 MPa
800°C
24 hr
175 MPa
900°C
175 MPa
1000°C
175 MPa
150 MPa
1100°C
150 MPa
100 MPa
1200°C
Room Temperature σ_f = 309 MPa

(a)

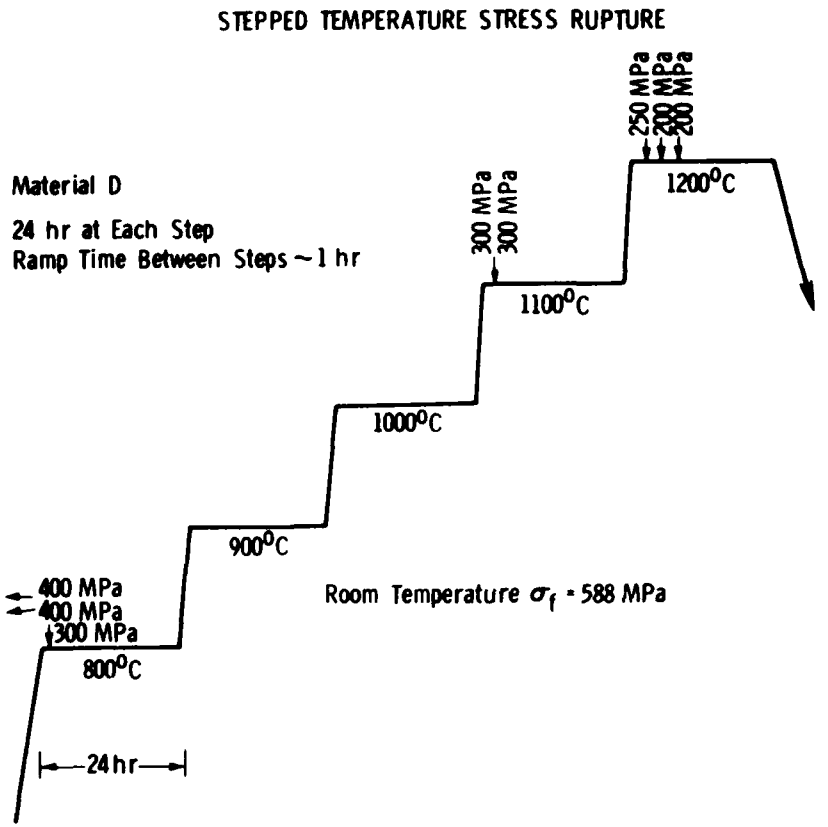
STEPPED TEMPERATURE STRESS RUPTURE
Material D
24 hr at Each Step
Ramp Time Between Steps ~ 1 hr
400 MPa
400 MPa
300 MPa
800°C
24 hr
900°C
1000°C
300 MPa
300 MPa
1100°C
250 MPa
250 MPa
200 MPa
1200°C
Room Temperature σ_f = 588 MPa

(b)

Figure 15.

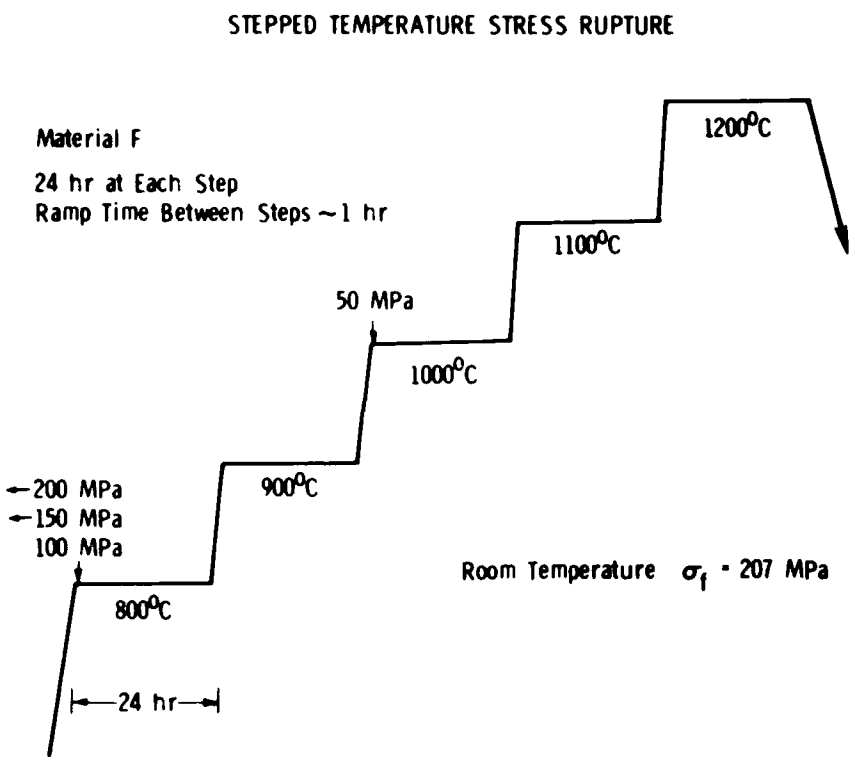
STEPPED TEMPERATURE STRESS RUPTURE
Material F
24 hr at Each Step
Ramp Time Between Steps ~ 1 hr
1200°C
1100°C
50 MPa
1000°C
900°C
200 MPa
150 MPa
100 MPa
800°C
24 hr
Room Temperature σ_f = 207 MPa

(c)

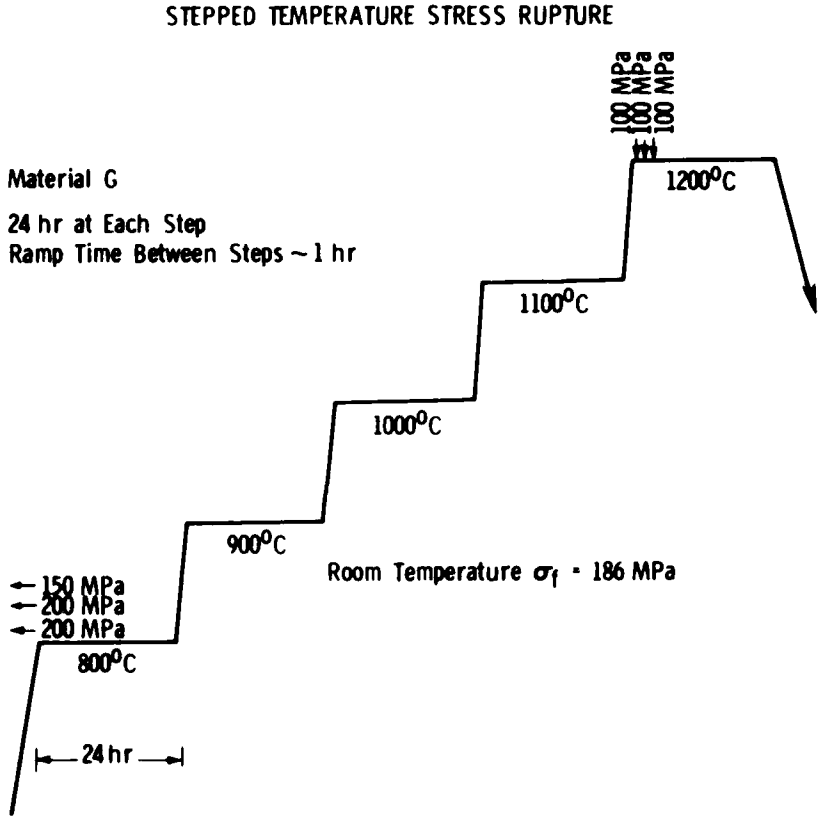
STEPPED TEMPERATURE STRESS RUPTURE
Material G
24 hr at Each Step
Ramp Time Between Steps ~ 1 hr
100 MPa
100 MPa
100 MPa
1200°C
1100°C
1000°C
900°C
Room Temperature σ_f = 186 MPa
150 MPa
200 MPa
200 MPa
800°C
24 hr

(d)

Figure 15.

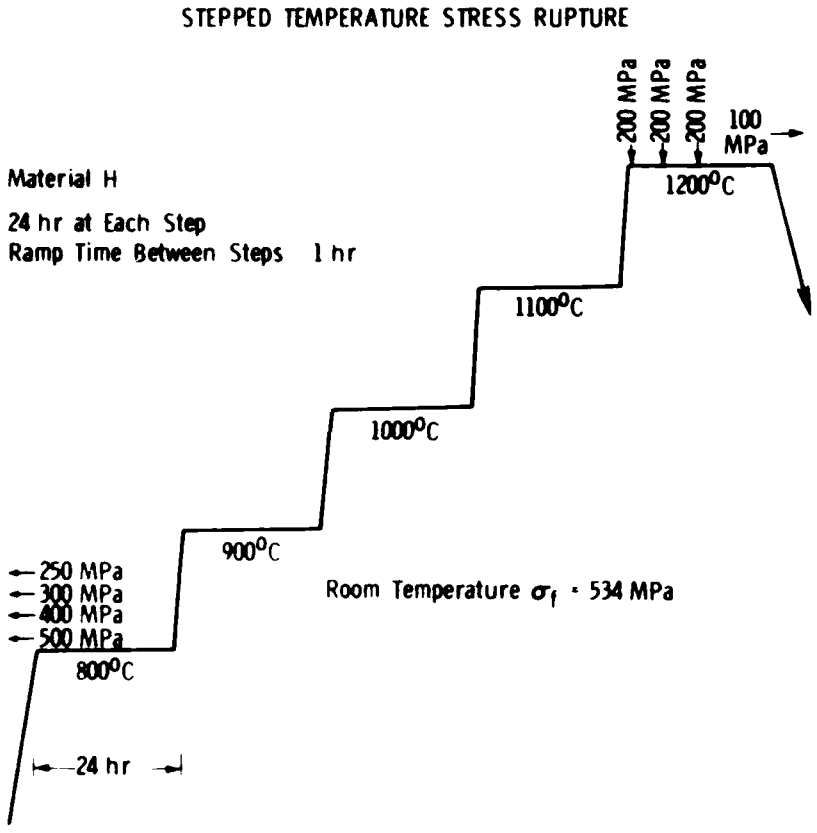
STEPPED TEMPERATURE STRESS RUPTURE
Material H
24 hr at Each Step
Ramp Time Between Steps 1 hr
200 MPa
200 MPa
200 MPa
100 MPa
1200°C
1100°C
1000°C
900°C
800°C
250 MPa
300 MPa
400 MPa
500 MPa
Room Temperature σ_f = 534 MPa
24 hr

(e)

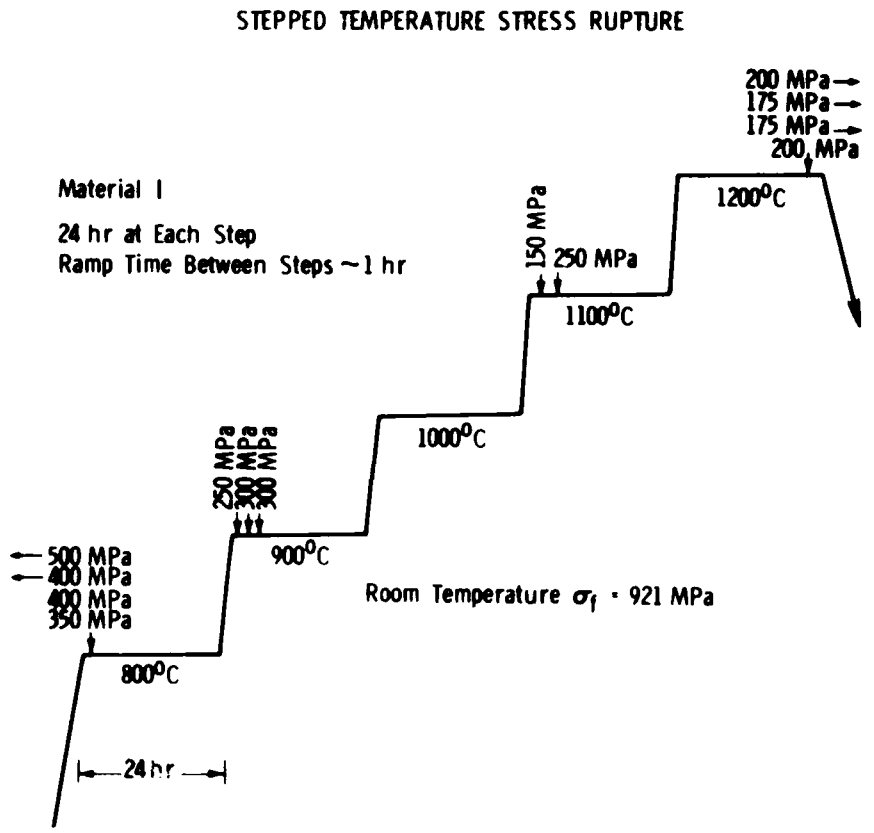
STEPPED TEMPERATURE STRESS RUPTURE
Material I
24 hr at Each Step
Ramp Time Between Steps ~1 hr
200 MPa
175 MPa
175 MPa
200 MPa
1200°C
150 MPa
250 MPa
1100°C
1000°C
250 MPa
300 MPa
300 MPa
900°C
500 MPa
400 MPa
400 MPa
350 MPa
800°C
Room Temperature σ_f = 921 MPa
24 hr

(f)

Figure 15.

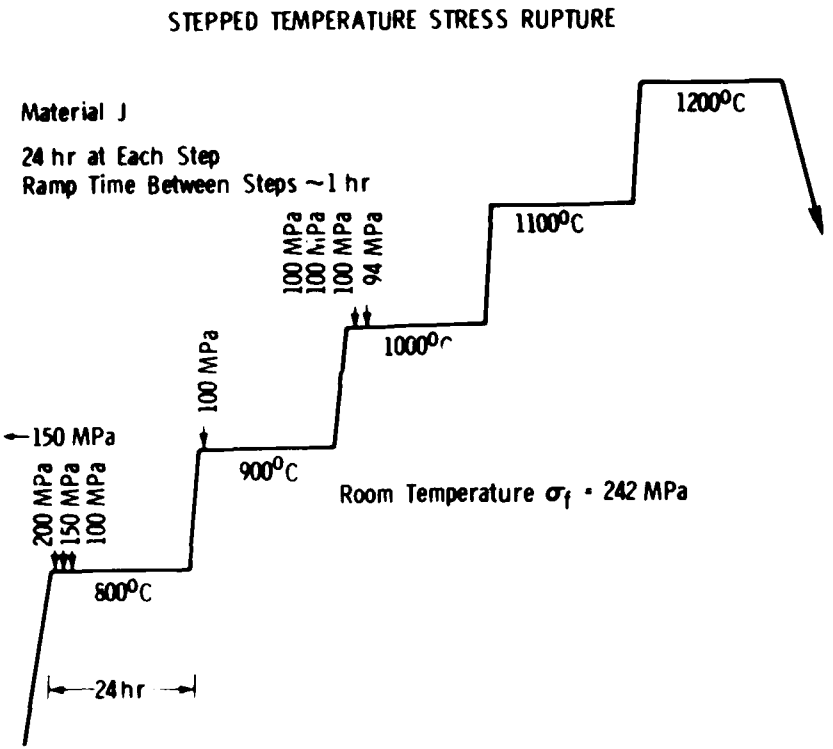
STEPPED TEMPERATURE STRESS RUPTURE
Material J
24 hr at Each Step
Ramp Time Between Steps ~1 hr
200 MPa
150 MPa
100 MPa
←150 MPa
800°C
100 MPa
900°C
100 MPa
100 MPa
100 MPa
94 MPa
1000°C
1100°C
1200°C
Room Temperature σ_f = 242 MPa
24 hr

(g)

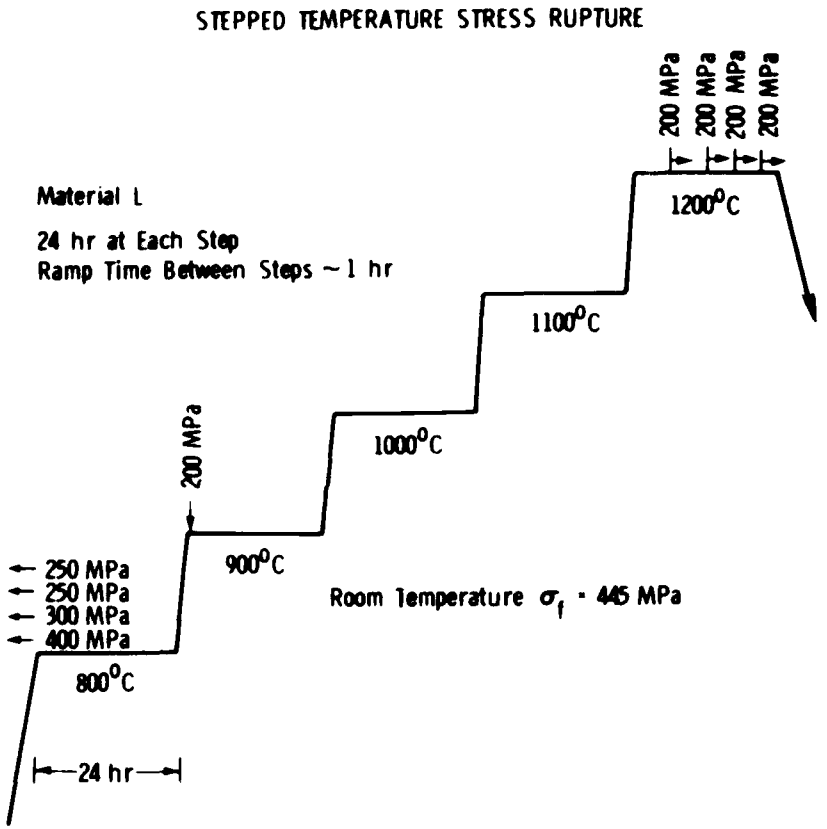
STEPPED TEMPERATURE STRESS RUPTURE
Material L
24 hr at Each Step
Ramp Time Between Steps ~1 hr
200 MPa
200 MPa
200 MPa
200 MPa
1200°C
1100°C
1000°C
200 MPa
900°C
← 250 MPa
← 250 MPa
← 300 MPa
← 400 MPa
800°C
Room Temperature σ_f = 445 MPa
24 hr

(h)

Figure 15.

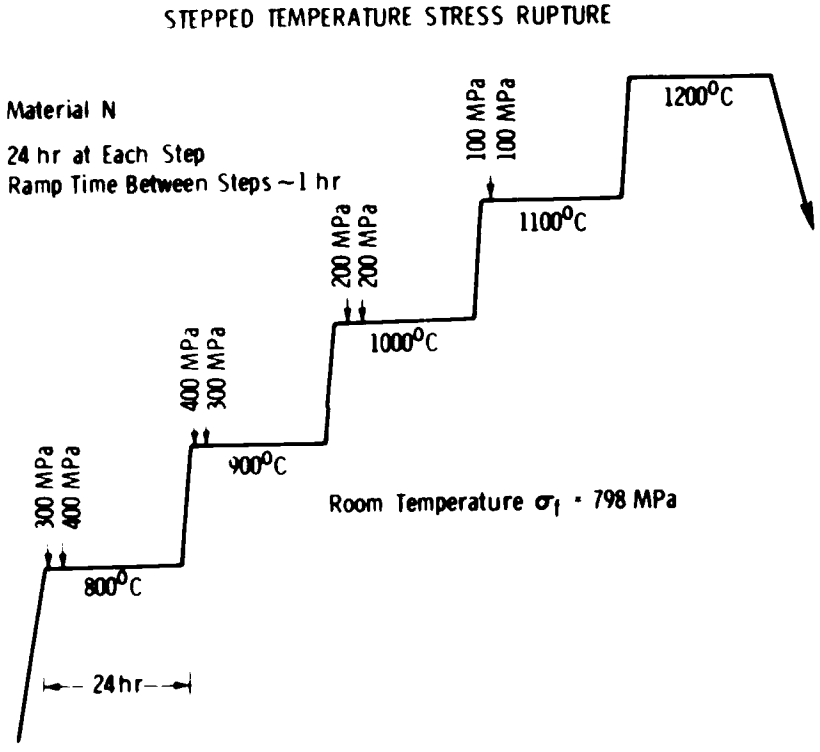
STEPPED TEMPERATURE STRESS RUPTURE
Material N
24 hr at Each Step
Ramp Time Between Steps ~ 1 hr
300 MPa
400 MPa
800°C
400 MPa
300 MPa
900°C
200 MPa
200 MPa
1000°C
100 MPa
100 MPa
1100°C
1200°C
Room Temperature σ_f = 798 MPa
24 hr

(i)

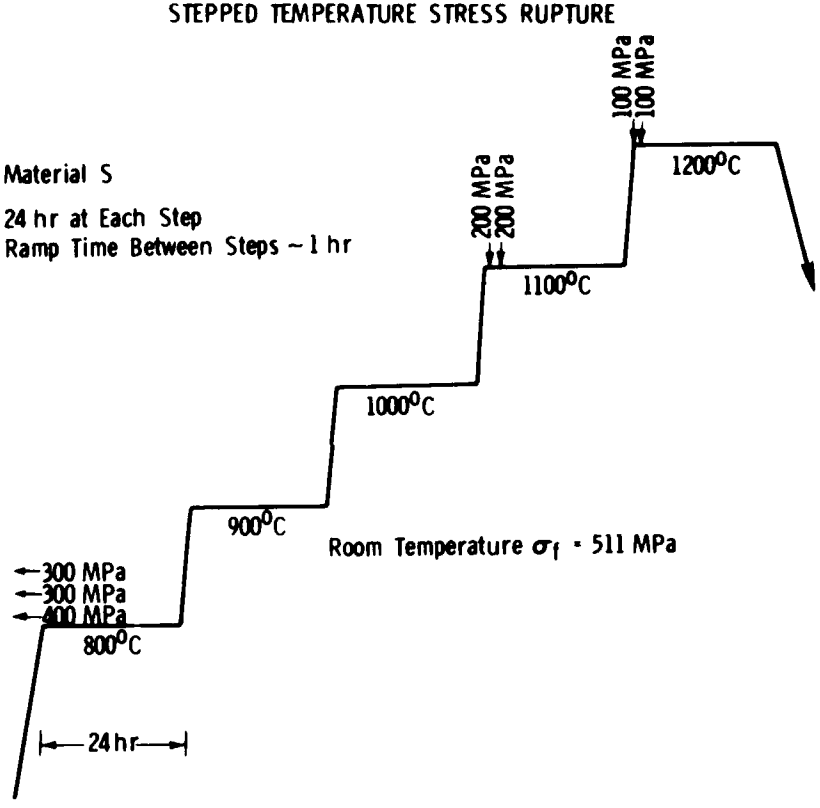
STEPPED TEMPERATURE STRESS RUPTURE
Material S
24 hr at Each Step
Ramp Time Between Steps ~ 1 hr
300 MPa
300 MPa
400 MPa
800°C
900°C
1000°C
200 MPa
200 MPa
1100°C
100 MPa
100 MPa
1200°C
Room Temperature σ_f = 511 MPa
24 hr

(j)

Figure 15.

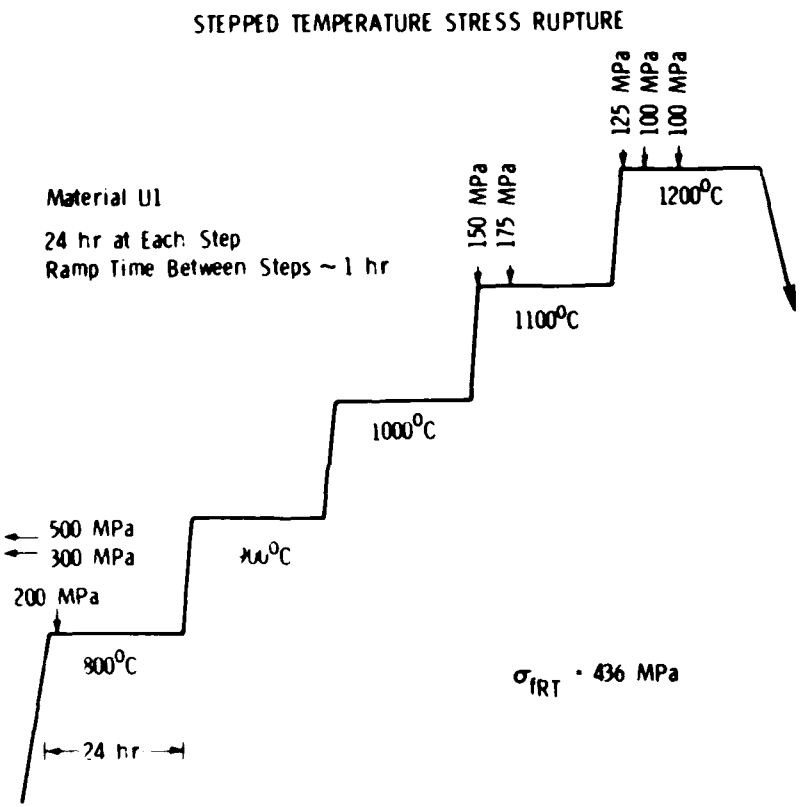
STEPPED TEMPERATURE STRESS RUPTURE
Material U1
24 hr at Each Step
Ramp Time Between Steps ~ 1 hr
125 MPa
100 MPa
100 MPa
150 MPa
175 MPa
1200°C
1100°C
1000°C
500 MPa
300 MPa
200 MPa
800°C
24 hr
σfRT = 436 MPa

(a)

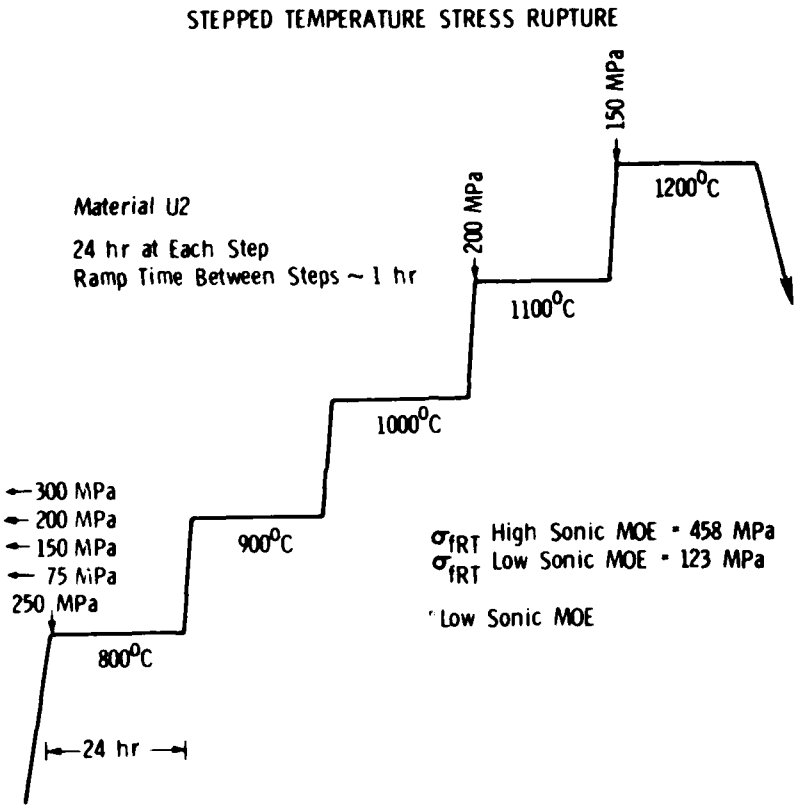
STEPPED TEMPERATURE STRESS RUPTURE
Material U2
24 hr at Each Step
Ramp Time Between Steps ~ 1 hr
150 MPa
200 MPa
1200°C
1100°C
1000°C
900°C
300 MPa
200 MPa
150 MPa
75 MPa
250 MPa
800°C
24 hr
σfRT High Sonic MOE = 458 MPa
σfRT Low Sonic MOE = 123 MPa
Low Sonic MOE

(b)

Figure 16.

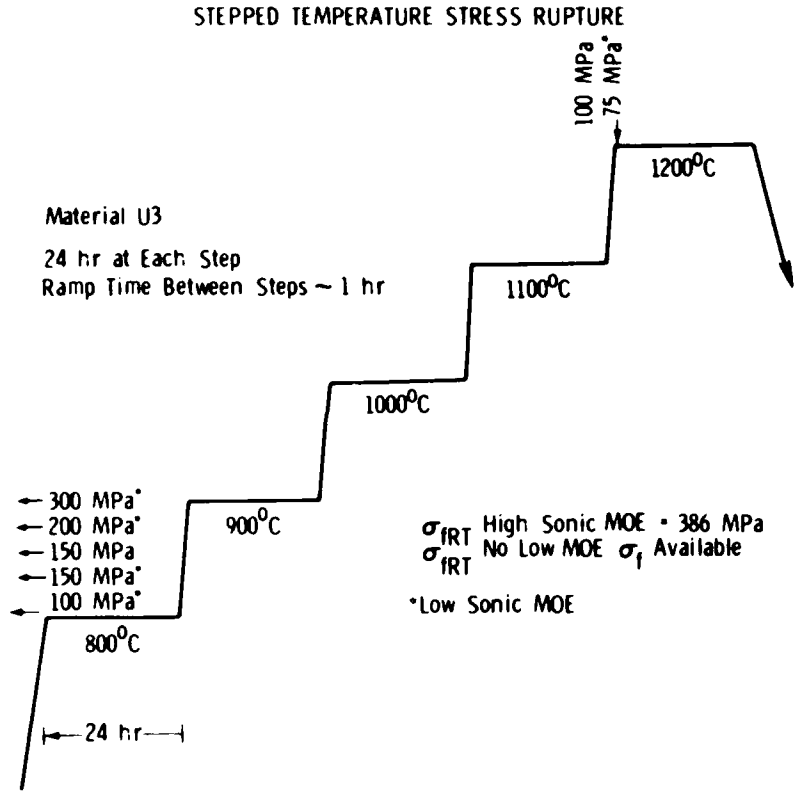

(c)

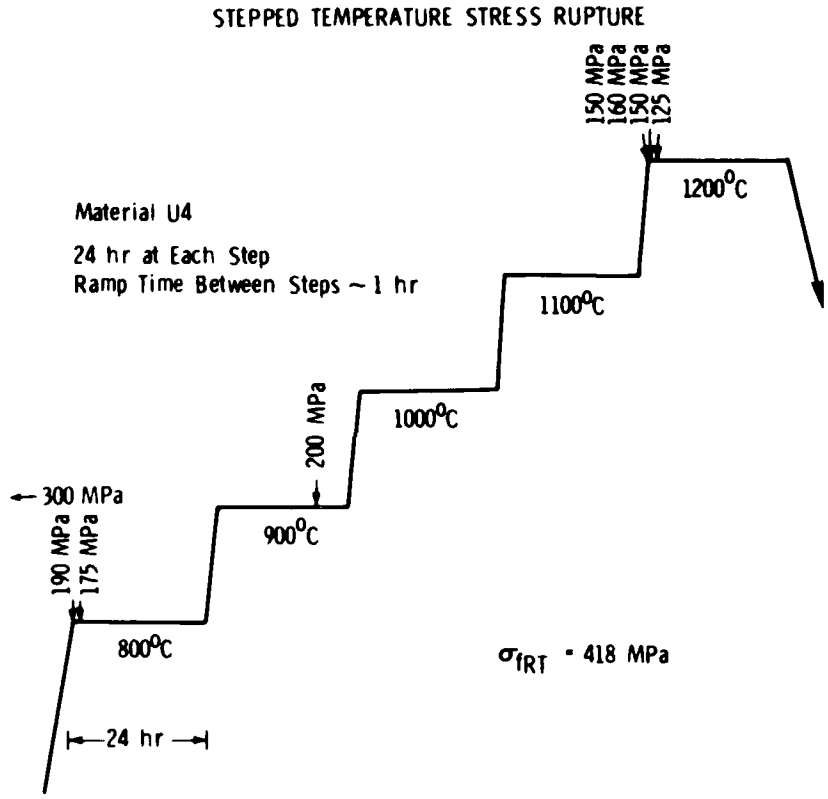

(d)

Figure 16. (Cont'd)

MATERIAL U1

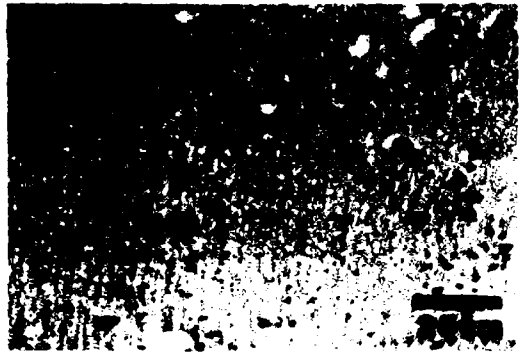

(not available)

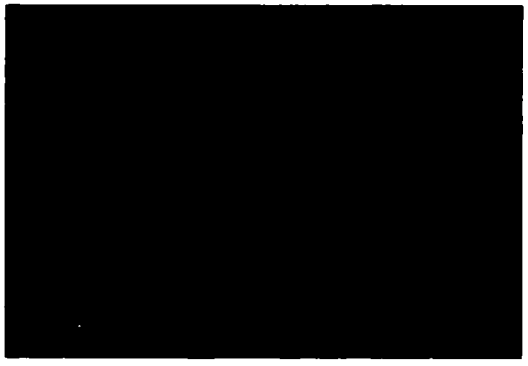

AS RECEIVED

100 HRS AT 1000°C

500 HRS AT 1000°C

Figure 17.

MATERIAL U2

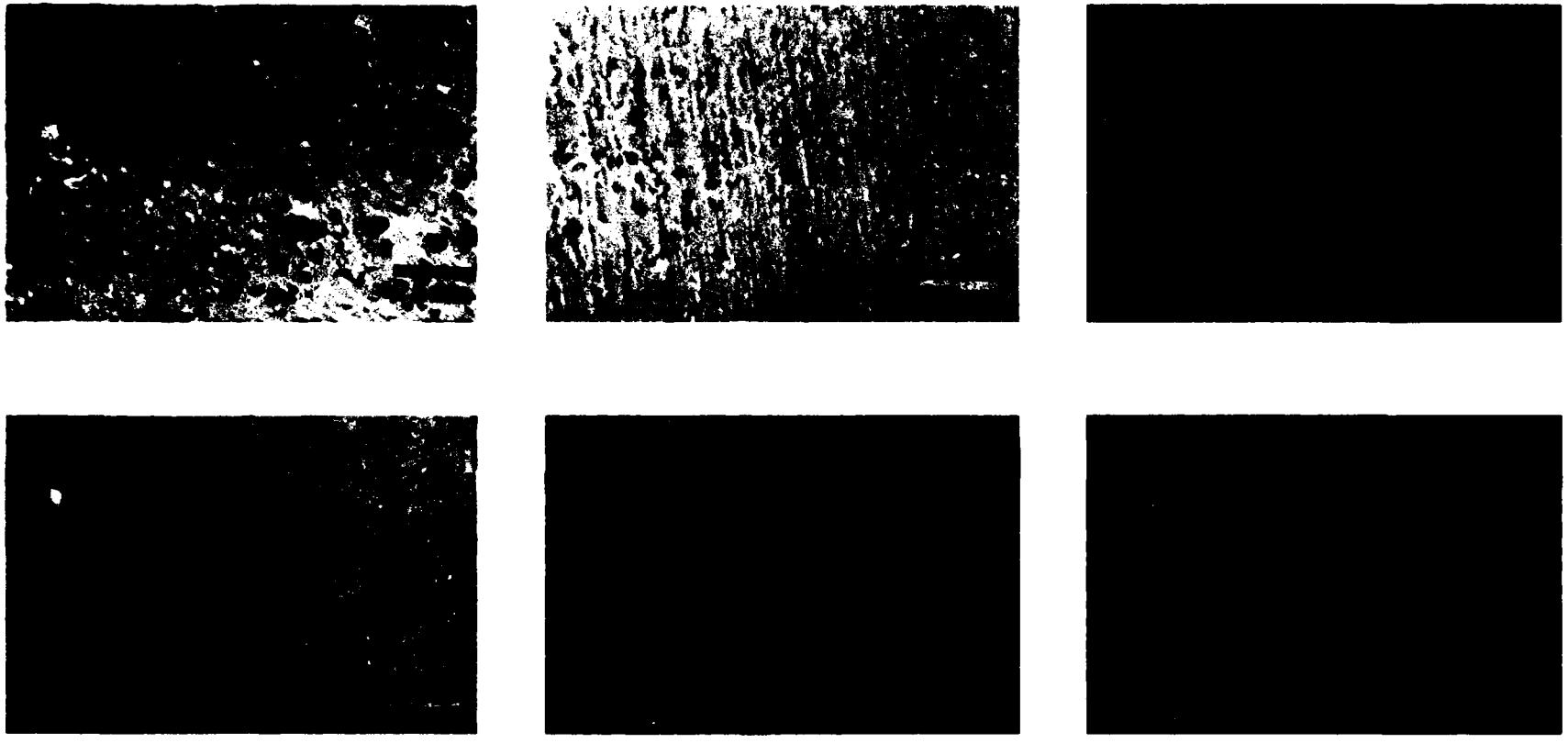

Figure 17. (Cont'd)

MATERIAL U3

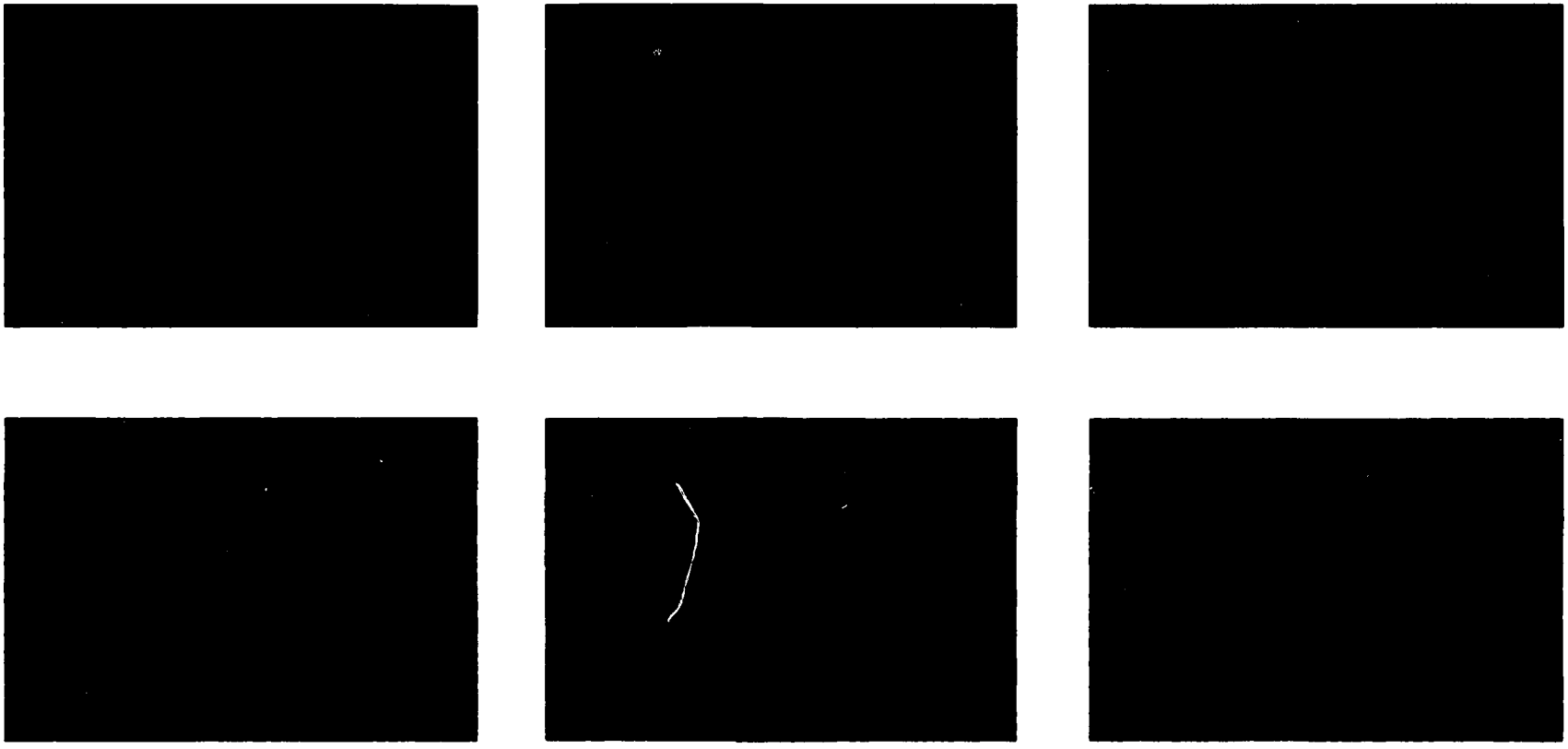

Figure 17. (Cont'd)

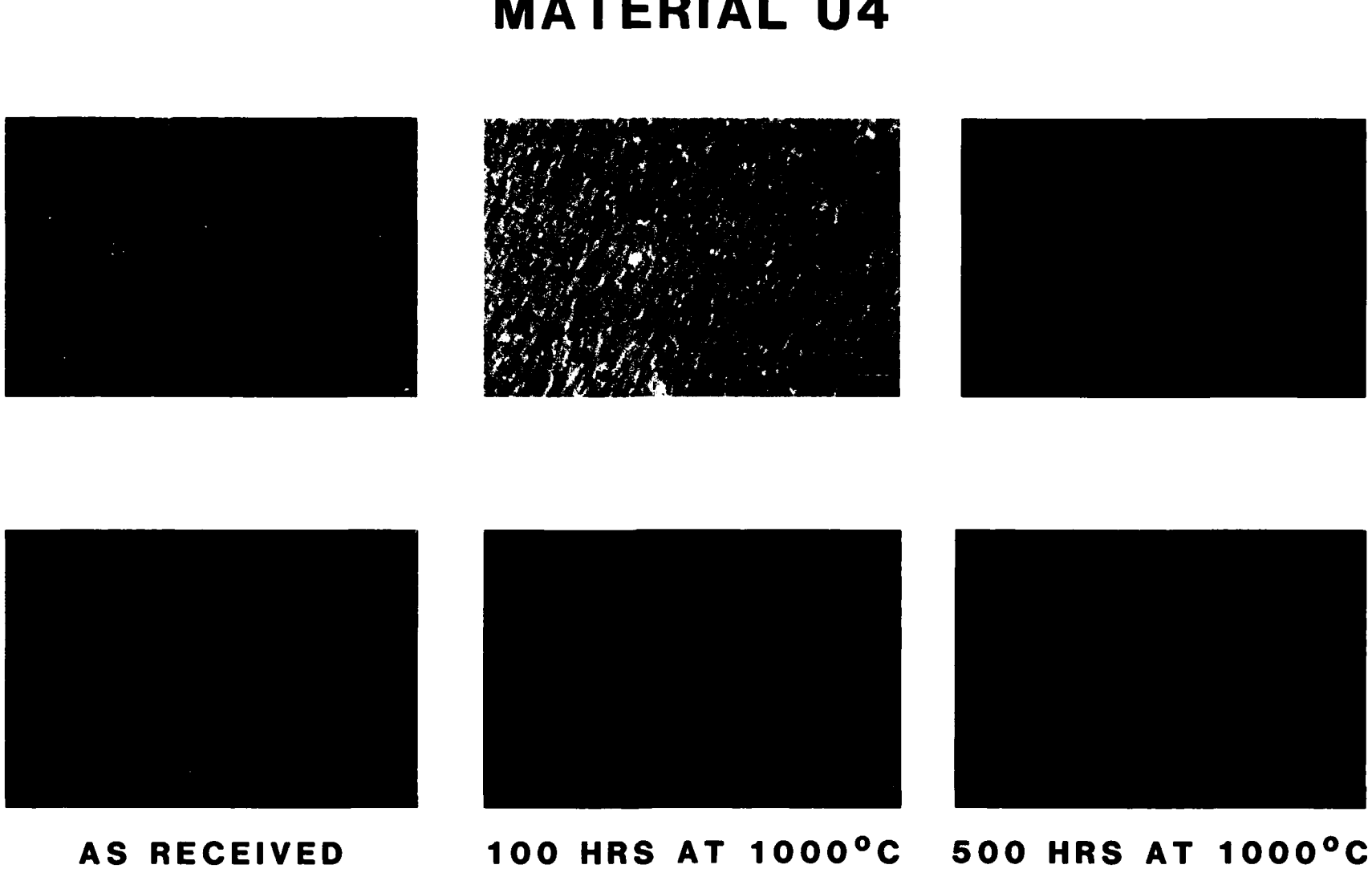

Figure 17. (Cont'd)

MATERIAL U5

(not available)

(not available)

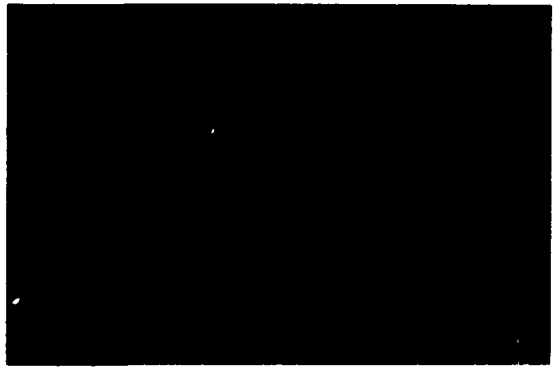

AS RECEIVED

500 HRS AT 1000°C

Figure 17. (Cont'd)

MATERIAL U6

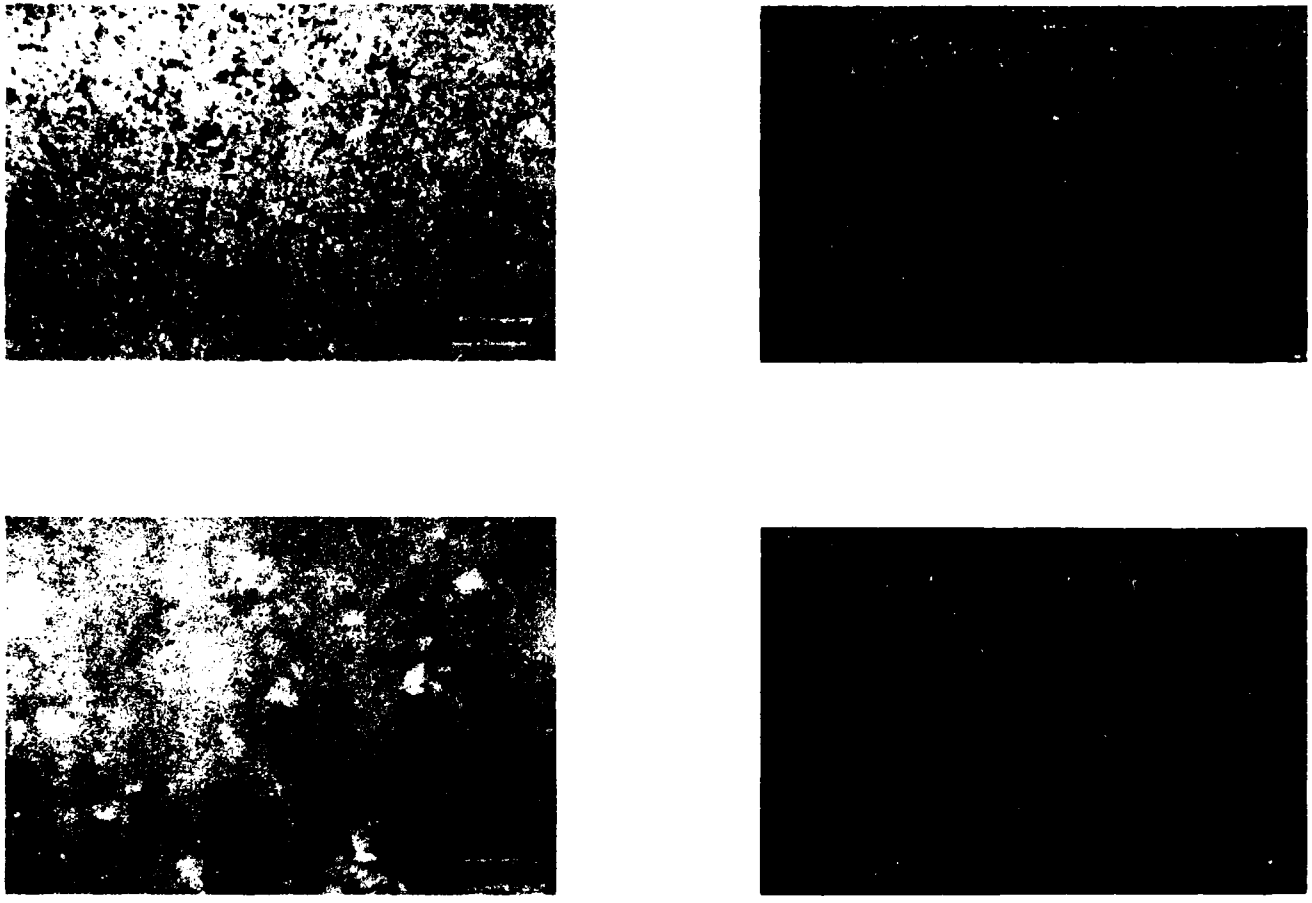

Figure 17. (Cont'd)

APPENDIX A. POLISHING PROCEDURE FOR ZIRCONIA TOUGHENED MATERIALS

Several different polishing procedures were tried before a successful method was found. The first procedure was as follows:

1. Flatten the sample with a 15 μm diamond wheel.

2. Rough polish with 6/12 μm diamond on a lead lap.

3. Final polish with cerium oxide on a phellon cloth.

This procedure resulted in surfaces that exhibited many "pop outs". These were caused by the transformation of the tetragonal precipitates due to the polishing; i.e., no longer constrained after the matrix was removed by polishing, they popped out from the surface. This problem indicated that the polishing might have caused surface damage such that the surface phase content was not that of the bulk.

Another procedure was tried in order to avoid the problem of pop outs and to ensure the polished surface represented a bulk phase content. In this procedure, colloidal silica on phellon cloth was used for the final polish rather than the ceria. In order to check that the polish had removed the transformed surface layer due to machining of the bend specimen and had not caused any more damage, the sample was polished and the surface x-rayed repeatedly until the x-ray diffraction pattern showed no changes from polishing. The first polishing cycle removed ~25 μm; subsequent polishes removed ~15 μm. It was found that, after 3 to 4 polishing cycles, the x-ray diffraction pattern remained unchanged.

Subsequent polished samples had 25 μm removed using the 15 μm diamond wheel and 5 μm removed with the 6/12 μm diamond paste before the final polishing with the colloidal silica.

APPENDIX B. PHASE ANALYSIS OF ZIRCONIA SYSTEM USING X-RAY DIFFRACTION

Analysis of a powder x-ray diffraction pattern is the most commonly used method of determining the phase content of an unknown sample. Usually the unknown contains two or more chemically dissimilar phases and the analysis is straightforward.[B1] In some cases (e.g., where the unknown is a transformation toughened partially-stabilized zirconia or TTZ), the sample may contain several phases, all of related lattice geometry. When this is the case, the phase analysis is less tractable. In the zirconia case, two factors that affect the analysis are the difficulty in resolving the tetragonal (101)* and cubic (111) peaks when copper radiation is used, and the common assumption that only two phases are present in the sample.

Three phases are normally found in partially stabilized zirconias: cubic, tetragonal, and monoclinic. The lattice parameters of the three phases depend on the radius of the substituted stabilizing cation and the amount of the stabilizer.

*The lattice parameters for the three phases of pure zirconia at room temperature were extrapolated from those given by Scott.[B2]

B1. KLUG, H.P., and ALEXANDER, L.E. *X-Ray Diffraction Procedures.* 2nd Ed., John Wiley and Sons, New York, 1974, p. 531-562.

B2. SCOTT, H.G. *Phase Relationships in the Zirconia-Yttria Systems.* J. Mater. Sci., v. 10, 1975, p. 1527-1535.

Table B-1 gives the interplanar spacing, d, and the calculated peak position for the first four peaks for CuKα radiation for pure ZrO_2 and for 2, 4, 6, and 8 mole % MgO, CaO, and $YO_{1.5}$ stabilized ZrO_2. From this table it can be seen that the most intense peaks of the cubic and tetragonal phases are very closely spaced in 2θ, and, in most cases, would not be resolvable on the diffractogram. The resolution of the two peaks is made more difficult by particle size broadening of the tetragonal peak due to the fine size of the tetragonal precipitates within the cubic matrix and by strain broadening due to the lattice mismatch between the cubic and tetragonal cells. Because of the resolution problem, it could be difficult to determine if there are two or three phases present in the sample. If three phases are present, the equations for the calculation of the phase content used in the past are incorrect, as only two phases are assumed, and the intensity due to a third phase is ignored.

Table B-1. CALCULATED INTERPLANAR SPACING AND PEAK POSITION FOR THE FIRST FOUR PEAKS OF SEVERAL ZIRCONIA AND STABILIZER SYSTEMS AT ROOM TEMPERATURE FOR CuKα RADIATION

Pure Zirconia	hkl	d (Å)	2θ (degrees)
Monoclinic	(111)	3.162	28.218
Tetragonal	(101)	2.955	30.246
Cubic	(111)	2.947	30.331
Monoclinic	(11$\bar{1}$)	2.839	31.516

	2 mole%		4 mole%		6 mole%		8 mole%	
	d (Å)	2θ	d (Å)	2θ	d (Å)	2θ	d (Å)	2θ
MgO Stabilized								
m(111)	3.166	28.817	3.165	28.198	3.163	28.029	3.163.	28.216
t(101)	2.953	30.265	2.952	30.277	2.951	30.288	2.949	30.306
c(111)	2.942	30.380	2.940	30.404	2.938	30.428	2.935	30.453
m(11$\bar{1}$)	2.981	31.942	2.839	31.511	2.838	31.524	2.837	31.538
CaO Stabilized								
m(111)	3.164	28.209	3.160	28.238	3.157	28.268	3.154	28.299
t(101)	2.956	30.239	2.956	30.235	2.956	30.229	2.957	30.226
c(111)	2.949	30.306	2.950	30.294	2.952	30.276	2.953	30.264
m(11$\bar{1}$)	2.842	31.477	2.843	31.471	2.843	31.465	2.844	31.459
$YO_{1.5}$ Stabilized								
m(111)	3.167	28.178	3.167	28.178	3.167	28.177	3.167	28.177
t(101)	2.956	30.232	2.957	30.220	2.959	30.220	2.961	31.184
c(111)	2.947	30.331	2.949	30.306	2.951	30.282	2.954	31.372
m(11$\bar{1}$)	2.844	31.449	2.846	31.428	2.849	31.401	2.851	31.372

Note: The lattice parameters used to calculate the d and 2θ values in Table B-1 were obtained from a least-squares fit to lattice parameters given in References B2, B3, and B5-B19.

In almost all previous work done on phase analysis of zirconia systems it has been assumed that only two phases were present, either monoclinic and cubic or monoclinic and tetragonal.* This assumption is not always valid, especially when the thermal history of the sample is not known. If all three phases are present, the original equations derived by Garvie and Micholson[B3] cannot be used.

*Porter and Heuer[B4] mention that "x-ray analysis of bulk samples could not be used for determining the presence or absence of (t)-ZrO_2 because of the overlap with peaks from the (c) matric". They used selected area electron diffraction to determine the phase content of their samples.

B3. GARVIE, R.C., and NICHOLSON, P.S. *Phase Analysis in Zirconia Systems* J. Amer. Ceram. Soc., v. 55, no. 6, 1972, p. 303-305.
B4. PORTER, D.L., and HEUER, A.H. *Microstructural Development in MgO-Partially Stabilized Zirconia (MG-PSZ)* J. Amer. Cer Soc., v. 62, no. 5-6, 1979, p. 298-405.

The resolution between the tetragonal (101) and the cubic (111) peaks can be increased by using CrKα radiation which has a longer wavelength than does CuKα radiation. Table B-2 gives the peak positions for the four main peaks of pure ZrO_2 and for 2, 4, 6, and 8 mole % ZrO_2 doped with MgO, CaO, and $YO_{1.5}$ for CrKα radiation. As can be seen by comparing Tables B-1 and B-2, the use of CrKα radiation increases the angular difference between the peaks used to calculate the phase content. Newer x-ray equipment often has the capability to step scan through the angular range of the four main peaks. This data can be used to perform a pattern decomposition and thus to determine the integrated intensity of all the peaks.

Table B-2. CALCULATED INTERPLANAR SPACING AND PEAK POSITION FOR THE FIRST FOUR PEAKS OF SEVERAL ZIRCONIA AND STABILIZER SYSTEMS AT ROOM TEMPERATURE FOR CrKα RADIATION

Pure Zirconia	hkl	d (Å)	2θ (degrees)
Monoclinic	(11ī)	3.162	42.477
Tetragonal	(101)	2.955	45.614
Cubic	(111)	2.947	45.745
Monoclinic	(111)	2.839	47.591

	2 mole%		4 mole%		6 mole%		8 mole%	
	d(Å)	2θ	d(Å)	2θ	d(Å)	2θ	d(Å)	2θ
MgO Stabilized								
m(111)	3.166	42.423	3.165	42.440	3.163	42.457	3.163.	42.468
t(101)	2.953	45.646	2.952	45.664	2.951	45.682	2.949	45.710
c(11ī)	2.949	45.711	2.950	45.692	2.952	45.663	2.953	45.645
m(11ī)	2.841	47.560	2.839	47.590	2.838	47.609	2.837	47.632
CaO Stabilized								
m(111)	3.164	42.456	3.160	42.502	3.157	42.549	3.154	42.596
t(101)	2.956	45.605	2.956	45.600	2.956	45.591	2.956	45.585
c(11ī)	2.949	45.711	2.950	45.692	2.952	45.633	2.953	45.645
m(11ī)	2.842	47.536	2.843	47.526	2.843	47.518	2.844	47.509
$YO_{1.5}$ Stabilized								
m(111)	3.167	42.410	3.167	42.410	3.167	42.410	3.167	42.408
t(101)	2.956	45.595	2.957	45.577	2.959	45.544	2.961	45.521
c(11ī)	2.947	45.749	2.949	45.711	2.951	45.673	2.954	49.635
m(11ī)	2.844	47.493	2.846	47.460	2.849	47.418	2.851	47.372

Note: The lattice parameters used to calculate the d and 2θ values in Table B-2 were obtained from a least-squares fit to lattice parameters given in References B2, B3, and B5-B19.

The measured integrated intensity of a powder x-ray diffraction peak can be assumed to be:

$$I_i = (K\, R_i\, V_i)/2\,\mu m \qquad \text{(B1)}$$

where K is a constant that includes machine parameters, R_i is the calculated intensity of that reflection, V_i is the volume fraction of phase i, and μm is the linear absorption coefficient of the mixture. R_i is given as:

$$R_i = \left(\frac{1}{v_i^2}\right)\left|F_i\right|^2 P_i \left(\frac{1 + \cos^2 2\theta_i}{\sin^2\theta_i \cos\theta_i}\right) e^{-2i} \qquad \text{(B2)}$$

where v_i is the unit cell volume of phase i, F_i is the structure factor, P_i is the multiplicity of that reflection, θ_i is the Bragg angle, and the exponential term is the temperature factor, which can be assumed to be similar for all three phases. Since K and the linear absorption coefficient of the mixture are constant for any one diffractogram and sample, Equation B1 can be rearranged to give:

$$V_i = I_i/R_i$$

The total phase content of a three component sample is:

$$V_m + V_t + V_c = 1 \tag{B3}$$

where m, t, and c denote monoclinic, tetragonal, and cubic phases, respectively. For the case where the tetragonal and cubic peaks can be resolved, the equations for the volume fraction of the three phases present become:

$$V_m = \frac{1}{1 + \frac{R_m}{I_m}\left[\frac{I_t}{R_t} + \frac{I_c}{R_c}\right]} \tag{B3a}$$

$$V_t = V_m\left[\frac{I_t}{R_c} \times \frac{R_m}{I_m}\right] \tag{B3b}$$

$$V_c = V_m\left[\frac{I_c}{R_c} \times \frac{R_m}{I_m}\right] \tag{B3c}$$

If the tetragonal (101) and the cubic (111) peaks cannot be resolved, then the integrated intensity of the peak on the diffractogram is a sum of intensity of the tetragonal (101) and cubic (111) peaks. In this case the volume fraction of phases present in the sample must be given as that of monoclinic and [tetragonal + cubic], and

$$V_m + V_{t+c} = 1 \quad . \tag{B4}$$

Rearranging and solving for V_{t+c}:

$$V_m = 1 - V_{t+c}$$

and

$$V_{t+c} = \frac{1}{1 + \left[\frac{I_m}{R_m} \times \frac{R_{t+c}}{I_{t+c}}\right]} \quad . \tag{B4a}$$

Table B-3 gives the calculated R_1 values for the monoclinic (111) and (111), tetragonal (101), and cubic (111) peaks for both copper and chromium Kα radiation. The sum of the R values, as well as the sum of the integrated intensities, of the two monoclinic peaks is used in the above equations.

Table B-3. THE R VALUES OF THE FOUR PEAKS FOR CuKα AND CrKα RADIATION

	R CuKα	R CrKα
m(111)	124.92	35.59
t(101)	187.96	73.96
c(111)	200.31	81.44
m(111)	102.10	23.74

The use of the rederived equations for calculating the phase content of the zirconia sample gives more accurate results than use of earlier equations, as these equations take into account the potential difficulty in resolving the two main peaks of the tetragonal and cubic phases.

Note: Throughout this appendix, the primative setting of the tetragonal cell will be used.

B5. DUWEZ, P., and ODELL, F. *Quantitative Analysis of Cubic and Monoclinic Zirconia by X-Ray Diffraction.* J. Amer. Cer. Soc., v. 32, no. 5, 1949, p. 180-183.

B6. DUWEZ, P., ODELL, F., and BROWN, F.H., Jr. *Stabilization of Zirconia with Calcia and Magnesia.* J. Amer. Cer. Soc., v. 35, no. 5, 1952, p. 107-113.

B7. McCULLOUGH, J.D., and TRUEBLOOD, K.N. *The Crystal Structure of Baddeleyite (Monoclinic ZrO_2).* Acta Cryst., v. 12, 1959, p. 507-511.

B8. ADAM, J., and ROGERS, M.D. *The Crystal Structure of ZrO_2 and HfO_2.* Acta Cryst., v. 12, 1959, p. 951.

B9. VIECHNICKI, D., and STUBICAN, V.S. *Mechanism of Decomposition of Cubic Solid Solution in the System ZrO_2 - MgO.* J. Amer. Cer. Soc., v. 48, no. 6, 1965, p. 292-297.

B10. GARVIE, R.C. *The Cubic Field in the System CaO-ZrO_2.* J. Amer. Cer. Soc., v. 51, no. 10, 1968, p. 553-556.

B11. PATIL, R.N., and SUBBARAO, E.C. *Axial Thermal Expansion of ZrO_2 and HfO_2 in the Range Room Temperature to 1400°C.* J. Appl. Cryst., v. 2, 1969, p. 281-288.

B12. PDF Card No. 26-341, Joint Committee on Powder Diffraction Standards, 1976.

B13 PDF Card No. 27-997, Joint Committee on Powder Diffraction Standards, 1977.

B14. HANNICK, R.H.J. *Growth Morphology of the Tetragonal Phase in Partially Stabilized Zirconia.* J. Mater. Sci., v. 13, 1978, p. 2487-2496.

B15. PORTER, D.L., EVANS, A.G., and HEUER, A.H. *Transformation Toughening in Partially-Stabilized Zirconia (PSZ).* Acta Metal., v. 27, 1979, p. 1649-1654.

B16. PDF Card No. 30-1468, Joint Committee on Powder Diffraction Standards, 1980.

B17. HANNICK, R.H.J., JOHNSTON, K.A., PASCOE, R.T., and GARVIE, R.C. *Microstructural Changes During Isothermal Aging of a Calcia Partially Stabilized Zirconia Alloy.* Science and Technology of Zirconia, Advances in Ceramics, v.3, A.H. Heuer and L.W. Hobbs, ed., American Ceramic Society, Columbus, Ohio, 1981.

B18. CHAIM, R., and BRANDON, D.G. *Microstructure Evolution and Ordering in Commercial Mg-PSZ.* J. Mater. Sci., v. 19, 1984, p. 2934-2942.

B19. CHAIM, R., and BRANDON, D.G. *Stability of the Polymorphs in Y_2O_3 Stabilized ZrO_2.* To be published.

DISTRIBUTION LIST

No. of Copies	To
1	Donald F. Adams, Composite Materials Research Group, Mechanical Engineering Department, University of Wyoming, Laramie, WY 82071
1	Jane W. Adams, Corning Glass Works, SP-DV-21, Corning, NY 14831
1	Anil K. Agarwal, Product Manager, High Performance Ceramics, Norton Company, One Bond Street, Worcester, MA 01606
1	Richard T. Alpaugh, Department of Energy, Office of Transportation Systems, CE-131 FORSTL, 1000 Independence Avenue, Washington, DC 20585
1	James P. Arnold, U.S. Army Belvoir, R&D Center, Fort Belvoir, VA 22060 ATTN: FTRBE-EMP
1	V. S. Avva, Dept. of Mechanical Engineering, North Carolina Agricultural and Technical State University, Greensboro, NC 27411
1	John M. Bailey, Research Consultant, Research Dept., Technical Center, Caterpillar Tractor Co., 100 NE Adams, Peoria, IL 61629
1	Murray Bailey, NASA Lewis Research Center, 21000 Brookpark Road, MS 77-6, Cleveland, OH 44135
1	J. Gary Baldoni, GTE Laboratories, INC. 40 Sylvan Road, Waltham, MA 02254
1	R. R. Baker, 34819 Lyndon Street, Livonia, MI 48154
1	Ken Baumert, Air Products and Chemicals, Inc., Box 538, Allentown, PA 18105
1	Ronald L. Beatty, ARCO Chemicals, Silag Operation, Route 6, Box A, Greer, SC 29651
1	A. L. Bement, Jr., Vice President, Technical Resources, TRW, Inc. 23555 Euclid Avenue, Cleveland, OH 44117
1	Clifton G. Bergeron, Head, Department of Ceramic Engineering, 204 Ceramics Building, University of Illinois, Urbana, IL 61801
1	William D. Bjorndahl, TRW, Inc., TRW Energy Development Group, Materials Characterization and Chemical Analysis Dept., One Space Park, Building 01, Room 2060, Redondo Beach, CA 90278
1	Paul N. Blumberg, President, Integral Technologies Inc., 415 E. Plaza Drive, Westmont, IL 60559
1	Wolfgang D. G. Boecker, SOHIO Engineered Materials Co., Niagara Falls R&D Center, P.O. Box 832 Niagara Falls, NY 14302

No. of Copies	To
1	Seymour A. Bortz, Manager, Nonmetallic Materials and Composites, Materials and Manufacturing Technology, IIT Research Institute, 10 West 35th Street, Chicago, IL 60616
1	H. K. Bowen, Department of Materials Science and Engineering, Room 12-009, Massachusetts Institute of Technology, Cambridge, MA 02139
1	Richard C. Bradt, University of Washington, Roberts Hall, FB-10, Seattle, WA 98195
1	Raymond J. Bratton, Manager, Ceramic Science, Westinghouse Research and Development Center, 1310 Beulah Road, Pittsburgh, PA 15235
1	W. Bryzik, US Army Tank Automotive Command (TACOM), R&D Center, Warren, MI 48090
1	S. T. Buljan, GTE Laboratories, Inc., 40 Sylvan Road, Waltham, MA 02154
1	John M. Byrne, Jr., Manager, Business Development, Corporate Development Department, PPG Industries, Inc., One PPG Place, Pittsburgh, PA 15272
1	Donald J. Campbell, Air Force Wright Aeronautical Laboratory, AFWAL/POX, Wright-Patterson AFB, OH 45433
1	Harry W. Carpenter, Rockwell International, Rocketdyne Division, J39-169:HC92, 6633 Canoga Avenue, Canoga Park, CA 91304
1	David Carruthers, Garrett Turbine Engine Company, 111 South 34 Street, P.O. Box 5217, Phoenix, AZ 85010
1	Se-Tak Chang, GTE Laboratories, 40 Sylvan Road, Dept. 312, Waltham, Ma 02254
1	En-sheng Chen, B&C Engineering Research, 13906 Dentwood Drive, Houston, TX 77014
1	Albert A. Chesnes, Director, Heat Engine Propulsion Division, Office of Transportation Systems, Department of Energy, CE-131 FORSTL, 1000 Independence Avenue, Washington, DC 20585
1	Melvin H. Chiogioji, Director, Office of Transportation Systems, Department of Energy, CE-13 FORSTL, 1000 Independence Avenue, SW, Washington, DC 20585
1	William J. Chmura, The Torrington Company, Corporate Research, 59 Field Street, Torrington, CT 06790
1	William L. Cleary, Associate Division Director, ORI, Inc., 1375 Piccard Drive, Rockville, MD 20850
1	Philip R. Compton, Energy Systems Office, National Aeronautics and Space Administration, Code REC-1, Washington, DC 20546

No. of Copies	To
1	John A. Coppola, Representative Director, Executive Vice President, Hitachi-Carborundum Company, Shinjuku-Mitsui Building, No. 1-1, 2-Chrome, Nishishinjuku, Shinjuku-ku, Tokyo 160, JAPAN
1	C. H. Craig, Department of Energy, 1000 Independence Avenue, CE-131 FORSTL, Washington, DC 20585
1	William J. Croft, U.S. Army Materials Technology Laboratory (MTL), Arsenal Street, Watertown, MA 02172
1	Gary M. Crosbie, Ford Motor Company, P.O. Box 2053, Room S-2079, Ceramics Materials Department, Dearborn, MI 48121
1	Floyd W. Crouse, Jr., Department of Energy, Morgantown Energy Technology Center, P.O. Box 880, Morgantown, WV 26505
1	Raymond Cutler, Ceramatec, Inc., 163 West 1700 South, Salt Lake City, UT 84115
1	Stanley J. Dapkunas, Office of Technical Coordination, Fossil Energy Technical Coordination Staff, FE-14, MS B127 GTN, Department of Energy, Washington, DC 20545
1	Robert F. Davis, North Carolina State University, Materials Engineering Department, 232 Riddick Laboratory, Raleigh, NC 27607
1	Alan L. Dragoo, Materials Scientist, Inorganic Materials Division, National Bureau of Standards, Center for Materials Science, Gaithersburg, MD 20899
1	Keith F. Dufrane, Battelle Columbus Laboratories, 505 King Avenue, Columbus, OH 43201
1	Robert J. Eagan, Manager, Chemistry and Ceramics Department 1840, Sandia National Laboratories, Albuquerque, NM 87185
1	Christopher A. Ebel, Program Manager, Norton Company, High Performance Ceramics, 1 New Bond Street, Worcester, MA 01606
1	J. J. Eberhardt, Office of Energy Utilization Research, Department of Energy, CE-142 FORSTL, 1000 Independence Avenue, Washington, DC 20585
1	E. E. Ecklund, Office of Transportation Systems, Department of Energy, CE-131 FORSTL, 1000 Independence Avenue, Washington, DC 20585
1	William A. Ellingson, Argonne National Laboratory, 9700 South Cass Avenue, Argonne, IL 60439
1	Director, Applied Technology Laboratory, U.S. Army Research and Technology Laboratory (AVSCOM), Fort Eustis, VA 23604 ATTN: SAVDL-ATL-ATP, Graydon A. Elliott

No. of Copies	To
1	A. Erdely, Chemical Engineer, 26 Avenue Gare Des Eaux-vives, 1208 Geneva, SWITZERLAND
1	Charles D. Estes, U.S. Senate, Professional Staff Member, Committee on Appropriations, Room SD-152, Dirksen Senate Office Building, Washington, DC 20510
1	Anthony G. Evans, University of California, Santa Barbara, CA 93106
1	Robert C. Evans, Asst. Manager, Vehicular Gas Turbine and Diesel Project Office, NASA-Lewis Research Center, 21000 Brookpark Road, Cleveland, OH 44135
1	John Facey, National Aeronautics and Space Administration, Energy Systems Office, Washington, DC 20546
1	John W. Fairbanks, Office of Advanced Energy Conversion, Department of Energy, FE-22 GTN, Washington, DC 20545
1	Larry Farrell, Babcock and Wilcox, P.O. Box 1260, Lynchburg, VA 24505
1	Matthew K. Ferber, University of Illinois-Urbana, 203 Ceramic Building, 105 S. Goodwin Avenue, Urbana, IL 61801
1	R. E. Fisher, President, Amercom, Inc., 8948 Fullbright Avenue, Chatsworth, CA 91311
1	H. W. Foglesong, Dow Corning Corporation, 3901 S. Saginaw Road, Midland, MI 48640
1	Robert G. Frank, Manager, Non-Metallic Materials, General Electric Company, One Neumann Way, Mail Drop M-87, P.O. Box 156301, Cincinnati, OH 45215-6301
1	Frank Gac, Department of Materials Science and Engineering, University of Washington, Seattle, WA 98195
1	Paul Glance, Director, R&D, Concept Analysis Corporation, 9145 General Court, Plymouth, MI 48170
1	Joseph W. Glatz, Naval Air Propulsion Center, Science and Technology Group, Systems Technology Division, Box 7176, PE 34, Trenton, JN 08628
1	S. Goguen, Office of Transportation Systems, Department of Energy, FORSTL, 1000 Independence Avenue, Washington, DC 20585
1	Stephen T. Gonczy, Allied Signal Research Center, Materials [illegible] 50 UOP Plaza, Des Plaines, IL 60016-6187
1	Robert J. Gottschall, Office of Material Sciences, [illegible] GTN, Washington, DC 20545

AD-A184 356 EFFECT OF TIME AND TEMPERATURE ON TRANSFORMATION TOUGHENED ZIRCONIAS(U) ARMY LAB COMMAND WATERTOWN MA MATERIAL TECHNOLOGY LAB L J SCHIOLER JUN 87 2/2

UNCLASSIFIED MTL-TR-87-29 DE-AI05-840R-21411 F/G 11/2 NL

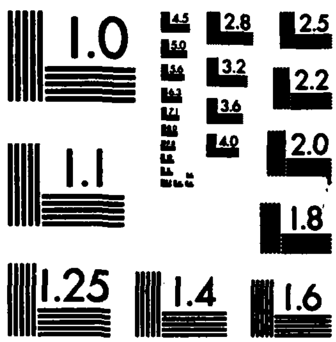

MICROCOPY RESOLUTION TEST CHART
NATIONAL BUREAU OF STANDARDS-1963-A

No. of Copies	To
1	Kenneth Green, Senior Development Engineer, Coors Porcelain Company, Golden, CO 80401
1	Michael Greenfield, National Aeronautics and Space Administration, Energy Systems Office, Washington, DC 20546
1	L. E. Groseclose, General Motors Corporation, Allison Gas Turbine Division, P.O. Box 420, Indianapolis, IN 46206-0420
1	T. D. Gulden, Manager, Ceramics and Chemistry, GA Technologies, Inc., P.O. Box 81608, San Diego, CA 92138
1	M. D. Gurney, NIPER, P.O. Box 2128, Bartlesville, OK 74005
1	H. T. Hahn, Mechanical Engineering Department, Washington Universtiy at St. Louis, Lindell and Skinker, Box 1087, St. Louis, MO 63130
1	Nabil S. Hakim, Staff Research Engineer, Engineering R&D, General Motors Corporation, Detroit Diesel Allison Division, 36880 Ecorse Road, Romulus, MI 48174
1	John M. Halstead, Manager, Business Development, Structural Ceramics Division, Standard Oil Engineered Materials Company, 1625 Buffalo Avenue, Bldg. 91-2, P.O. Box 1054, Niagara Falls, NY 14302
1	R. A. Harmon, 25 Schalren Drive, Latham, NY 12110
1	Stephen D. Hartline, Norton Company, One New Bond Street, Worcester, MA 01606
1	Willard E. Hauth, Section Manager - Composite Development Ceramics Program, Dow Corning Corporation, Midland, MI 48640
1	Norman L. Hecht, University of Dayton Research Institute, 300 College Park, Dayton, OH 45469-0001
1	S. S. Hecker, Chairman, Center for Materials Science, Los Alamos National Laboratory, Mail Stop K765, Los. Alamos, NM 87545
1	Peter W. Heitman, General Motors Corporation, Allison Gas Turbine Operations, P.O. Box 420, W-5, Indianapolis, IN 46206-0420
1	H. E. Helms, General Motors Corporation, Allison Gas Turbine Operations, P.O. Box 420, Indianapolis, IN 46206-0420
1	Thomas L. Henson, Director of Research and Engineering, Chemical & Metallurgical Division, GTE Products Corporation, Hawes Street, Towanda, PA 18848-0504
1	Thomas P. Herbell, NASA Lewis Research Center, 21000 Brookpark Road, M/S 49-3, Cleveland, OH 44135
1	Robert V. Hillery, Manager, Coating Materials & Processes, General Electric Company, Cincinnati, OH 45215

No. of Copies	To
1	Jonathan W. Hinton, Vice President and General Manager, Structural Ceramics Division, SOHIO Engineered Materials Company, P.O. Box 1054, Niagara Falls, NY 14302
1	Stephen M. Hsu, Inorganic Materials Div., Center for Materials Science, U.S. Department of Commerce, National Bureau of Standards, Gaithersburg, MD 20899
1	Harold A. Huckins, President, Princeton Advanced Technology, Inc., 56 Finley Road, Princeton, NJ 08540
1	Joseph E. Hunter, Jr., Metallurgy Department, General Motors Research Lab., 12 Mile and Mound Road, Warren, MI 48090-9055
1	Louis C. Ianniello, Director, Office of Materials Sciences, Department of Energy, ER-13 GTN, Washington, DC 20545
1	Curtis A. Johnson, General Electric Company, Ceramics Branch, P.O. Box 8, Schenectady, NY 12301
3	D. Ray Johnson, Ceramic Technology for Advanced Heat Engines Project, Building 4515, Oak Ridge National Laboratory, P.O. Box X, Oak Ridge, TN 37831-6066
1	Larry Johnson, Director, Center for Transportation Research, Argonne National Laboratory, Building 362, 9700 S. Cass Avenue, Argonne, IL 60439
1	R. A. Johnson, General Motors Corporation, Allison Gas Turbine Division, P.O. Box 420, Indianapolis, IN 46206-0420
1	L. A. Joo, Associate Director of Research, Great Lakes Research Corp., P.O. Box 1031, Elizabethton, TN 37643
1	Roy Kamo, President, Adiabatics, Inc., 630 S. Mapleton, Columbus, IN 47201
1	Allan Katz, Air Force Wright Aeronautical Laboratory, Materials Laboratory, Metals and Ceramics Division, AFWAL/MLLM, Wright-Patterson AFB, OH 45433
1	P. Victor Kelsey, Ceramics Technical Leader, Materials Science Division, Alcoa Aluminum Company of America, Alcoa Technical Center B, Alcoa Center, PA 15061
1	Frederick L. Kennard, III, Supervisor, Ceramic Research, AC Spark Plug Division of General Motors, 1300 N. Dort Highway, Flint, MI 48556
1	J. R. Kidwell, AGT 101 Assistant Project Engineer, Garrett Turbine Engine Company, 111 S. 34th Street, P.O. Box 5217, Phoenix, AZ 85010
1	A. S. Kobayashi, Mechanical Engineering Dept., MS FU10, University of Washington, Seattle, WA 98195

No. of Copies	To
1	John Mason, Vice President-Engineering, The Garrett Corporation, 9851 Sepulveda Boulevard, P.O. Box 92248, Los Angeles, CA 90009
1	K. S. Mazdiyasni, Air Force Wright Aeronautical Laboratory, Materials Laboratory, Metals and Ceramics Division, AFWAL/MLLM, Wright-Patterson AFB, OH 45433
1	Thomas D. McGee, Department of Materials Science and Engineering, Iowa State University, Ames, IA 50011
1	Malcolm G. McLaren, Head, Department of Ceramics, Rutgers University, Busch Campus, Box 909, Bowser Road, Piscataway, NJ 08854
1	Arthur F. McLean, Ceramics Materials Department, Ford Motor Company, P.O. Box 2053, Dearborn, MI 48121
1	Brian L. Mehosky, Development Engineer, R&D, Standard Oil Engineered Materials Company, 4440 Warrensville Center Road, Cleveland, OH 44128
1	P. K. Mehrotra, Kennametal Inc., P.O. Box 639, Greensburg, PA 15601
1	Arthur G. Metcalfe, Director, Research Department, Solar Turbines, Inc., P.O. Box 80966, 2200 Pacific Highway, San Diego, CA 92138
1	Thomas N. Meyer, Senior Technical Specialist, Alumina, Chemicals and Ceramics Div., Aluminum Company of America, Alcoa Technical Center, Alcoa Center, PA 15069
1	W. Miloscia, Standard Oil Engineered Materials Company, Research and Development, 4440 Warrensville Center Road, Cleveland, OH 44128
1	Helen Moeller, Babcock & Wilcox, P.O. Box 1260, Lynchburg, VA 24505
1	Peter E. D. Morgan, Member Technical Staff, Structural Ceramics, Science Center, Rockwell International, 1049 Camino Dos Rios, P.O. Box 1085, Thousand Oaks, CA 91360
1	Solomon Musikant, General Electric, VFSC, Building 100, U-3027, P.O. Box 8555, Philadelphia, PA 19101
1	Dale E. Niesz, Manager, Materials Department, Battelle Columbus Laboratories, 505 King Avenue, Columbus, OH 43201
1	W. Richard Ott, New York State College of Ceramics, Alfred University, Alfred, NY 14802
1	Hayne Palmour III, Engineering Research Services Division, 2158 Burlington Engineering Laboratories, North Carolina State University, P.O. Box 5995, Raleigh, NC 27607

No. of Copies	To
1	David M. Kotchick, AiResearch Manufacturing Company, 2525 W. 190th Street, Torrance, CA 90509
1	Saunders B. Kramer, Manager, AGT Program, Office of Transportation Systems, Department of Energy, GE-131 FORSTL, 1000 Independence Avenue, Washington, DC 20585
1	D. M. Kreiner, AGT 101 Project Manager, Garrett Turbine Engine Company, 111 S. 34th Street, P.O. Box 5217, Phoenix, AZ 85010
1	W. J. Lackey, Georgia Tech Research Institute, Energy and Materials Sciences Laboratory, Georgia Institute of Technology, Atlanta, GA 30332
1	Everett A. Lake, Air Force Wright Aeronautical Laboratory, AFWAL/POOS, Wright-Patterson AFB, OH 45433
1	Fred F. Lange, Science Center, Rockwell International, 1049 Camino Dos Rios, P.O. Box 1085, Thousand Oaks, CA 91360
1	John G. Lanning, Corning Glass Works, Advanced Engine Components, HP-BB-2, Corning, NY 14830
1	David C. Larsen, IIT Research Center, 10 W. 35th Street, Chicago, IL 60616
1	Stanley R. Levine, NASA-Lewis Research Center, 21000 Brookpark Road, Cleveland, OH 44135
1	David Lewis, Naval Research Laboratory, Code 6360, Materials Science & Technology Division, 4555 Overlook Avenue, S.W., Washington, DC 20375
1	Winston W. Liang, Project Manager, Industrial Materials Research, Gas Research Institute, 8600 W. Bryn Mawr Avenue, Chicago, IL 60631
1	Bill Long, Elektroschmetlzwerk Kempten GmbH, P.O. Box 590, Tonawanda, NY 14151-0590
1	L. A. Lott, EG&G, Inc., Idaho National Engineering Laboratory, P.O. Box 1625, Idaho Falls, ID 83415
1	Bryan K. Luftglass, Staff Consultant, Chem Systems, Inc., 303 S. Broadway, Tarrytown, NY 10591
1	Michael J. Lynch, General Electric Company, Medical Systems Group, P.O. Box 414, 7B-36, Milwaukee, WI 53201
1	Tai-il Mah, Technical Manager, Ceramics and Composites Research, Universal Energy Systems, 4401 Dayton-Xenia Road, Dayton, OH 45432

No. of Copies	To
1	Michael A. Rigdon, Babcock and Wilcox, 1735 I Street, NW, Washington DC 20006
1	John E. Ritter, Jr., University of Massachusetts, Mechanical Engineering Department, Amherst, MA 01003
1	Giulio A. Rossi, Norton Company, High Performance Ceramics, Goddard Road, Northboro, MA 01532
1	Barry R. Rossing, Aluminum Company of America, Alcoa Technical Center, Alcoa Center, PA 15069
1	David J. Rowcliffe, SRI International, 333 Ravenswood Avenue, Menlo Park, CA 94025
1	Donald W. Roy, Manager, Carbide and Optical Material Research and Development, Coors Porcelain Company, Golden, CO 80401
1	Bruce Rubinger, Gobal, 50 Milk Street, 15th Floor, Boston, MA 02109
1	Robert Ruh, Air Force Wright Aeronautical Laboratory, Materials Laboratory Metals and Ceramics Division, AFWAL/MLLM, Wright-Patterson AFB, OH 45433
1	Robert J. Russell, Sr., Divisional Vice President, Technology and Planning, High Performance Ceramics, Norton Company, One New Bond Street, Worcester, MA 01606
1	J. Sankar, North Carolina Agricultural and Technical State University, Mechanical Engineering Dept., Greenboro, NC 27411
1	Maxine Savitz, 5019 Lowell Street, NW, Washington, DC 20016
1	Richard Schapery, Civil Engineering Department, Texas A&M University, College Station, TX 77843
1	Liselotte J. Schioler, Department 900, Aerojet Tech Systems Co., P.O. Box 13222, Sacremento, CA 95813
1	Matthew Schreiner, Gas Research Institute, 8600 West Bryn Mawr Avenue, Chicago, IL 60631
1	Peter C. Schultz, Manager, Materials Research, Corning Research and Development Division, Corning Glass Works, Corning, NY 14831
3	R. B. Schulz, Office of Transportation Systems, Department of Energy, CE-151 FORSTL, 1000 Independence Avenue, Washington, DC 20585
1	Murray A. Schwartz, Bureau of Mines, 2401 I Street, N.W., Washington, DC 20241
1	Thomas M. Sebestyen, U.S. Army Tank Automotive Command, AMSTA-RGRT, Warren, MI 48397-5000

No. of Copies	To
1	Joseph N. Panzarino, Norton Company, Director, Research and Development, High Performance Ceramics, 1 New Bond Street, Worcester, MA 01606
1	Pellegrino Papa, Manager, Technical and Business Development, Corning Technical Products Division, Corning Glass Works, Corning, NY 14831
1	Arvid E. Pasto, Member of Technical Staff, Precision Materials Technology, GTE Laboratories, Inc., 40 Sylvan Road, Waltham, MA 02254
1	James W. Patten, Director, Materials Engineering, Cummins Engine Company, Inc., Mail Code 50183, Box 3005, Columbus, IN 47201
1	Dan Petrak, Babcock and Wilcox, P.O. Box 1260, Lynchburg, VA 24505
1	R. Byron Pipes, Center for Composite Materials, 2001 Spencer Laboratory, University of Delaware, Newark, DE 19716
1	Robert C. Pohanka, Office of Naval Research, Code 431, 800 North Quincy Street, Arlington, VA 22217
1	Karl M. Prewo, United Technologies Research Center, Silver Lane, MS 24, East Hartford, CT 06108
1	Hubert B. Probst, Chief Scientist, Materials Division, MS 49-1, NASA-Lewis Research Center, 21000 Brookpark Road, Cleveland, OH 44135
1	Carr Lane Quackenbush, GTE Products Corporation, Hawes Street, Towanda, PA 18848-0504
1	Dennis T. Quinto, Phillip M. McKenna Laboratory, Kennametal, Incorporated, P.O. Box 639, Greensburg, PA 15601
1	Dennis Readey, Department Chairman, Ceramic Engineering Department, Ohio State University, 2041 College Road, Columbus, OH 43210
1	Robert R. Reeber, U.S. Army Research Office, P.O. Box 12211, Research Triangle Park, NC 27709
1	K. L. Reifsnider, Department of Engineering Science and Mechanics, Virginia Polytechnic Institute and State University, Blacksburg, VA 24061
1	K. T. Rhee, College of Engineering, Rutgers University, P.O. Box 909, Piscataway, NJ 08854
1	Roy W. Rice, W.R. Grace and Company, 7379 Route 32, Columbus, MD 21044
1	David W. Richerson, Ceramatec, Inc., 163 West 1700 South, Salt Lake City, UT 84115
1	Paul Rieth, Ferro Corporation, 661 Willet Road, Buffalo, NY 14218

No. of Copies	To
1	Roger Storm, Director, Niagara Falls R&D Center, Standard Oil Engineered Materials Company, P.O. Box 832, Niagara Falls, NY 14302
1	E. E. Strain, Program Manager, Garrett Turbine Engine Company, 111 S. 34th Street, P.O. Box 5217, Mail Stop 301-2N, Phoenix, AZ 85010
1	Thomas N. Strom, NASA Lewis Research Center, 21000 Brookpark Road, 77-6, Cleveland, OH 44135
1	Karsten Styhr, AiResearch Casting Co., 19800 Van Ness Avenue, Torrance, CA 90509
1	Lewis R. Swank, Ford Motor Company, P.O. Box 2053, Building SRL, Room E3172, Dearborn, MI 48121
1	Anthony C. Taylor, Staff Director, Subcommittee on Transportation, Aviation and Materials, Committee on Science and Technology, U.S. House of Representatives, Room 2321 Rayburn Building, Washington, DC 20515
1	W. H. Thielbahr, Chief, Energy Programs Branch, Idaho Operations Office, U.S. Department of Energy, 550 2nd Street, Idaho Falls, ID 83401
1	John K. Tien, Director of Center for Strategic Materials, 1137 S.W. Mudd Building, Columbia University, New York, NY 10027
1	T. Y. Tien, University of Michigan, Dept. of Materials & Metallurgical Engineering, Dow Building, Ann Arbor, MI 48109-2136
1	Nancy J. Tighe, National Bureau of Standards, Inorganic Materials Division 420, Gaithersburg, MD 20899
1	Julian M. Tishkoff, Air Force Office of Scientific Research, Directorate of Aerospace Sciences, Bolling AFB, Washington, DC 20332
1	Maurice L. Torti, Senior Scientist, High Performance Ceramics, Norton Company, One New Bond Street, Worcester, MA 01606
1	Louis E. Toth, Division of Materials Research, National Science Foundation, 1800 G Street, N.W., Washington, DC 20550
1	Richard E. Tressler, Chairman, Ceramic Science and Engineering Department, The Pennsylvania State University, 201 Steidle Building, University Park, PA 16802
1	V. Venkateswaran, Standard Oil Engineered Materials Company, P.O. Box 832, Niagara Falls, NY 14302
1	John B. Wachtman, Jr., Rutgers University, Department of Ceramics, P.O. Box 901, Piscataway, NJ 08854

No. of Copies	To
1	Brian Seegmiller, Senior Development Engineer, Coors Porcelain Company, 17750 North 32 Street, Golden, CO 80401
1	S. G. Seshadri, Research Associate, Standard Oil Engineered Materials Company, Niagara Falls R&D Center, P.O. Box 832, Niagara Falls, NY 14302
1	Peter T. B. Shaffer, Executive Vice President, Advanced Refractory Technologies, Inc., 699 Hertel Avenue, Buffalo, NY 14207
1	Dinesh K. Shetty, The University of Utah, Dept. of Materials Science & Engrg., Salt Lake City, UT 84112
1	Jack D. Sibold, Coors Porcelain Company, 17750 North 32 Street, Golden, CO 80401
1	Neal Sigmon, Appropriations Committee, Subcommittee on Interior and Related Events, U.S. House of Representatives, B-308 Rayburn Building, Washington, DC 20515
1	Richard Silberglitt, DHR, Inc., 6849 Old Dominion Drive, Suite 228, McLean, VA 22101
1	S. R. Skaggs, MS F-682, Program Office, Los Alamos National Laboratory, P.O. Box 1663, Los Alamos, NM 87545
1	Ed Skorupski, Air Products and Chemicals, Inc., P.O. Box 538, Allentown, PA 18105
1	J. Thomas Smith, Director, Precision Materials Tech., GTE Laboratories, Inc., 40 Sylvan Road, Waltham, MA 02254
1	Jay R. Smyth, Senior Development Specialist, Garrett Turbine Engine Company, 2739 E. Washington, MS 93-172/1302-2K, Phoenix, AZ 85034
1	Rafel Sobotowski, Standard Oil Engineered Materials Company, Research and Development, 3092 Broadway Avenue, Cleveland, OH 44115
1	Richard M. Spriggs, National Materials Advisory Board, National Research Council, 2101 Constitution Avenue, Washington, DC 20418
1	M. Srinavasan, Standard Oil Engineered Materials Company, Niagara Falls R&D Center, P.O. Box 832, Niagara Falls, NY 14302
1	Gordon L. Starr, Manager, Metallic/Ceramic Materials Dept., Cummins Engine Company, Inc., Mail Code 50183, Box 3005, Columbus, IN 47202-3005
1	Harold L. Stocker, Manager, Low Heat Rejection Program, General Motors Corporation, Allison Gas Turbine Operations, P.O. Box 420, T-23, Indianapolis, IN 46206-0420

No. of Copies	To
1	Richard B. Wallace, Manager, Government Research and Development Programs, General Motors Corporation, Detroit Diesel Allison Division, 36880 Ecorse Road, Romulus, MI 48174
1	Harlan L. Watson, Subcommittee on Energy Research and Production, U.S. House of Representatives, Committee on Science and Technology, Suite 2321, Rayburn House Office Building, Washington, DC 20515
1	Steven G. Wax, Materials Science Division, Advanced Research Projects Agency, Department of Defense, 1400 Wilson Boulevard, Arlington, VA 22209
1	Albert R. C. Westwood, Corporate Director, Martin Marietta Laboratories, 1450 South Rolling Road, Baltimore, MD 21227
1	Thomas J. Whalen, Principal Research Scientist, Ford Motor Company, Scientific Lab., Room 2023, Dearborn, MI 48121
1	Sheldon M. Wiederhorn, Inorganic Materials Division, Mechanical Properties Group, U.S. Department of Commerce, National Bureau of Standards, Gaithersburg, MD 20899
1	James C. Williams, Dean, Carnegie Institute of Technology, Carnegie-Mellon University, Schenley Park, Pittsburgh, PA 15213
1	Roger R. Wills, Manager, Advanced Ceramic Components, TRW Inc., Automotive Worldwide Sector, Valve Division, 1455 East 185th Street, Cleveland, OH 44110
1	David Gordon Wilson, Massachusetts Institute of Technology, Mechanical Engineering Department, Room 3-455, Cambridge, MA 02139
1	J. M. Wimmer, Supervisor, Nonmetallic Materials Group, Garrett Turbine Engine Company, 111 S. 34th Street, P.O. Box 5217, Phoenix, AZ 85010
1	David Wirth, Vice President, Technical Operations and Engr., Coors Porcelain Company, 17750 North 32 Street, Golden, CO 80401
1	Thomas J. Wissing, Manager, Government Contract Administration, Eaton Corporation, Engineering & Research Center, 25201 Northwestern Highway, P.O. Box 766, Southfield, MI 48037
1	James C. Wood, NASA Lewis Research Center, 21000 Brookpark Road, Mail Stop 77-6, Cleveland, OH 44135
1	Hun C. Yeh, Ceramic Supervisor, AiResearch Casting Company, A Division of the Garrett Corp., 19800 Van Ness Avenue, Torrance, CA 90509
1	Thomas M. Yonushonis, Cummins Engine Company, Box 3005, Mail Code 50183, Columbus, IN 47202-3005

No. of Copies	To
1	Don Zabierek, Air Force Wright Aeronautical Laboratory, AFWAL/POTC, Wright-Patterson AFB, OH 45433
1	Klaus M. Zwilsky, Executive Director, National Materials Advisory Board, National Research Council, 2101 Constitution Avenue, Washington, DC 20418
1	Department of Energy, Oak Ridge Operations Office, Office of Assistant Manager for Energy Research and Development, P.O. Box E, Oak Ridge, TN 37831
1	Department of Energy, Technical Information Center, Office of Information Services, P.O. Box 62, Oak Ridge, TN 37831
	Commander, U.S. Army Laboratory Command, 2800 Powder Mill Road, Aldelphi, MD 20783-1145
1	ATTN: SLCIS-IM-TL
	Commander, Defense Technical Information Center, Cameron Station, Building 5, 5010 Duke Street, Alexandria, VA 22304-6145
2	ATTN: DTIC-FDAC
	Commander, U.S. Army Materiel Command, 5001 Eisenhower Avenue, Alexandria, VA 22333
1	ATTN: AMCLD
	Director, U.S. Army Materials Technology Laboratory, Watertown, MA 02172-0001
2	ATTN: SLCMT-IML
1	Author

U.S. Army Materials Technology Laboratory
Watertown, Massachusetts 02172-0001
EFFECT OF TIME AND TEMPERATURE ON
TRANSFORMATION TOUGHENED ZIRCONIAS
Liselotte J. Schioler

AD______________
UNCLASSIFIED
UNLIMITED DISTRIBUTION

Key Words

Zirconia
Toughened ceramics
Ceramics

Technical Report MTL TR 87-29, June 1987, 91 pp-
illus-tables, Contract Number DE-AI05-
840R 21411

The effects of exposure to elevated temperatures (900 to 1300°C) for times ranging from 50 to 500 hours on toughened oxide ceramics intended for use in heat engines were examined. The materials were magnesia stabilized transformation toughened zirconia, yttria stabilized tetragonal zirconia polycrystal, and zirconia toughened alumina, as well as untoughened zirconias for comparison. The materials were heat treated, and physical and mechanical properties were then measured at room temperature. High temperature mechanical tests performed were stress rupture and stepped temperature stress rupture. The results of the tests indicate that the mechanical properties of magnesia stabilized transformation toughened zirconia degrade substantially after relatively short times at the moderate temperatures expected in low-heat-rejection diesel engines. The ytrria stabilized tetragonal zirconia polycrystal and the untoughened partially stabilized zirconia materials appear to be more stable against the effects of time-at-temperature.

U.S. Army Materials Technology Laboratory
Watertown, Massachusetts 02172-0001
EFFECT OF TIME AND TEMPERATURE ON
TRANSFORMATION TOUGHENED ZIRCONIAS
Liselotte J. Schioler

AD______________
UNCLASSIFIED
UNLIMITED DISTRIBUTION

Key Words

Zirconia
Toughened ceramics
Ceramics

Technical Report MTL TR 87-29, June 1987, 91 pp-
illus-tables, Contract Number DE-AI05-
840R 21411

The effects of exposure to elevated temperatures (900 to 1300°C) for times ranging from 50 to 500 hours on toughened oxide ceramics intended for use in heat engines were examined. The materials were magnesia stabilized transformation toughened zirconia, yttria stabilized tetragonal zirconia polycrystal, and zirconia toughened alumina, as well as untoughened zirconias for comparison. The materials were heat treated, and physical and mechanical properties were then measured at room temperature. High temperature mechanical tests performed were stress rupture and stepped temperature stress rupture. The results of the tests indicate that the mechanical properties of magnesia stabilized transformation toughened zirconia degrade substantially after relatively short times at the moderate temperatures expected in low-heat-rejection diesel engines. The ytrria stabilized tetragonal zirconia polycrystal and the untoughened partially stabilized zirconia materials appear to be more stable against the effects of time-at-temperature.

U.S. Army Materials Technology Laboratory
Watertown, Massachusetts 02172-0001
EFFECT OF TIME AND TEMPERATURE ON
TRANSFORMATION TOUGHENED ZIRCONIAS
Liselotte J. Schioler

AD______________
UNCLASSIFIED
UNLIMITED DISTRIBUTION

Key Words

Zirconia
Toughened ceramics
Ceramics

Technical Report MTL TR 87-29, June 1987, 91 pp-
illus-tables, Contract Number DE-AI05-
840R 21411

The effects of exposure to elevated temperatures (900 to 1300°C) for times ranging from 50 to 500 hours on toughened oxide ceramics intended for use in heat engines were examined. The materials were magnesia stabilized transformation toughened zirconia, yttria stabilized tetragonal zirconia polycrystal, and zirconia toughened alumina, as well as untoughened zirconias for comparison. The materials were heat treated, and physical and mechanical properties were then measured at room temperature. High temperature mechanical tests performed were stress rupture and stepped temperature stress rupture. The results of the tests indicate that the mechanical properties of magnesia stabilized transformation toughened zirconia degrade substantially after relatively short times at the moderate temperatures expected in low-heat-rejection diesel engines. The ytrria stabilized tetragonal zirconia polycrystal and the untoughened partially stabilized zirconia materials appear to be more stable against the effects of time-at-temperature.

U.S. Army Materials Technology Laboratory
Watertown, Massachusetts 02172-0001
EFFECT OF TIME AND TEMPERATURE ON
TRANSFORMATION TOUGHENED ZIRCONIAS
Liselotte J. Schioler

AD______________
UNCLASSIFIED
UNLIMITED DISTRIBUTION

Key Words

Zirconia
Toughened ceramics
Ceramics

Technical Report MTL TR 87-29, June 1987, 91 pp-
illus-tables, Contract Number DE-AI05-
840R 21411

The effects of exposure to elevated temperatures (900 to 1300°C) for times ranging from 50 to 500 hours on toughened oxide ceramics intended for use in heat engines were examined. The materials were magnesia stabilized transformation toughened zirconia, yttria stabilized tetragonal zirconia polycrystal, and zirconia toughened alumina, as well as untoughened zirconias for comparison. The materials were heat treated, and physical and mechanical properties were then measured at room temperature. High temperature mechanical tests performed were stress rupture and stepped temperature stress rupture. The results of the tests indicate that the mechanical properties of magnesia stabilized transformation toughened zirconia degrade substantially after relatively short times at the moderate temperatures expected in low-heat-rejection diesel engines. The ytrria stabilized tetragonal zirconia polycrystal and the untoughened partially stabilized zirconia materials appear to be more stable against the effects of time-at-temperature.

END

10-87

DTIC